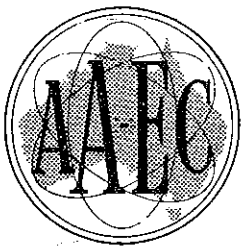

AAEC/E171

AUSTRALIAN ATOMIC ENERGY COMMISSION

RESEARCH ESTABLISHMENT
LUCAS HEIGHTS

DIFFERENTIAL NEUTRON ENERGY SPECTRUM MEASUREMENTS ON U233/BeO AND U235/BeO ASSEMBLIES IN THE REACTOR MOATA

by

R. B. TATTERSALL*

*Attached, from U.K.A.E.A. Reactor Group

March 1967

AUSTRALIAN ATOMIC ENERGY COMMISSION

RESEARCH ESTABLISHMENT

LUCAS HEIGHTS

DIFFERENTIAL NEUTRON ENERGY SPECTRUM MEASUREMENTS ON U233/BeO AND U235/BeO ASSEMBLIES IN THE REACTOR MOATA

by

R. B. TATTERSALL *

* Attached, from U.K.A.E.A. Reactor Group

ABSTRACT

Differential spectrum measurements were made on a series of U233 and U235 fuelled, beryllia moderated assemblies with fuel to moderator atomic ratios ranging from 1/6500 to 1/700. A preliminary comparison has been made with calculations of the spectra and, in the thermal region, fair agreement was found for the U235 lattices, but for U233 the experimental thermal flux was significantly higher than that calculated. In the epithermal region above 50eV, the experimental flux was higher than that calculated for the U235 assemblies, but was in reasonable agreement with calculation for U233.

CONTENTS

(continued)

CONTENTS (continued)

(continued)

CONTENTS (continued)

1. INTRODUCTION

A series of measurements on small (12 inch cube) beryllia moderated assemblies fuelled with U233 and U235 has been made using the UTR–10 reactor MOATA. The assemblies were placed at the centre of the reactor and a variety of reactivity, perturbation, and integral and differential spectrum measurements were made.

This paper presents the results of the differential spectrum measurements which were made on a neutron beam from the centre of each assembly using the MOATA chopper. The detailed theory and methods used to reduce the time of flight measurements to neutron energy spectra have been described (Tattersall 1966), so this report is confined to an account of the experimental layouts used and the spectra found.

The spectra measured were compared with calculations based on the cross section libraries of the code GYMEA (Pollard and Robinson 1966) and the initial results of this comparison are also presented.

2. DESCRIPTION OF ASSEMBLIES

All the assemblies were in the form of horizontal slab lattices with either 1 inch or 2 inches between adjacent layers of fuel (see Figure 1). These lattices were assembled inside an aluminium box whose internal dimensions were 12 inches cube and whose walls were 0.25 inch thick.

The compositions of the assemblies are given in Table 1. These compositions are the mean values found by assuming that the assemblies were uniform slab lattices.

As far as the moderator is concerned the assemblies were in two groups, those without thorium and those with thorium. For those without thorium, the moderator consisted of 1 inch thick slabs of BeO of density 2.86 g/cm^3, and in all cases a single layer of BeO was used between each layer of fuel.

The moderator in the thorium–containing assemblies was a uniform mixture of ThO_2 and BeO (2.5 per cent. ThO_2 by weight). This material was also formed into 1 inch thick slabs with a density of 2.96 g/cm^3. A single layer of slabs was used between fuel layers for all but the two most dilute assemblies, and for these two (U235/Th/BeO = 1/3.6/1500 and U233/Th/BeO = 1/6.8/2800) a double layer of slabs was used.

The U235 fuel was in the form of metal foil 2 inches by 4 inches by 0.002 inch thick with a U235 content of approximately 90 per cent. atomic. The foils in each fuel layer were evenly distributed over the area available, the number of foils per layer ranging from 2 to 18 as the composition was changed from U235/BeO ratio of 1/6545 to 1/740. In the last case and also for the U235/Th assemblies, the whole 12 inches by 12 inches area was completely covered with foils. The foils in each layer were stuck on to a 0.0625 inch thick aluminium plate for ease of handling, except in the case of the most dilute assembly.

The U233 fuel was in the form of a UO_2–aluminium compact 0.022 inch thick by 1.08 inch wide, clad in 0.010 inch thick aluminium. The resulting fuel elements were 11.8 inches long and were laid side by side to form a layer of fuel. For the assembly with the composition U233/Th/BeO = 1/1.7/700, a double layer of fuel was used between layers of moderator. In all other cases a single layer of fuel was used. The mean thickness of a single fuel layer was 0.058 inch.

A channel 1 inch high by 1.14 inch wide by 6 inches deep leading from the centre to the middle of one face of the assembly was used to extract a neutron beam for spectrum measurements. This channel lay mid–way between two layers of fuel so that its upper and lower boundaries were formed by the fuel layers, in those cases where the moderator layer was 1 inch thick, and by 0.5 inch thick pieces of moderator when the moderator layer was 2 inches thick. In both cases the neutron source for the spectrum measurements originated from an area of moderator approximately 0.7 inch square mid–way between fuel layers. There was a 0.010 inch thick aluminium window over the end of the channel in the side of the aluminium box which held the assembly.

3. GEOMETRIC ARRANGEMENT OF REACTOR AND NEUTRON FLIGHT PATH

MOATA is a light water moderated graphite reflected system fuelled with U235 (Marks 1962). It has two core tanks each approximately 20 inches by 6 inches by 57 inches high which contain the H_2O moderator and U235–aluminium alloy fuel (the fuelled height is 23 inches). The tanks are about 18 inches apart and are completely surrounded with graphite to give an overall reactor size of 56 inches by 44 inches by 48 inches high. The assemblies described above were inserted in a 12½ inch cubical cavity between the core tanks so that there was a layer of graphite approximately 3 inches thick between the core tanks and the assemblies.

Figure 2 is a vertical section through the reactor and shows the channels along which the neutron beam passes. As noted above, the channel within the assembly itself is 1.14 inch wide by 1 inch high by 6 inches deep. In the reactor graphite the channel is initially 2 inches square for a distance of 4 inches followed by a 4 inch square section for a distance of 12 inches to the outside of the graphite. The chopper rotor is mounted on the inside of a concrete door in the reactor shielding. A cavity in the shield between the door and the graphite reflector is filled with a steel shot loaded concrete block 18 inches deep with a 5 inch square hole through it. The channel through the shield door is 3 inches square by 4 feet 6 inches long, and the neutron detector station is about 25 feet from the chopper rotor.

Various collimators and evacuated flight tubes were installed along the flight path as shown in Figures 3 and 4. These are illustrated in detail in Figure 5 and are described below. Table 2 gives details of the combinations used in the individual experimental runs.

The graphite and boron–wax collimators are used to minimize the neutron background, whilst the lead and steel collimators reduce the gamma ray background (the Li–glass scintillation detector described in Section 4 is quite sensitive to gamma rays).

There are 6 collimators.

(i) Inner Graphite Collimator

This is a piece of graphite 4 inches square by 17 inches long with a rectangular section beam hole 1.125 inch high by 1.25 inch wide along its axis. This is placed in the 4 inch square hole in the reactor graphite. The outer face of this collimator is faced with cadmium.

(ii) Steel Collimator

This is a block of steel 4 inches square by 18 inches long with a 0.75 inch square beam hole along its axis. This is placed in the 5 inches square hole in the steel shot loaded concrete block.

(iii) Boron–Wax Collimator

This is a block about 8 inches square by 3 inches thick made of a mixture of boron carbide and paraffin wax. It fits over the end of the 5 inches square hole in the steel shot concrete block, between it and the chopper rotor. There is a 0.75 inch square beam hole along its axis.

(iv) Boron–Lead Collimator

This is a block 3 inches square by 6 inches long which fits in the 3 inches square hole through the concrete shield door, and which is positioned as close to the chopper rotor as possible. It has a 0.75 inch square beam hole along its axis. Proceeding from the chopper rotor the first 3 inches of this collimator is made from a mixture of boric acid and paraffin wax, and the other 3 inches from lead.

(v) Outer Graphite Collimator

This is a piece of graphite 3 inches square by 3 feet 6 inches long with a rectangular section beam hole along its axis. It is placed in the 3 inches square hole through the shield door and the beam hole is 1.15 inch high by 1.22 inch wide at the rotor end and 1.40 inch by 1.45 inch at the other end.

(vi) Lead Collimator and Flight Tube

This consists of a 3 inch diameter aluminium flight tube 30 inches long attached to a lead collimator 4 inches square by 7 inches long with a tapered rectangular beam hole along its axis. This beam hole is 1.0 inch square at the end nearest the flight tube and 0.75 inch square at the other end. The outer ends of this flight tube/collimator combination are covered with 0.005 inch thick aluminium foil and the unit is evacuated to a pressure of less than 0.1 mmHg.

In addition there are three other evacuated flight tubes, one 3 inches diameter by 60 inches long which fits in the shield door as an alternative to the Outer Graphite Collimator, and two 7 inches diameter by 5 feet 6 inches and 11 feet 6 inches long respectively, which are used between the shield door and the detector. The ends of all tubes are closed with 0.005 inch thick aluminium foil and they are evacuated to a pressure of less than 0.1 mmHg. These evacuated flight tubes reduce attenuation of the neutron beam by the air along the flight path. The length of air traversed by the neutron beam in each run is given in Table 2.

4. DETECTORS

Two detector systems were used, one consisting of BF_3 counters and the other a Li–glass scintillator. The BF_3 counters were of comparatively low efficiency (about 10 per cent. for neutrons of energy 0.025 eV) and gave rather poor statistical accuracy (see Section 6.8). They were replaced when the scintillator detector became available.

The BF_3 counter system consisted of 3 counters each approximately 0.5 inch diameter by 2 inches long, filled with enriched BF_3 to a pressure of about 0.70 cmHg (type 5 EB 70/13). Their layout is shown in Figure 6. The height (1.28 inch = 3.26 cm) of the neutron beam detected was determined by the height of the counter system and the width (1.57 inch = 4.0 cm) was determined by a collimator made from a boric oxide–paraffin wax mixture which screened the ends of the counters. The counters were housed in a box lined with a boric oxide–epoxy resin mixture to minimize neutron background.

The position of time zero in the flight time analyzer output was determined by measuring the position in time of the gamma rays transmitted along the flight path from the reactor (see Tattersall 1966, Section 11). To detect these gamma rays a Na–I crystal, 1.5 inch diameter by 1 inch thick was used in the position indicated in Figure 6.

The Li–glass scintillation detector type NE908 was 1.5 inch diameter by 1 inch thick and was mounted on a 2 inch diameter photomultiplier tube EMI type 6097B. The layout is shown in Figure 7. In this case the area of neutron beam detected (1 inch square) was defined by a boric acid–paraffin wax collimator as indicated in the figure. The scintillating glass contained 77 per cent. lithium enriched to 95 per cent. Li^6, and had a mean free path for absorption of neutrons of energy E of $0.34\sqrt{E}$. For the 1 inch thick glass used this gave a counting efficiency of 100 per cent. for neutrons of energies up to 1 eV. This fell to 50 per cent. at 100 eV and 20 per cent. at 1 keV. This was very much better than the BF_3 counters but the Li–glass had the disadvantage of being sensitive to gamma rays. To minimize this gamma ray sensitivity the output of the photomultiplier was taken through a single channel analyzer and, in addition, the detector was shielded with 6 inches of steel and 4 inches of borated wax blocks.

When this scintillation detector was in use a measurement on gamma rays to determine the position of the Time Analyzer zero could be made simply by resetting the single channel analyzer outside the range of neutron pulse heights.

The BF_3 counter system was used for measurements on the three most dilute U235 assemblies (U235/BeO ratios of 1/6545, 1/4360, and 1/2185). The Li-glass scintillator was used for all other measurements.

5. ROTORS

Two rotors were used during the experiments. They were basically similar except that the main rotor body was made in stainless steel in one case and Monel metal (65/30 alloy of Ni and Cu) in the other. The difficulty in the use of steel for the rotor body was that the very low total cross section of Fe at about 20 keV led to a considerable neutron leakage through the rotor. This, coupled with the use of the high efficiency detectors and measurements on fairly hard neutron spectra, resulted in a high background count. The change to a Monel rotor reduced this background by a factor of about two in the case of the assembly with a U235/BeO ratio of 1/740.

Figure 8 shows sections through the rotor. The rectangular section slit insert was made of Monel metal whilst the main body was of stainless steel or Monel metal. There were 3 slits each 0.424 inch wide by 0.065 inch high (1.077 cm by 0.1656 cm) and their length was 5.63 inches (14.3 cm) with the stainless steel rotor body and 5.54 inches (14.06 cm) with the Monel rotor. The thickness of the Monel strip defining the top and bottom of each slit was 0.103 inch (0.261 cm).

The rotor was belt driven from a 3 phase induction motor and speed changes were made by changing pulley sizes. The speeds used in the present experiments were approximately 1800 and 7200 r.p.m.

The stainless steel rotor was used for the experiments on all the U235 fuelled assemblies, and the Monel rotor for the U233 fuelled assemblies.

6. EXPERIMENTAL RESULTS

6.1 Introduction

In this section the various stages in the reduction of the experimental data to an energy spectrum are discussed. The detailed theoretical background is given in Tattersall (1966), so the present discussion is primarily concerned with stating the magnitudes of the corrections involved and the experimental checks made.

For each assembly, experimental runs were made with rotor speeds of 1800 and 7200 r.p.m. to provide a complete coverage of the neutron energy range. The only exceptions to this were the runs in which BF_3 counters were used (U235/BeO ratios of 1/6545, 1/4360, and 1/2185), where only the speed of 1800 r.p.m. was used because the low counting efficiency at the higher neutron energies would have resulted in extremely poor counting statistics for the high speed run.

The Time of Flight Analyzer used had 512 channels. Channel widths of 32 μs and 8 μs were used for the rotor speeds of 1800 r.p.m. and 7200 r.p.m. respectively, the time widths being about one third of the neutron burst width produced by the rotor.

Each experimental run lasted about 3 hours and was made with a thermal neutron flux level of about $10^9 n/cm^2/sec$ (Westcott sub-Cd flux) at the chopper source. The length of run was restricted to avoid activating the fuel in the assemblies too much because assembly components had to be altered by hand to change the composition.

Typical count distributions obtained from the Time of Flight Analyzer at the two rotor speeds are shown in Figure 9 (these were obtained in the run on the U233/Th/BeO ratio of 1/6.8/2800). Zero flight time occurs at about channel 100, so channels 1 to 100 measure background. Beyond channel 200 the background is roughly equal to or greater than the genuine counts so that only channels 100 to 200 are utilized to obtain a spectrum. It is interesting to note the high counting rate in the channels corresponding to short flight times. For a 1/E spectrum and a counter whose efficiency varies as $1/\sqrt{E}$ (for example a 'thin' BF_3 counter) a flat count distribution is obtained. In the present case where a 'thick' Li-glass counter is used the efficiency falls more slowly than $1/\sqrt{E}$ so that a rise in count rate occurs as the flight time falls.

6.2 Dead Time Corrections

The Time of Flight Analyzer used could record only the first count occurring after the initiation of a timing cycle. The method of calculating dead time losses is described in Section 8.2 of Tattersall (1966). Over the channels used to produce spectra the magnitude of this loss ranged up to 12 per cent. and 3 per cent. at rotor speeds of 1800 r.p.m. and 7200 r.p.m. respectively. Errors in this correction will be small compared to the statistical errors in the channel counts which are about 5 per cent. (see Section 6.8).

6.3 Background Correction

Details of the methods used in correcting for background are given in Section 8.3 of Tattersall (1966). Three different methods were used, one for the BF_3 counter system, one for the Li-glass counter and stainless steel rotor, and one for the Li-glass counter and Monel rotor.

In the simplest case, the BF_3 counters, there was no gamma ray component to the background and the very low counting efficiency at high neutron energies also meant that the component of background from neutrons transmitted via the rotor was negligible. The background was accordingly not a function of rotor angle, and could be found by averaging the counts in the channels earlier than that corresponding to zero flight time.

With the Li-glass in use there were considerable gamma ray and neutron components to the background which were transmitted from the reactor via the rotor. This meant that the background was dependent on rotor angle, that is, it varied from channel to channel on the Time of Flight Analyzer. As described in Section 8.3 of Tattersall (1966) the background was deduced for flight times near zero from the count distribution in the channels immediately before time zero. The extrapolation of this distribution to longer flight times was based on a measurement of counting rates for a stationary rotor with the slit set at angles of 90° and 25°.

For the Monel rotor, the distribution of background counts was a minimum when the rotor slits were at 90° to the beam and rose as they approached zero because gamma rays and neutrons from the reactor have less rotor material to traverse as the slit angle approaches zero. A similar effect occurred with the stainless steel rotor but the situation was further complicated because the rotor body was virtually transparent for neutrons near 20 keV. Such neutrons would interact with the Monel slit insert which was essentially like a thin slab rotating in the beam. Thus except when the slits were actually open, the minimum length of material traversed was when the slits were at 90° to the beam. There was thus a small peak (about 6 per cent. above the mean level) in the background when the slits were at 90°.

The estimation of background could be checked in the case of runs at 1800 r.p.m. because the genuine neutron counting rate fell to zero by about channel 300 because of the small flux and small rotor transmission at these low energies. Thus channels 300 to 512 provided a further measurement of background which was found to agree with that calculated as indicated above.

As already noted only those channels in which the genuine counts exceeded the background counts were used to deduce spectra. In view of the above check and also because the background in any one channel was essentially deduced from an average over many channels, it was concluded that the uncertainty in the background was not a significant contribution to the error in the channel counts.

6.4 Air Attenuation Correction

The correction for air attenuation was calculated (see Section 8.4 of Tattersall 1966) using total cross section data for nitrogen and oxygen given by Hughes and Schwartz (1958). Reference to Table 2 shows that two path lengths in air were used, and the magnitudes of the corrections in these two cases were:

(i) Air length equal to 390 cm: Correction varied from 18 per cent. at high ($\sim$ 100 eV) neutron energy to 25 per cent. at low ($\sim$ 0.02 eV) energy.

(ii) Air length equal to 140 cm: Correction varied from 7 per cent. at high energy to 10 per cent. at low energy.

In a spectrum measurement it is the change of the correction with energy rather than its absolute value which is important. This change is 7 per cent. and 3 per cent. in the above two cases and these reasonably small values are unlikely to lead to errors in the measured spectra. A pair of runs was made on the same spectrum with different lengths of air in the beam and the results showed that the errors in the correction were certainly less than the statistical errors in a typical run.

The magnitude of the correction for the various aluminium foils in the beam (these were over the ends of evacuated flight tubes) was about 2 per cent. so no significant errors could arise from this correction.

6.5 Slit Transmission Probabilities

The slit transmission probabilities were calculated allowing for neutron leakage through the slit walls by the method described in Tattersall (1966) (see the calculation of $\tau'(E)$ in Section 3 and Appendices II and IV of that report). This method was checked previously by Rocke (A.A.E.C., unpublished) by measuring the same spectrum at several rotor speeds and has been shown to give satisfactory results. In these calculations the total cross section of the Monel metal forming the slits is required as a function of energy and this was found from a chemical analysis of this material and the cross section curves given by Hughes and Schwartz (1958).

6.6 Detector Efficiencies

The efficiencies of the detector systems as a function of energy were calculated from the absorption cross section of the detecting material (boron or lithium) in the counters. If the absorption cross section per cm^3 is Σ then the probability of detecting a neutron with a path length ℓ in the counter is:

$$p = 1 - \exp(-\Sigma \ell) \quad . \qquad 6.1$$

For the BF_3 counter system it is necessary to average p over the various path lengths possible, but for the Li-glass detector all path lengths are the same.

Manufacturer's data were used initially for Σ. The BF_3 counters had an efficiency of 10 per cent. at 0.025 eV which meant that they were essentially thin over all the energy ranges of interest so Equation 6.1 reduced to:

$$p = \Sigma \ell \quad .$$

The dependence of p on energy is thus exactly that of Σ so $p \propto 1/\sqrt{E}$ and the absolute value of Σ does not matter.

In the case of the Li-glass detector it is only when the efficiency has fallen below about 50 per cent. (that is, for neutron energies above 100 eV) that it becomes at all sensitive to the value of Σ. Thus for the energy range covered in the present experiments precise knowledge of Σ is not necessary. However, to check the manufacturer's value used, measurements on the same spectrum were made with the BF_3 and Li-glass detectors. The results are shown in Figure 10 where the effect of changing Σ_o for the Li-glass from 16.6 to 20.4 cm^{-1} (Σ_o is the absorption cross section for 0.025 eV) is indicated. From these curves the value of Σ_o to give best agreement was estimated to be:

$$\Sigma_o = 18.7 \pm 0.6 \text{ cm}^{-1} \quad .$$

This is to be compared with the manufacturer's value of 18.5 cm^{-1}. The error of 0.6 cm^{-1} is equivalent to an error in a deduced spectrum of about 1.5 per cent. at the highest energies quoted in this report, and much less elsewhere. This error is much less than the statistical errors (see Section 6.8).

The data used to give Figure 10 also extended down to about 0.03eV and excellent agreement between the Li-glass and BF_3 counters was found throughout the range.

6.7 Air Source Correction

As well as receiving neutrons from the centre of the assembly the chopper also received neutrons scattered from the air in the probe hole leading through the reactor to the centre of the assembly. This effect was quite important at thermal energy for the assemblies with the higher fuel concentrations. The spectra of these assemblies were quite hard, and, in fact, the thermal flux level along the probe hole (apart from the last few inches at the outside of the reactor) was at its lowest level at the centre of these assemblies. The harder spectra were thus liable to be contaminated by thermal neutrons.

If the flux at the centre of the assembly is ϕ_S, then the effective source strength per unit area at the chopper source plane is:

$$S = \phi_S / 4 \ ,$$

(this is the flux directed into one hemisphere).

If the flux at a point in the probe hole is ϕ, then the source strength per unit area arising from air scatter in a length $\delta\ell$ and directed into the hemisphere towards the chopper is:

$$\delta S_A = \frac{\phi \Sigma \delta \ell}{2} \ ,$$

where Σ is the macroscopic scattering cross section of air.

The total air source is thus:

$$S_A = \frac{1}{2} \Sigma \int \phi \, d\ell \ .$$

Reference to Equation 4.3 of Section 4 of Tattersall (1966) which relates source flux and channel counts shows that this relation is independent of the distance between the source and rotor, so that the total source strength seen by the chopper is:

$$S_T = S + S_A \ ,$$

Note: There is a variation in A_S, the area of source viewed, but this is small along the length of the probe hole (see Equation 3.1 of Tattersall 1966).

Thus the chopper results must be multiplied by a factor:

$$F = \frac{S}{S_A + S} = \frac{\phi/4}{\phi/4 + \frac{1}{2} \Sigma \int \phi \, d\ell} \ ,$$

at each energy, to correct for the air source.

To find this ratio, a calculation of the flux distribution in the reactor was made using the diffusion code CRAM (Section 7 gives further details of the geometric model and energy group structure used). The resulting correction factors are shown in Figures 11 to 20 (curves labelled "Air Source") from which it will be seen that the correction is significant only for lethargies above 18 (energies less than 0.2 eV). In the worst case (U235/BeO ratio of 1/740 in Figure 15) the maximum correction to an experimental point is 1.09 at a lethargy of 19.5 (energy 0.03eV). Although the flux distributions are of limited accuracy the discussion in Section 8 indicates that the error in the correction should not exceed 3 per cent. Since this is the maximum error, and it would fall for smaller lethargies, it is concluded that error in this correction will not add significantly to the statistical errors (Section 6.8).

6.8 Resolution and Statistical Accuracy

No correction was necessary to the measured spectra for the finite resolution of the chopper.

The typical count distributions illustrated in Figure 9 show that the statistical accuracy varies considerably from channel to channel. It was decided to keep this steady at about 5 per

cent. by grouping channels together where necessary. This worsened the resolution but it was felt that this procedure would give a reasonable balance between statistical accuracy and resolution. This procedure was applied to all the results taken using the Li-glass counter, but the much lower count rate given by the BF_3 counters meant that a statistical accuracy of 15 per cent. had to be adopted as the standard value in these cases.

The resolution of the chopper (quoted as energy and lethargy error in the tabulation of the results) was based on the variance of the flight time calculated as described in Section 6 of Tattersall (1966). The major contribution to the flight time variance was from the neutron burst width when single channel results were quoted. The channel width was the main contribution when more than four channels were grouped together.

6.9 Miscellaneous Experimental Checks

As noted in Section 6.7, the arrangement of the chopper and the hard spectra measured make significant thermal neutron contamination of the spectrum a possibility. To check further on this a run was made with the inner graphite collimator (see Figures 3 and 5) replaced by a 4 inches square section cadmium tube with a 1 inch square aperture at one end. The purpose of this was to screen the neutron beam from thermal neutrons as much as possible. Since the presence of the cadmium led to no significant reduction in the thermal flux, it was concluded that thermal contamination of the spectra was certainly less than the statistical errors in the measurements.

Quite a variety of collimation systems, and chopper rotors made of two different materials, were used during the measurements. The variations were mainly attempts to reduce the fairly high gamma ray and neutron backgrounds. To check that these changes had no effect on the spectra, the measurement on the assembly with a U235/BeO ratio of 1/740 was repeated. The original measurement (see Table 2) used the steel and graphite collimators etc., and the stainless steel rotor. The repeat measurement used additional flight tubes and the Monel rotor; these were in fact the arrangements used with the U233 assemblies. No significant difference was found between the spectra measured in the two cases.

6.10 Experimental Spectra

In obtaining both the experimental and theoretical spectra the aim was to find the spectrum at the centre of an assembly, when it was in place in the reactor, to permit direct comparison between these results and other related measurements made on the assemblies. Accordingly the experimental results were corrected for the air source contribution (Section 6.7) before being listed in Tables 5 to 14 and plotted in Figures 21 to 30. These Figures also include the calculated spectra (Section 7) and the comparison between these and the experimental results is discussed in Section 8.

Each set of experimental results, except those for the three most dilute U235 assemblies, includes data at two rotor speeds. For each assembly, the runs at both rotor speeds and the calculated spectrum are normalized to one another over a lethargy range of about 14 to 16.

7. CALCULATED SPECTRA

The codes used in the calculations of the spectra in the assemblies were GYMEA (Pollard and Robinson 1966), DSN (Carlson et al. 1960) and CRAM (Hassitt 1962). The purpose for which each code was used was as follows:

GYMEA and its data libraries NDXD and NDSC, were used to prepare group cross section data for the other codes. A crystal scattering model was used for BeO at energies less than 15 eV.

DSN was used to make 18 group transport theory calculations on one dimensional slab representations of the assemblies.

CRAM was used to make 13 group diffusion theory calculations on a two dimensional representation of the reactor MOATA for assessing the effect of environment on the spectra in the assemblies.

Tables 3 and 4 show the energy group structures used in the DSN and CRAM calculations. The 18 groups used for the DSN calculations were chosen to give reasonable detail in the spectrum calculations near thermal energies and also over the lethargy range 15 to 15.7 (energies near 2 eV) since in this latter range the 1.5 eV and 1.8 eV resonances in U233 cause a marked step in the spectrum, particularly at the higher concentrations of U233. For the CRAM calculation the number of groups had to be reduced to 13 because of excessive computation time. This was done mainly by omitting the fine structure in the 15 to 15.7 lethargy range.

The chopper measurements were made on a moderator position in a slab type lattice (see Section 2), forming a 12 inch cube at the centre of a reactor. Since this geometry is too complicated to make an exact calculation of the system, it was assumed initially that the spectrum near the centre of the assembly would be unaffected by the reactor environment. Accordingly, using group cross section data prepared by GYMEA, an 18 group transport calculation (DSN) was carried out on a slab reactor with infinite lateral dimensions and with a height chosen to make the system critical. For each assembly the first two lattice cells, that is, the first two layers of fuel working out from the centre, were represented exactly. Outside this, an homogeneous mixture of the mean assembly composition was assumed (see Figure 31 for a typical case). The thickness of the homogeneous layer was adjusted for criticality.

These calculations yielded an 18 group energy spectrum. The chopper measurements were much more detailed than this group structure so some method of interpolating between the group energies was needed. The spectrum in a bare critical homogeneous system could be calculated in 120 groups using GYMEA, and as this was a first approximation to the above 18 group spectrum it was useful for interpolation. In practice it was more convenient to regard the GYMEA spectrum as a first approximation and to use the 18 group calculation to correct it to a moderator position. The correction factors needed were found by condensing the 120 group GYMEA spectrum to 18 groups and finding the ratios of these fluxes to the 18 group DSN fluxes.

A small complication arose because the spectrum and the sensitivity of the chopper vary across the source (see Appendix I of Tattersall 1966). The calculated sensitivity or source weighting factor for the chopper is shown in Figure 32 as a function of height above the centre of the source (the spectrum is constant in the horizontal direction parallel to the fuel plates). Using this curve and the DSN spectra, the spectrum correction factors averaged over the source area were found.

In practice the spectrum variation was small, being most marked at lower energies in the harder spectra. For a U235/BeO ratio of 1/740, the ratio of the flux at the centre of the source to the mean flux over the source differed from unity only for lethargies above 17.5, being about 1.01 at lethargy 18.8 (energy 0.07 eV) and rising to 1.03 at lethargy 21.8 (energy 0.003 eV).

The calculated spectrum correction factors normalized to unity at a lethargy of 14 are shown in Figures 11 to 20 (curves labelled GYMEA to Moderator).

In the curves for the U233 assemblies it is interesting to note the peak at about a lethargy of 15.5. The effect of this was to flatten the step in the spectrum produced by the 1.5 eV and 1.8 eV resonances in U233.

The above procedure gave a spectrum characteristic of a critical system with the composition of the assembly concerned. To determine the effect of the reactor environment on the spectrum in an experimental assembly, calculations were made on the reactor as a whole. Figure 33 is a reasonable two dimensional cylindrical model of MOATA. The axis of this model was horizontal, being the line joining the centres of the core tanks.

Distances along this axis were the same as in MOATA itself, but the aluminium forming the walls of core tanks and the box containing the assemblies was not represented. It was necessary, therefore, to reduce the density of the graphite surrounding the core tank to give the correct total amount between the tanks and the assembly. It was assumed that the reflector in the annular region outside the core tanks was H_2O. In the calculations the radii of the core tanks and hence the fuel loading were adjusted for criticality.

Calculations on this system were made in 13 groups using the diffusion theory code CRAM, and group cross section data provided by GYMEA. The CRAM spectra were compared to the 13 group GYMEA spectra exactly as was done for the DSN calculations. In this case no averaging over the source was necessary, because spectrum variations over the source volume were not significant (less than about 3 per cent.). The source volume concerned was roughly a hemisphere with a radius of about one mean free path ($\sim$ 2 cm) centred on the base of the probe hole into the experimental assembly. The flux was nearly constant with respect to position over this volume so the assumption of a source strength of $\phi/4$ made in the derivation of channel counts (see Section 3 of Tattersall 1966) was justified.

The calculated correction factors normalized to unity at a lethargy of 14 are shown in Figures 11 to 20 (curves labelled 'Environment'). To correct the GYMEA spectrum to both a moderator position and for environment effects, the product of two appropriate factors given in these Figures was used.

The resulting calculated spectra are shown in Figures 21 to 30.

8. DISCUSSION OF THE RESULTS

8.1 General Comments

In considering the results plotted in Figures 21 to 30 it should be noted that experiment and theory have been normalized to each other over a lethargy range from about 14 to 16. Any discrepancies discussed below are therefore relative to this normalization.

The main feature common to all results is the discrepancy between the experimental and calculated fluxes in the thermal region (lethargies above 18). For the three most dilute U235 lattices the differences between experiment and theory are not really significant because of the high statistical errors in these cases which arose from the use of the low efficiency BF_3 counters (Section 4). However a trend is still apparent in that the theoretical flux near the thermal peak is higher than the experimental one for the most dilute assembly but falls below it as the fuel concentration rises.

In the epithermal region, as the lethargy falls below about 13, the experimental fluxes rise more steeply than the calculated fluxes for all assemblies, though the differences are barely significant where the fuel is U233 (this comment excludes the three most dilute U235 assemblies for which experimental data at these lethargies was not available).

The trend of the thermal flux discrepancies is illustrated in Table 15 which gives the ratios of the experimental to theoretical fluxes at the thermal peaks. The errors quoted are a rough guide only as it is rather difficult to estimate the height of the experimental peaks from the limited data available.

8.2 U235/BeO Assemblies

Considering the results for the five U235 assemblies it is noted that the reversal in trend of the ratios in Table 15 between U235/BeO ratios of 1/1120 and 1/740 probably arises, at least in part, from errors in the 'GYMEA to Moderator' correction factors for all but the most concentrated assembly. In all cases except the assembly with a U235/BeO ratio of 1/740, the fuel foils did not form a complete layer across the base (Section 2). This would tend to give more moderator between the fuel and the chopper source than in the DSN calculations which assumed a uniform fuel layer. The correction factors resulting from the DSN calculation are quite sensitive to moderator, and this is illustrated by comparing the 'GYMEA to Moderator' correction factors near the thermal flux peak for a 2 inch moderator layer (for example Figure 16 where the correction is 1.15 at a lethargy of 18.5) with those for a 1 inch layer at comparable fuel concentrations (for example Figures 13 and 14 where the corrections are 1.01 and 1.03).

The above source of error would increase the correction factors for the four assemblies with U235/BeO ratios in the range 1/6545 to 1/1120, possibly by up to about 10 per cent. for the 1/1120, and by smaller amounts in the other cases as the magnitude of the correction falls.

A further source of error in the 'GYMEA to Moderator' correction can arise from the finite width of the energy groups used in the calculation. However, comparison of 12 and 18 group DSN calculations for the assembly with a U235/BeO ratio of 1/740 indicated that for lethargies less than 20 this source of error should not exceed 1 per cent.

There are indications that error arising from the finite group width may be rather more important in the CRAM calculations for the environment effect. For the assembly with U235/BeO ratio of 1/740 calculations have been made in 13 and 18 groups and the latter gave an environment correction about 2 per cent. lower than the former at a lethargy of 10, and one about 4 per cent. higher at a lethargy of 18.5. The geometries of the two calculations were not quite the same and this may have accounted for some of the differences, but the discussion in the following paragraphs indicates that geometric effects are small.

To check on the effect of the geometry assumed for the CRAM runs, further calculations were made using rectangular geometry for a U235/BeO ratio of 1/740. In these calculations a horizontal section through MOATA was represented in XY geometry and the finite height of the reactor was represented by a buckling which was adjusted for criticality. Two different graphite densities were assumed, with the physical distance between the assembly and core tanks adjusted in each case to give the correct amount of graphite in this region (compare with discussion of CRAM model in Section 7). This model gave the same environment corrections as obtained previously to within 1 per cent.

The above model was also used to check the air source correction. The flux distribution needed for this calculation was that along a radius of the cylindrical model. This is of limited accuracy when used to represent the actual rectangular geometry of MOATA so the flux distributions calculated with the above model were also used to find the air source correction. Comparison of the results from the two models indicated that error in the air source correction arising from inadequacies in the flux calculation were less than 3 per cent.

Some error will also be associated with the assumption that the 'GYMEA to Moderator' and environment correction can simply be multiplied together to obtain the total correction. No quantitative data are available on this but it should be a reasonable approximation.

For the assembly with a U235/BeO ratio of 1/740 the following conclusions can be drawn.

(i) There is a discrepancy of about 10 per cent. in the height of the calculated and experimental thermal flux peaks. About half of this is probably caused by an error in the environment correction arising from too wide an energy group structure in the CRAM calculations. The remainder could well arise from a variety of smaller contributions from sources such as thermal neutron leakage into the beam, error in the fuel ratio in the assembly and errors in the data in the GYMEA libraries for U235 or BeO. The first of these was discussed in Section 6.9 and experimental checks indicated that it should contribute less than about 4 per cent. to the thermal flux. Composition errors probably contribute about 2 per cent.

(ii) In the epithermal region below a lethargy of 13 the experimental flux changes more rapidly with lethargy than calculated. There is no indication of the reason for this discrepancy in any of the calculations so an error in the GYMEA data library is indicated.

For the remaining U235/BeO assemblies there is an additional error in the calculation of the 'GYMEA to Moderator' correction which arises from the inadequate geometric representation in the DSN calculation. Because of this the discrepancy between experimental and calculated thermal flux for the assembly with a U235/BeO ratio of 1/1120 is similar in magnitude to that for a ratio of 1/740 and the conclusions drawn above apply to this case also. The error sources already discussed, coupled with the higher statistical errors, lead to the conclusion that no discrepancies exist for the other U235/BeO assemblies.

8.3 U235/Th/BeO Assemblies

The relations between experimental and theoretical results for the U235/Th/BeO assemblies are very similar to those for the assembly with a U235/BeO ratio of 1/740, and similar conclusions can be drawn for both the thermal and epithermal regions.

8.4 U233/Th/BeO Assemblies

The situation for the U233 assemblies is different from that for U235 in that the discrepancies in the thermal region of the spectrum are much larger. The environment correction is also much larger because it refers to the spectrum in a bare critical assembly. For U233, such an assembly is smaller than for U235 with the same atomic ratio, so that there is a larger change in leakage between the bare critical and the MOATA situations. However, even allowing extra errors for this, there will still be discrepancies of at least 15 per cent. at the peak of the thermal spectrum. In view of the much closer agreement between theory and experiment for the U235 assemblies, and the similar experimental conditions used in all runs, these results indicate errors in the GYMEA data library for U233 at thermal energies. At epithermal energies however, the discrepancy noted for the U235 assemblies is barely significant for U233.

8.5 GYMEA Data Libraries

The above discussion has indicated possible errors in the GYMEA data libraries but it is not immediately apparent which data are involved. The worst discrepancies are for the thermal flux in the U233 assemblies but although errors of about 3 per cent. are known to be present in the GYMEA cross section data used for U233, these would certainly not account for the size of the observed differences.

Another possible source of error is in the transport cross section for BeO which could affect the leakage calculation. Pulsed source measurements of diffusion length by A.I.M. Ritchie (unpublished) have indicated that the cross section in GYMEA is much too high for energies below about 0.04 eV. This is below the energy range of the present measurements, but if the error persisted to higher energies it could be of some consequence. However it seems most unlikely that this could account for the different trends in the U233 and U235 experiments. Further calculations will be required to locate the origin of the discrepancies observed.

9. ACKNOWLEDGEMENTS

The author wishes to acknowledge the assistance given by other members of the Chopper Group, in particular F.A. Rocke and Mrs. L. Wall, in the initial setting up of the experimental equipment and other general assistance in the initial stages of this work. He also wishes to acknowledge the work carried out by staff of the Fuel Element Development Section at Lucas Heights, who prepared the fuel and BeO moderator bricks.

10. REFERENCES

Carlson, B., Lee, C., and Worlton, J. (1960). – The DSN and TDC neutron transport codes, LAMS 2346. The DSN code LAMS 2346, Appendix 1.

Hassitt, A. (1962). – A computer programme to solve the multigroup diffusion equations. TRG Report 229(R).

Hughes, D.J. and Schwartz, R.B. (1958). – Neutron Cross-Sections. BNL 325, Second Edition and Supplement.

Marks, A.P. (1962). – MOATA Reactor. Atomic Energy in Australia, Vol. 5, No. 4, Page 9, published by the Australian Atomic Energy Commission.

Pollard, J.P. and Robinson, G.S. (1966). – GYMEA – A nuclide depletion, space independent multigroup neutron diffusion, data preparation code. AAEC/E147.

Tattersall, R.B. (1966). – Methods used to analyse experimental data obtained with the MOATA time of flight analyser. AAEC/E169.

TABLE 1

COMPOSITIONS OF ASSEMBLIES

Nominal Composition				Composition (Atoms/cm³ x 10^{-24})									
U233	U235	Th	BeO	U233	U234	U235	U236	U238	Th	BeO	Al	O in ThO_2	O in UO_2
	1		6545		1.228×10^{-7}	1.051×10^{-5}	3.524×10^{-7}	7.248×10^{-7}		6.872×10^{-2}			
	1		4360		1.732×10^{-7}	1.482×10^{-5}	4.970×10^{-7}	1.022×10^{-6}		6.461×10^{-2}	3.540×10^{-3}		
	1		2185		3.456×10^{-7}	2.957×10^{-5}	9.916×10^{-7}	2.039×10^{-6}		6.461×10^{-2}	3.535×10^{-3}		
	1		1120		6.728×10^{-7}	5.757×10^{-5}	1.931×10^{-6}	3.970×10^{-6}		6.456×10^{-2}	3.535×10^{-3}		
	1		740		1.024×10^{-6}	8.759×10^{-5}	2.937×10^{-6}	6.040×10^{-6}		6.458×10^{-2}	3.529×10^{-3}		
	1	3.6	1500		5.281×10^{-7}	4.519×10^{-5}	1.515×10^{-6}	3.116×10^{-6}	1.638×10^{-4}	6.741×10^{-2}	1.823×10^{-3}	3.273×10^{-4}	
	1	1.8	750		1.023×10^{-6}	8.755×10^{-5}	2.936×10^{-6}	6.038×10^{-6}	1.586×10^{-4}	6.529×10^{-2}	3.532×10^{-3}	3.171×10^{-4}	
1		6.8	2800	2.421×10^{-5}	5.907×10^{-7}	5.483×10^{-8}	6.480×10^{-8}		1.644×10^{-4}	6.766×10^{-2}	9.545×10^{-4}	3.286×10^{-4}	4.991×10^{-5}
1		3.4	1400	4.707×10^{-5}	1.148×10^{-6}	1.066×10^{-7}	1.260×10^{-7}		1.598×10^{-4}	6.578×10^{-2}	1.856×10^{-3}	3.195×10^{-4}	9.704×10^{-5}
1		1.7	700	8.918×10^{-5}	2.176×10^{-6}	2.020×10^{-7}	2.387×10^{-7}		1.514×10^{-4}	6.230×10^{-2}	3.516×10^{-3}	3.026×10^{-4}	1.837×10^{-4}

Note: The BeO composition is molecules/cm³ x 10^{-24}

The oxygen associated with ThO_2 and UO_2 is listed in the last two columns

TABLE 2

DATA ON COLLIMATORS USED AND FLIGHT PATH LENGTHS

Nominal Assembly Composition				Collimators in Use						Flight Path Lengths (cm)		
U233	U235	Th	BeO	Inner Graphite	Steel	Boron Wax	Boron Lead	Outer Graphite	Lead With Flight Tube	Rotor Source	Rotor Detector	Length in Air
	1		6545	x				x		137.5	697.2	387.0
	1		4360	x				x		137.5	697.2	387.0
	1		2185	x				x		137.5	697.2	387.0
	1		1120	x	x		x	x		137.5	776.7	390.9
	1		740	x	x	x	x	x		137.5	776.7	390.9
	1	3.6	1500	x	x		x	x		137.5	776.7	390.9
	1	1.8	750	x	x		x	x		137.5	776.7	390.9
1		6.8	2800				x		x	138.5	775.7	143.3
1		3.4	1400				x		x	138.5	775.7	143.3
1		1.7	700				x		x	138.5	775.7	143.3

Collimators in use marked 'x'

TABLE 3

18 GROUP STRUCTURE USED FOR DSN CALCULATIONS

Group	Lethargy at Centre	Group	Lethargy at Centre	Group	Lethargy at Centre
1	2.00	7	15.30	13	18.25
2	6.00	8	15.50	14	18.75
3	9.50	9	15.80	15	19.25
4	12.00	10	16.50	16	19.75
5	14.00	11	17.25	17	20.25
6	15.10	12	17.75	18	21.75

TABLE 4

13 GROUP STRUCTURE USED FOR CRAM CALCULATIONS

Group	Lethargy at Centre	Group	Lethargy at Centre	Group	Lethargy at Centre
1	2.25	5	14.00	9	18.50
2	6.75	6	16.00	10	19.10
3	10.00	7	17.30	11	19.70
4	12.00	8	17.90	12	20.25
				13	21.75

TABLE 5

SPECTRUM FOR ASSEMBLY WITH COMPOSITION U235/BeO = 1/6545

ROTOR SPEED = 1800 r.p.m.

Lethargy	Flux Per Unit Lethargy	Flux Per Unit Energy	Energy (eV)
$14.48^{+0.47}_{-0.41}$	1.91 ± 0.46	0.371 ± 0.090	$5.1^{+2.6}_{-1.9}$
$15.41^{+0.30}_{-0.27}$	2.88 ± 0.52	1.42 ± 0.26	$2.03^{+0.63}_{-0.52}$
$16.03^{+0.21}_{-0.20}$	2.26 ± 0.49	2.08 ± 0.45	$1.09^{+0.24}_{-0.21}$
$16.68^{+0.26}_{-0.22}$	2.34 ± 0.35	4.11 ± 0.62	$0.57^{+0.14}_{-0.13}$
$17.34^{+0.19}_{-0.16}$	2.67 ± 0.37	9.0 ± 1.2	$0.296^{+0.052}_{-0.050}$
$17.83^{+0.14}_{-0.13}$	4.03 ± 0.43	22.2 ± 2.4	$0.181^{+0.025}_{-0.024}$
18.135 ± 0.073	7.53 ± 0.78	56.6 ± 5.8	0.1330 ± 0.0097
18.313 ± 0.066	8.44 ± 0.82	75.8 ± 7.4	0.1114 ± 0.0074
18.475 ± 0.061	11.80 ± 0.95	124 ± 10	0.0947 ± 0.0058
18.626 ± 0.057	13.2 ± 1.0	162 ± 12	0.0814 ± 0.0046
18.766 ± 0.053	13.1 ± 1.0	185 ± 14	0.0708 ± 0.0037
18.897 ± 0.050	14.4 ± 1.1	233 ± 17	0.0621 ± 0.0031
19.020 ± 0.047	15.7 ± 1.1	286 ± 20	0.0549 ± 0.0026
19.135 ± 0.044	14.0 ± 1.1	286 ± 22	0.0489 ± 0.0022
19.245 ± 0.042	13.3 ± 1.0	300 ± 24	0.0439 ± 0.0018
19.348 ± 0.040	11.22 ± 0.97	284 ± 25	0.0396 ± 0.0016
19.447 ± 0.038	11.30 ± 0.98	316 ± 28	0.0358 ± 0.0014
19.541 ± 0.036	11.72 ± 0.99	359 ± 31	0.0326 ± 0.0012
19.631 ± 0.035	8.60 ± 0.89	289 ± 30	0.0298 ± 0.0010
19.716 ± 0.033	7.75 ± 0.86	283 ± 31	0.02737 ± 0.00090
19.837 ± 0.050	7.30 ± 0.60	301 ± 25	0.0243 ± 0.0012
19.990 ± 0.046	6.27 ± 0.58	301 ± 25	0.02082 ± 0.00097
20.195 ± 0.078	4.83 ± 0.38	285 ± 23	0.0170 ± 0.0013
20.444 ± 0.069	3.25 ± 0.36	246 ± 27	0.01322 ± 0.00091
20.665 ± 0.062	2.20 ± 0.35	207 ± 33	0.01060 ± 0.00066
20.95 ± 0.10	1.61 ± 0.27	202 ± 35	0.00796 ± 0.00083

TABLE 6

SPECTRUM FOR ASSEMBLY WITH COMPOSITION U235/BeO = 1/4360

ROTOR SPEED = 1800 r.p.m.

Lethargy	Flux Per Unit Lethargy	Flux Per Unit Energy	Energy (eV)
$14.22^{+0.54}_{-0.46}$	1.98 ± 0.46	0.296 ± 0.069	$6.7^{+3.9}_{-2.8}$
$15.25^{+0.32}_{-0.29}$	1.94 ± 0.46	0.82 ± 0.19	$2.38^{+0.80}_{-0.65}$
$15.92^{+0.23}_{-0.21}$	2.21 ± 0.48	1.82 ± 0.39	$1.22^{+0.29}_{-0.25}$
$16.60^{+0.27}_{-0.23}$	2.62 ± 0.36	4.22 ± 0.59	$0.62^{+0.16}_{-0.15}$
$17.28^{+0.19}_{-0.17}$	2.40 ± 0.35	7.6 ± 1.1	$0.314^{+0.057}_{-0.055}$
$17.78^{+0.15}_{-0.13}$	3.35 ± 0.40	17.7 ± 2.1	$0.189^{+0.027}_{-0.026}$
18.097 ± 0.074	5.99 ± 0.70	43.3 ± 5.1	0.138 ± 0.010
18.277 ± 0.068	7.24 ± 0.77	62.7 ± 6.6	0.1154 ± 0.0078
18.443 ± 0.062	8.06 ± 0.80	82.5 ± 8.2	0.0978 ± 0.0061
18.596 ± 0.058	9.25 ± 0.85	111 ± 10	0.0839 ± 0.0049
18.738 ± 0.054	9.92 ± 0.89	136 ± 12	0.0728 ± 0.0039
18.871 ± 0.050	10.80 ± 0.93	170 ± 15	0.0638 ± 0.0032
18.995 ± 0.047	7.82 ± 0.81	137 ± 15	0.0563 ± 0.0027
19.112 ± 0.045	11.11 ± 0.94	221 ± 19	0.0501 ± 0.0022
19.223 ± 0.042	9.50 ± 0.89	211 ± 20	0.0448 ± 0.0019
19.328 ± 0.040	9.59 ± 0.90	238 ± 23	0.0404 ± 0.0016
19.473 ± 0.060	8.25 ± 0.61	236 ± 17	0.0349 ± 0.0021
19.655 ± 0.055	5.62 ± 0.53	193 ± 18	0.0291 ± 0.0016
19.821 ± 0.051	5.03 ± 0.52	204 ± 20	0.0247 ± 0.0012
19.975 ± 0.047	3.33 ± 0.46	158 ± 21	0.02114±0.00099
20.182 ± 0.080	2.84 ± 0.32	165 ± 18	0.0172 ± 0.0013
20.54 ± 0.13	1.26 ± 0.20	104 ± 17	0.0121 ± 0.0015

TABLE 7

SPECTRUM FOR ASSEMBLY WITH COMPOSITION U235/BeO = 1/2185

ROTOR SPEED = 1800 r.p.m.

Lethargy	Flux Per Unit Lethargy	Flux Per Unit Energy	Energy (eV)
$14.54^{+0.46}_{-0.40}$	3.56 ± 0.57	0.74 ± 0.11	$4.8^{+2.4}_{-1.8}$
$15.45^{+0.29}_{-0.27}$	3.81 ± 0.59	1.95 ± 0.30	$1.96^{+0.60}_{-0.49}$
$16.06^{+0.21}_{-0.20}$	3.65 ± 0.58	3.44 ± 0.55	$1.06^{+0.23}_{-0.20}$
$16.70^{+0.26}_{-0.22}$	2.96 ± 0.39	5.29 ± 0.69	$0.56^{+0.14}_{-0.13}$
$17.35^{+0.18}_{-0.16}$	3.04 ± 0.39	10.4 ± 1.3	$0.292^{+0.051}_{-0.049}$
$17.83^{+0.14}_{-0.13}$	5.09 ± 0.47	28.4 ± 2.6	$0.179^{+0.025}_{-0.024}$
18.144 ± 0.072	8.86 ± 0.83	67.2 ± 6.3	0.1318 ± 0.0097
18.321 ± 0.066	10.12 ± 0.88	91.5 ± 8.0	0.1105 ± 0.0074
18.483 ± 0.061	11.58 ± 0.93	123 ± 10	0.0940 ± 0.0058
18.633 ± 0.057	10.91 ± 0.92	135 ± 12	0.0809 ± 0.0046
18.773 ± 0.053	12.15 ± 0.97	172 ± 14	0.0703 ± 0.0037
18.903 ± 0.049	10.16 ± 0.90	164 ± 15	0.0617 ± 0.0031
19.026 ± 0.047	11.10 ± 0.94	203 ± 18	0.0546 ± 0.0025
19.141 ± 0.044	11.23 ± 0.95	231 ± 19	0.0487 ± 0.0021
19.250 ± 0.042	8.71 ± 0.85	199 ± 19	0.0436 ± 0.0018
19.353 ± 0.040	9.55 ± 0.90	243 ± 23	0.0394 ± 0.0016
19.452 ± 0.038	10.05 ± 0.93	282 ± 26	0.0357 ± 0.0013
19.545 ± 0.036	7.54 ± 0.83	232 ± 25	0.0325 ± 0.0011
19.677 ± 0.055	7.07 ± 0.58	248 ± 20	0.0285 ± 0.0015
19.841 ± 0.050	4.94 ± 0.52	205 ± 21	0.0242 ± 0.0012
19.993 ± 0.047	3.67 ± 0.48	177 ± 23	0.02075 ± 0.00096
20.199 ± 0.080	3.27 ± 0.34	194 ± 20	0.0169 ± 0.0013
20.55 ± 0.13	1.75 ± 0.23	147 ± 19	0.0119 ± 0.0015
20.95 ± 0.11	0.93 ± 0.26	117 ± 33	0.00795 ± 0.00083

TABLE 8 A

SPECTRUM FOR ASSEMBLY WITH COMPOSITION U235/BeO = 1/1120

ROTOR SPEED = 7200 r.p.m.

Lethargy	Flux Per Unit Lethargy	Flux Per Unit Energy	Energy (eV)
$11.16^{+0.34}_{-0.41}$	5.40 ± 0.21	0.0378 ± 0.0015	143^{+73}_{-41}
$11.47^{+0.30}_{-0.35}$	4.73 ± 0.21	0.0453 ± 0.0020	104^{+43}_{-27}
$11.74^{+0.26}_{-0.30}$	5.12 ± 0.22	0.0645 ± 0.0028	79^{+28}_{-18}
$11.98^{+0.23}_{-0.26}$	5.45 ± 0.23	0.0871 ± 0.0037	63^{+19}_{-13}
$12.20^{+0.21}_{-0.23}$	5.01 ± 0.23	0.0992 ± 0.0045	51^{+13}_{-10}
$12.39^{+0.19}_{-0.21}$	5.11 ± 0.24	0.1227 ± 0.0057	$41.7^{+9.8}_{-7.3}$
$12.56^{+0.18}_{-0.19}$	4.63 ± 0.23	0.1325 ± 0.0067	$34.9^{+7.4}_{-5.6}$
$12.73^{+0.16}_{-0.18}$	5.17 ± 0.25	0.1740 ± 0.0084	$29.7^{+5.8}_{-4.5}$
$12.88^{+0.15}_{-0.16}$	4.95 ± 0.25	0.1933 ± 0.0098	$25.6^{+4.6}_{-3.6}$
13.08 ± 0.16	4.39 ± 0.18	0.2097 ± 0.0084	20.9 ± 3.3
13.32 ± 0.14	4.65 ± 0.19	0.284 ± 0.011	16.4 ± 2.3
13.54 ± 0.12	4.76 ± 0.20	0.362 ± 0.015	13.2 ± 1.6
13.74 ± 0.11	4.03 ± 0.19	0.372 ± 0.018	10.8 ± 1.2
13.92 ± 0.10	4.42 ± 0.21	0.490 ± 0.023	9.03 ± 0.93
14.082 ± 0.094	4.25 ± 0.22	0.554 ± 0.028	7.66 ± 0.73
14.234 ± 0.088	4.18 ± 0.22	0.635 ± 0.034	6.58 ± 0.58
14.44 ± 0.10	3.96 ± 0.16	0.737 ± 0.031	5.36 ± 0.56
14.687 ± 0.091	4.01 ± 0.18	0.958 ± 0.042	4.18 ± 0.38
14.908 ± 0.081	3.87 ± 0.19	1.153 ± 0.056	3.36 ± 0.27
15.107 ± 0.073	3.63 ± 0.20	1.319 ± 0.072	2.75 ± 0.20
15.287 ± 0.067	3.97 ± 0.22	1.728 ± 0.094	2.30 ± 0.16
15.527 ± 0.097	4.13 ± 0.17	2.288 ± 0.094	1.81 ± 0.17
15.812 ± 0.084	3.96 ± 0.19	2.92 ± 0.14	1.36 ± 0.11
16.062 ± 0.074	3.77 ± 0.20	3.57 ± 0.19	1.057 ± 0.078
16.284 ± 0.066	4.29 ± 0.23	5.07 ± 0.27	0.847 ± 0.056
16.57 ± 0.11	4.05 ± 0.19	6.37 ± 0.29	0.636 ± 0.068
16.906 ± 0.091	4.11 ± 0.22	9.03 ± 0.48	0.454 ± 0.041

TABLE 8B

SPECTRUM FOR ASSEMBLY WITH COMPOSITION U235/BeO = 1/1120

ROTOR SPEED 1800 r.p.m.

Lethargy	Flux Per Unit Lethargy	Flux Per Unit Energy	Energy (eV)
$13.22^{+0.46}_{-0.60}$	4.32 ± 0.11	0.2386 ± 0.0061	18^{+15}_{-7}
$13.66^{+0.38}_{-0.47}$	4.26 ± 0.12	0.364 ± 0.010	$11.7^{+7.0}_{-3.7}$
$14.01^{+0.32}_{-0.39}$	4.32 ± 0.13	0.526 ± 0.016	$8.2^{+3.9}_{-2.3}$
$14.32^{+0.28}_{-0.33}$	4.09 ± 0.14	0.675 ± 0.022	$6.1^{+2.3}_{-1.5}$
$14.58^{+0.25}_{-0.28}$	4.13 ± 0.14	0.886 ± 0.031	$4.7^{+1.5}_{-1.0}$
$14.81^{+0.22}_{-0.25}$	4.12 ± 0.15	1.114 ± 0.041	$3.7^{+1.0}_{-0.7}$
$15.02^{+0.20}_{-0.22}$	3.83 ± 0.16	1.276 ± 0.052	$3.00^{+0.75}_{-0.55}$
$15.21^{+0.18}_{-0.20}$	3.77 ± 0.16	1.517 ± 0.065	$2.49^{+0.56}_{-0.42}$
$15.38^{+0.17}_{-0.19}$	3.45 ± 0.16	1.647 ± 0.078	$2.09^{+0.43}_{-0.33}$
$15.54^{+0.16}_{-0.17}$	4.06 ± 0.18	2.27 ± 0.10	$1.79^{+0.33}_{-0.26}$
$15.68^{+0.15}_{-0.16}$	3.76 ± 0.19	2.44 ± 0.12	$1.54^{+0.26}_{-0.21}$
$15.82^{+0.14}_{-0.15}$	4.02 ± 0.20	2.99 ± 0.15	$1.35^{+0.21}_{-0.17}$
$15.94^{+0.13}_{-0.14}$	4.04 ± 0.21	3.41 ± 0.17	$1.18^{+0.17}_{-0.14}$
16.12 ± 0.14	3.50 ± 0.15	3.52 ± 0.15	0.99 ± 0.13
16.34 ± 0.12	3.95 ± 0.16	4.92 ± 0.20	0.802 ± 0.096
16.53 ± 0.11	4.03 ± 0.17	6.10 ± 0.26	0.660 ± 0.072
16.71 ± 0.10	4.07 ± 0.19	7.37 ± 0.34	0.553 ± 0.056
16.874 ± 0.092	3.76 ± 0.19	8.01 ± 0.40	0.470 ± 0.044
17.024 ± 0.085	4.03 ± 0.20	9.98 ± 0.51	0.404 ± 0.035
17.23 ± 0.10	3.82 ± 0.15	11.58 ± 0.46	0.330 ± 0.033
17.474 ± 0.090	4.40 ± 0.17	17.09 ± 0.67	0.258 ± 0.023
17.693 ± 0.080	5.00 ± 0.20	24.17 ± 0.94	0.207 ± 0.017
17.891 ± 0.072	5.26 ± 0.21	30.9 ± 1.3	0.170 ± 0.012
18.071 ± 0.066	6.27 ± 0.24	44.2 ± 1.7	0.1419 ± 0.0094
18.236 ± 0.061	7.18 ± 0.27	59.6 ± 2.3	0.1203 ± 0.0073
18.388 ± 0.057	8.22 ± 0.29	79.6 ± 2.8	0.1033 ± 0.0058
18.529 ± 0.052	8.50 ± 0.31	94.8 ± 3.5	0.0897 ± 0.0047
18.662 ± 0.049	8.99 ± 0.33	114.5 ± 4.3	0.0786 ± 0.0039
18.786 ± 0.046	9.09 ± 0.35	130.9 ± 5.0	0.0694 ± 0.0032
18.902 ± 0.044	8.37 ± 0.36	135.4 ± 5.8	0.0618 ± 0.0027
19.013 ± 0.042	7.34 ± 0.35	132.6 ± 6.4	0.0553 ± 0.0023
19.117 ± 0.039	6.78 ± 0.36	136.0 ± 7.3	0.0498 ± 0.0020
19.263 ± 0.059	6.74 ± 0.28	156.2 ± 6.3	0.0431 ± 0.0026
19.444 ± 0.054	5.35 ± 0.27	148.7 ± 7.7	0.0360 ± 0.0020
19.683 ± 0.091	4.30 ± 0.21	151.8 ± 7.4	0.0283 ± 0.0026

TABLE 9 A

SPECTRUM FOR ASSEMBLY WITH COMPOSITION U235/BeO = 1/740

ROTOR SPEED = 7200 r.p.m.

Lethargy	Flux Per Unit Lethargy	Flux Per Unit Energy	Energy (eV)
$10.42^{+0.48}_{-0.62}$	8.49 ± 0.26	0.02860 ± 0.00087	300^{+260}_{-110}
$10.86^{+0.39}_{-0.48}$	7.95 ± 0.26	0.0415 ± 0.0013	191^{+120}_{-62}
$11.22^{+0.33}_{-0.40}$	7.55 ± 0.26	0.0565 ± 0.0019	134^{+65}_{-38}
$11.53^{+0.29}_{-0.34}$	6.84 ± 0.26	0.0695 ± 0.0026	98^{+39}_{-25}
$11.79^{+0.25}_{-0.29}$	6.82 ± 0.26	0.0902 ± 0.0035	76^{+26}_{-17}
$12.02^{+0.23}_{-0.26}$	6.38 ± 0.26	0.1066 ± 0.0044	60^{+18}_{-12}
$12.24^{+0.21}_{-0.23}$	6.28 ± 0.27	0.1293 ± 0.0055	49^{+13}_{-9}
$12.43^{+0.19}_{-0.21}$	6.42 ± 0.28	0.1599 ± 0.0069	$40.2^{+9.3}_{-6.9}$
$12.60^{+0.17}_{-0.19}$	6.58 ± 0.29	0.1946 ± 0.0085	$33.8^{+7.1}_{-5.4}$
$12.76^{+0.16}_{-0.17}$	5.78 ± 0.28	0.2007 ± 0.0097	$28.8^{+5.5}_{-4.3}$
$12.90^{+0.15}_{-0.16}$	6.15 ± 0.29	0.247 ± 0.012	$24.9^{+4.4}_{-3.5}$
13.10 ± 0.15	5.80 ± 0.21	0.284 ± 0.010	20.4 ± 3.1
13.35 ± 0.14	5.57 ± 0.22	0.348 ± 0.014	16.0 ± 2.2
13.56 ± 0.12	5.72 ± 0.23	0.443 ± 0.018	12.9 ± 1.6
13.76 ± 0.11	5.64 ± 0.24	0.531 ± 0.022	10.6 ± 1.2
13.93 ± 0.10	5.42 ± 0.24	0.610 ± 0.028	8.88 ± 0.91
14.097 ± 0.094	5.54 ± 0.26	0.734 ± 0.034	7.54 ± 0.71
14.248 ± 0.087	5.01 ± 0.26	0.773 ± 0.040	6.49 ± 0.57
14.45 ± 0.10	4.69 ± 0.19	0.885 ± 0.036	5.29 ± 0.54
14.699 ± 0.091	4.68 ± 0.21	1.133 ± 0.050	4.14 ± 0.37
14.918 ± 0.082	4.86 ± 0.23	1.463 ± 0.068	3.32 ± 0.27
15.116 ± 0.074	4.80 ± 0.24	1.761 ± 0.088	2.72 ± 0.20
15.296 ± 0.067	4.68 ± 0.26	2.06 ± 0.11	2.28 ± 0.15
15.534 ± 0.097	4.84 ± 0.20	2.70 ± 0.11	1.79 ± 0.17
15.819 ± 0.084	4.92 ± 0.23	3.65 ± 0.17	1.35 ± 0.11
16.068 ± 0.074	4.87 ± 0.25	4.63 ± 0.24	1.051 ± 0.078
16.289 ± 0.066	4.91 ± 0.28	5.83 ± 0.33	0.843 ± 0.056
16.58 ± 0.11	4.78 ± 0.23	7.55 ± 0.36	0.633 ± 0.067

TABLE 9B

SPECTRUM FOR ASSEMBLY WITH COMPOSITION U235/BeO = 1/740

ROTOR SPEED = 1800 r.p.m.

Lethargy	Flux Per Unit Lethargy	Flux Per Unit Energy	Energy (eV)
$13.70^{+0.37}_{-0.45}$	5.80 ± 0.19	0.517 ± 0.017	$11.2^{+6.4}_{-3.4}$
$14.05^{+0.31}_{-0.37}$	5.42 ± 0.20	0.686 ± 0.025	$7.9^{+3.6}_{-2.1}$
$14.34^{+0.27}_{-0.32}$	5.01 ± 0.21	0.853 ± 0.035	$5.9^{+2.2}_{-1.4}$
$14.61^{+0.24}_{-0.28}$	5.31 ± 0.23	1.170 ± 0.050	$4.5^{+1.4}_{-1.0}$
$14.84^{+0.22}_{-0.24}$	5.01 ± 0.23	1.388 ± 0.065	$3.61^{+0.99}_{-0.71}$
$15.04^{+0.20}_{-0.22}$	4.90 ± 0.24	1.669 ± 0.084	$2.94^{+0.72}_{-0.53}$
15.31 ± 0.20	4.74 ± 0.19	2.107 ± 0.082	2.25 ± 0.45
15.62 ± 0.17	4.63 ± 0.20	2.82 ± 0.12	1.64 ± 0.28
15.90 ± 0.15	4.39 ± 0.21	3.52 ± 0.17	1.25 ± 0.19
16.14 ± 0.13	4.55 ± 0.24	4.64 ± 0.24	0.98 ± 0.13
16.35 ± 0.12	4.92 ± 0.26	6.22 ± 0.33	0.792 ± 0.094
16.63 ± 0.13	4.87 ± 0.20	8.11 ± 0.33	0.600 ± 0.081
16.96 ± 0.11	4.81 ± 0.22	11.10 ± 0.52	0.433 ± 0.050
17.24 ± 0.10	4.56 ± 0.24	13.93 ± 0.74	0.327 ± 0.033
17.58 ± 0.14	4.87 ± 0.20	21.08 ± 0.87	0.231 ± 0.032
17.98 ± 0.11	5.87 ± 0.25	37.8 ± 1.6	0.155 ± 0.017
18.313 ± 0.096	6.72 ± 0.28	60.4 ± 2.5	0.111 ± 0.011
18.597 ± 0.083	6.97 ± 0.32	83.2 ± 3.8	0.0838 ± 0.0069
18.95 ± 0.13	6.19 ± 0.25	105.0 ± 4.3	0.0589 ± 0.0076
19.35 ± 0.11	3.99 ± 0.29	101.3 ± 7.2	0.0394 ± 0.0042

TABLE 10 A

SPECTRUM FOR ASSEMBLY WITH COMPOSITION U235/Th/BeO = 1/3.6/1500

ROTOR SPEED = 7200 r.p.m.

Lethargy	Flux Per Unit Lethargy	Flux Per Unit Energy	Energy (eV)
$10.63^{+0.43}_{-0.56}$	5.17 ± 0.21	0.02138 ± 0.00085	242^{+180}_{-85}
$11.03^{+0.36}_{-0.44}$	4.80 ± 0.21	0.0296 ± 0.0013	162^{+90}_{-49}
$11.36^{+0.31}_{-0.37}$	4.64 ± 0.21	0.0400 ± 0.0018	116^{+52}_{-31}
$11.65^{+0.27}_{-0.31}$	4.59 ± 0.21	0.0525 ± 0.0024	87^{+32}_{-21}
$11.90^{+0.24}_{-0.27}$	4.29 ± 0.21	0.0630 ± 0.0031	68^{+21}_{-15}
$12.12^{+0.22}_{-0.24}$	4.49 ± 0.22	0.0825 ± 0.0041	54^{+15}_{-11}
$12.32^{+0.20}_{-0.22}$	3.99 ± 0.22	0.0896 ± 0.0049	45^{+11}_{-8}
$12.50^{+0.18}_{-0.20}$	3.96 ± 0.22	0.1064 ± 0.0060	$37.2^{+8.2}_{-6.2}$
12.74 ± 0.19	4.05 ± 0.17	0.1383 ± 0.0056	29.3 ± 5.5
13.03 ± 0.16	3.46 ± 0.16	0.1573 ± 0.0076	22.0 ± 3.6
13.28 ± 0.14	4.11 ± 0.18	0.241 ± 0.011	17.1 ± 2.4
13.50 ± 0.13	3.81 ± 0.19	0.279 ± 0.014	13.7 ± 1.8
13.70 ± 0.11	3.58 ± 0.19	0.320 ± 0.017	11.2 ± 1.3
13.89 ± 0.10	3.26 ± 0.19	0.349 ± 0.021	9.32 ± 0.96
14.13 ± 0.12	3.45 ± 0.15	0.472 ± 0.020	7.32 ± 0.88
14.41 ± 0.10	3.31 ± 0.16	0.602 ± 0.029	5.49 ± 0.57
14.666 ± 0.092	3.24 ± 0.17	0.758 ± 0.040	4.27 ± 0.39
14.889 ± 0.082	3.37 ± 0.19	0.984 ± 0.054	3.42 ± 0.28
15.18 ± 0.12	3.35 ± 0.15	1.307 ± 0.057	2.56 ± 0.29
15.513 ± 0.098	2.70 ± 0.16	1.474 ± 0.086	1.83 ± 0.18
15.800 ± 0.085	3.07 ± 0.18	2.24 ± 0.13	1.37 ± 0.12
16.16 ± 0.13	3.22 ± 0.15	3.35 ± 0.16	0.96 ± 0.13

TABLE 10 B

SPECTRUM FOR ASSEMBLY WITH COMPOSITION U235/Th/BeO = 1/3.6/1500

ROTOR SPEED = 1800 r.p.m.

Lethargy	Flux Per Unit Lethargy	Flux Per Unit Energy	Energy (eV)
$13.36^{+0.43}_{-0.55}$	3.64 ± 0.11	0.2316 ± 0.0073	$15.7^{+11.5}_{-5.5}$
$13.77^{+0.36}_{-0.44}$	3.64 ± 0.12	0.348 ± 0.012	$10.5^{+5.7}_{-3.1}$
$14.11^{+0.31}_{-0.36}$	3.46 ± 0.13	0.464 ± 0.018	$7.5^{+3.2}_{-2.0}$
$14.40^{+0.27}_{-0.31}$	3.39 ± 0.14	0.607 ± 0.025	$5.6^{+2.0}_{-1.3}$
$14.65^{+0.24}_{-0.27}$	3.38 ± 0.15	0.780 ± 0.034	$4.3^{+1.3}_{-0.9}$
$14.88^{+0.21}_{-0.24}$	3.25 ± 0.15	0.939 ± 0.045	$3.46^{+0.94}_{-0.67}$
$15.08^{+0.19}_{-0.21}$	2.82 ± 0.15	0.995 ± 0.055	$2.83^{+0.68}_{-0.50}$
15.34 ± 0.20	2.87 ± 0.12	1.315 ± 0.055	2.18 ± 0.43
15.65 ± 0.17	3.21 ± 0.14	2.009 ± 0.085	1.60 ± 0.27
15.92 ± 0.15	3.24 ± 0.15	2.66 ± 0.12	1.22 ± 0.18
16.16 ± 0.13	3.24 ± 0.16	3.37 ± 0.17	0.96 ± 0.12
16.37 ± 0.12	3.17 ± 0.17	4.08 ± 0.22	0.777 ± 0.092
16.65 ± 0.14	3.30 ± 0.13	5.60 ± 0.23	0.590 ± 0.079
16.97 ± 0.11	3.22 ± 0.15	7.54 ± 0.34	0.427 ± 0.049
17.25 ± 0.10	3.29 ± 0.16	10.19 ± 0.51	0.323 ± 0.032
17.491 ± 0.088	3.50 ± 0.18	13.82 ± 0.71	0.253 ± 0.022
17.709 ± 0.079	4.25 ± 0.21	20.9 ± 1.0	0.204 ± 0.016
17.905 ± 0.071	5.00 ± 0.24	29.8 ± 1.4	0.168 ± 0.012
18.084 ± 0.065	6.08 ± 0.27	43.4 ± 1.9	0.1401 ± 0.0091
18.248 ± 0.060	7.09 ± 0.30	59.6 ± 2.5	0.1189 ± 0.0072
18.399 ± 0.056	7.95 ± 0.32	77.9 ± 3.2	0.1022 ± 0.0057
18.540 ± 0.052	7.93 ± 0.34	89.3 ± 3.8	0.0888 ± 0.0046
18.671 ± 0.049	8.79 ± 0.37	112.9 ± 4.8	0.0778 ± 0.0038
18.795 ± 0.046	9.76 ± 0.41	141.8 ± 5.9	0.0688 ± 0.0032
18.911 ± 0.043	8.52 ± 0.41	139.1 ± 6.6	0.0613 ± 0.0027
19.021 ± 0.041	8.39 ± 0.43	152.9 ± 7.6	0.0549 ± 0.0022
19.125 ± 0.039	8.17 ± 0.43	165.1 ± 8.8	0.0495 ± 0.0019
19.270 ± 0.059	6.85 ± 0.32	160.3 ± 7.3	0.0428 ± 0.0025
19.450 ± 0.054	5.62 ± 0.32	157.3 ± 9.1	0.0357 ± 0.0019
19.689 ± 0.090	3.69 ± 0.24	131.0 ± 8.4	0.0281 ± 0.0025

TABLE 11 A

SPECTRUM FOR ASSEMBLY WITH COMPOSITION U235/Th/BeO = 1/1.8/750

ROTOR SPEED = 7200 r.p.m.

Lethargy	Flux Per Unit Lethargy	Flux Per Unit Energy	Energy (eV)
$10.75^{+0.41}_{-0.52}$	6.46 ± 0.23	0.0300 ± 0.0011	215^{+146}_{-73}
$11.13^{+0.35}_{-0.42}$	6.13 ± 0.24	0.0417 ± 0.0016	147^{+77}_{-43}
$11.46^{+0.30}_{-0.35}$	5.66 ± 0.24	0.0529 ± 0.0022	107^{+45}_{-28}
$11.72^{+0.26}_{-0.30}$	5.62 ± 0.24	0.0692 ± 0.0030	81^{+29}_{-19}
$11.96^{+0.23}_{-0.27}$	5.51 ± 0.25	0.0863 ± 0.0038	64^{+19}_{-13}
$12.18^{+0.21}_{-0.24}$	5.81 ± 0.26	0.1130 ± 0.0050	51^{+13}_{-10}
$12.37^{+0.19}_{-0.21}$	5.44 ± 0.26	0.1284 ± 0.0061	42^{+10}_{-7}
$12.55^{+0.18}_{-0.19}$	5.35 ± 0.26	0.1508 ± 0.0074	$35.5^{+7.6}_{-5.8}$
$12.71^{+0.16}_{-0.18}$	4.99 ± 0.26	0.1657 ± 0.0087	$30.1^{+5.9}_{-4.6}$
$12.86^{+0.15}_{-0.16}$	4.96 ± 0.26	0.191 ± 0.010	$25.9^{+4.6}_{-3.7}$
13.07 ± 0.16	4.43 ± 0.19	0.2093 ± 0.0089	21.2 ± 3.4
13.31 ± 0.14	4.59 ± 0.20	0.277 ± 0.012	16.5 ± 2.3
13.53 ± 0.12	4.57 ± 0.21	0.344 ± 0.016	13.3 ± 1.6
13.73 ± 0.11	4.75 ± 0.22	0.436 ± 0.020	10.9 ± 1.2
13.91 ± 0.10	4.12 ± 0.22	0.453 ± 0.024	9.10 ± 0.94
14.15 ± 0.12	4.40 ± 0.17	0.614 ± 0.024	7.17 ± 0.86
14.43 ± 0.10	4.29 ± 0.18	0.796 ± 0.034	5.39 ± 0.55
14.682 ± 0.091	3.97 ± 0.19	0.945 ± 0.046	4.21 ± 0.38
14.903 ± 0.081	3.52 ± 0.20	1.045 ± 0.060	3.37 ± 0.27
15.19 ± 0.11	3.69 ± 0.16	1.455 ± 0.064	2.53 ± 0.29
15.52 ± 0.097	3.78 ± 0.19	2.08 ± 0.10	1.81 ± 0.18
15.81 ± 0.084	3.56 ± 0.20	2.61 ± 0.15	1.36 ± 0.12
16.16 ± 0.13	3.63 ± 0.17	3.80 ± 0.18	0.95 ± 0.12

TABLE 11 B

SPECTRUM FOR ASSEMBLY WITH COMPOSITION U235/Th/BeO = 1/1.8/750

ROTOR SPEED = 1800 r.p.m.

Lethargy	Flux Per Unit Lethargy	Flux Per Unit Energy	Energy (eV)
$13.66^{+0.38}_{-0.46}$	4.23 ± 0.13	0.363 ± 0.011	$11.7^{+6.9}_{-3.7}$
$14.02^{+0.32}_{-0.38}$	4.41 ± 0.15	0.541 ± 0.018	$8.2^{+3.8}_{-2.2}$
$14.32^{+0.28}_{-0.32}$	4.03 ± 0.15	0.668 ± 0.025	$6.0^{+2.3}_{-1.5}$
$14.58^{+0.25}_{-0.28}$	3.62 ± 0.15	0.779 ± 0.033	$4.6^{+1.5}_{-1.0}$
$14.81^{+0.22}_{-0.25}$	3.74 ± 0.17	1.016 ± 0.045	$3.7^{+1.0}_{-0.7}$
$15.02^{+0.20}_{-0.22}$	3.96 ± 0.18	1.325 ± 0.060	$2.99^{+0.74}_{-0.54}$
$15.21^{+0.18}_{-0.20}$	4.03 ± 0.19	1.623 ± 0.078	$2.48^{+0.55}_{-0.41}$
$15.38^{+0.17}_{-0.18}$	3.61 ± 0.19	1.729 ± 0.093	$2.09^{+0.42}_{-0.32}$
15.61 ± 0.17	3.79 ± 0.15	2.279 ± 0.090	1.66 ± 0.29
15.88 ± 0.15	3.77 ± 0.16	2.98 ± 0.13	1.26 ± 0.19
16.13 ± 0.13	3.71 ± 0.18	3.74 ± 0.18	0.99 ± 0.13
16.34 ± 0.12	3.69 ± 0.19	4.62 ± 0.24	0.800 ± 0.095
16.62 ± 0.14	3.65 ± 0.15	6.03 ± 0.24	0.605 ± 0.082
16.95 ± 0.12	3.85 ± 0.17	8.82 ± 0.38	0.436 ± 0.050
17.23 ± 0.10	3.78 ± 0.18	11.48 ± 0.56	0.329 ± 0.033
17.475 ± 0.089	3.96 ± 0.21	15.37 ± 0.79	0.258 ± 0.023
17.694 ± 0.079	4.17 ± 0.23	20.1 ± 1.1	0.207 ± 0.016
17.98 ± 0.11	4.83 ± 0.19	31.0 ± 1.2	0.156 ± 0.018
18.310 ± 0.096	5.74 ± 0.22	51.4 ± 2.0	0.112 ± 0.010
18.594 ± 0.083	5.12 ± 0.24	60.9 ± 2.9	0.0841 ± 0.0070
18.843 ± 0.073	5.11 ± 0.27	77.9 ± 4.1	0.0656 ± 0.0048
19.064 ± 0.066	4.19 ± 0.28	79.8 ± 5.3	0.0526 ± 0.0034
19.35 ± 0.11	3.03 ± 0.22	76.8 ± 5.5	0.0395 ± 0.0042

TABLE 12 A

SPECTRUM FOR ASSEMBLY WITH COMPOSITION U233/Th/BeO = 1/6.8/2800

ROTOR SPEED = 7200 r.p.m.

Lethargy	Flux Per Unit Lethargy	Flux Per Unit Energy	Energy (eV)
$11.02^{+0.37}_{-0.45}$	4.45 ± 0.18	0.0272 ± 0.0011	164^{+94}_{-51}
$11.35^{+0.32}_{-0.38}$	4.67 ± 0.19	0.0399 ± 0.0016	117^{+54}_{-32}
$11.64^{+0.28}_{-0.32}$	4.17 ± 0.19	0.0474 ± 0.0022	88^{+33}_{-21}
$11.89^{+0.25}_{-0.28}$	3.91 ± 0.19	0.0572 ± 0.0028	68^{+22}_{-15}
$12.12^{+0.22}_{-0.25}$	3.98 ± 0.20	0.0728 ± 0.0036	55^{+16}_{-11}
$12.32^{+0.20}_{-0.22}$	4.07 ± 0.20	0.0909 ± 0.0045	45^{+11}_{-8}
12.57 ± 0.20	3.63 ± 0.14	0.1053 ± 0.0041	34.5 ± 7.1
12.89 ± 0.18	3.42 ± 0.15	0.1350 ± 0.0058	25.3 ± 4.5
13.16 ± 0.15	3.51 ± 0.15	0.1814 ± 0.0080	19.3 ± 3.0
13.39 ± 0.14	3.32 ± 0.16	0.218 ± 0.010	15.3 ± 2.1
13.60 ± 0.12	3.05 ± 0.16	0.247 ± 0.013	12.4 ± 1.5
13.88 ± 0.14	2.91 ± 0.12	0.310 ± 0.012	9.4 ± 1.3
14.20 ± 0.12	3.32 ± 0.13	0.489 ± 0.020	6.79 ± 0.80
14.48 ± 0.10	3.16 ± 0.14	0.615 ± 0.027	5.14 ± 0.52
14.724 ± 0.090	3.10 ± 0.15	0.770 ± 0.037	4.03 ± 0.36
14.942 ± 0.081	3.15 ± 0.16	0.970 ± 0.049	3.24 ± 0.26
15.22 ± 0.11	2.94 ± 0.12	1.201 ± 0.049	2.45 ± 0.28
15.552 ± 0.097	3.18 ± 0.14	1.806 ± 0.077	1.76 ± 0.17
15.835 ± 0.084	3.12 ± 0.15	2.35 ± 0.11	1.33 ± 0.11
16.19 ± 0.13	2.81 ± 0.11	3.01 ± 0.13	0.93 ± 0.12
16.59 ± 0.11	3.02 ± 0.14	4.83 ± 0.23	0.626 ± 0.067
16.920 ± 0.091	3.08 ± 0.16	6.86 ± 0.37	0.449 ± 0.040

TABLE 12 B

SPECTRUM FOR ASSEMBLY WITH COMPOSITION U233/Th/BeO = 1/6.8/2800

ROTOR SPEED = 1800 r.p.m.

Lethargy	Flux Per Unit Lethargy	Flux Per Unit Energy	Energy (eV)
$13.87^{+0.35}_{-0.42}$	3.23 ± 0.11	0.343 ± 0.012	$9.4^{+4.9}_{-2.8}$
$14.20^{+0.29}_{-0.35}$	3.09 ± 0.12	0.453 ± 0.017	$6.8^{+2.9}_{-1.8}$
$14.48^{+0.26}_{-0.30}$	3.25 ± 0.13	0.629 ± 0.025	$5.2^{+1.8}_{-1.2}$
$14.72^{+0.23}_{-0.26}$	2.82 ± 0.13	0.697 ± 0.032	$4.0^{+1.2}_{-0.8}$
$14.94^{+0.21}_{-0.24}$	3.20 ± 0.15	0.982 ± 0.045	$3.26^{+0.87}_{-0.62}$
$15.13^{+0.19}_{-0.21}$	3.15 ± 0.15	1.176 ± 0.057	$2.68^{+0.63}_{-0.47}$
$15.31^{+0.18}_{-0.19}$	2.97 ± 0.16	1.327 ± 0.070	$2.24^{+0.47}_{-0.36}$
15.55 ± 0.18	2.92 ± 0.12	1.651 ± 0.067	1.77 ± 0.33
15.83 ± 0.16	2.97 ± 0.13	2.229 ± 0.097	1.33 ± 0.21
16.08 ± 0.14	3.07 ± 0.14	2.95 ± 0.13	1.04 ± 0.14
16.30 ± 0.12	3.03 ± 0.15	3.63 ± 0.18	0.83 ± 0.10
16.50 ± 0.11	3.03 ± 0.16	4.43 ± 0.23	0.684 ± 0.076
16.68 ± 0.10	2.95 ± 0.17	5.17 ± 0.29	0.571 ± 0.058
16.92 ± 0.12	3.01 ± 0.13	6.69 ± 0.28	0.450 ± 0.053
17.20 ± 0.10	3.31 ± 0.14	9.80 ± 0.43	0.338 ± 0.034
17.452 ± 0.091	3.75 ± 0.16	14.23 ± 0.62	0.263 ± 0.024
17.674 ± 0.081	4.50 ± 0.19	21.32 ± 0.88	0.211 ± 0.017
17.874 ± 0.073	5.34 ± 0.21	30.9 ± 1.2	0.173 ± 0.013
18.055 ± 0.067	7.60 ± 0.25	52.7 ± 1.8	0.1441 ± 0.0096
18.222 ± 0.062	9.77 ± 0.30	80.1 ± 2.4	0.1220 ± 0.0075
18.375 ± 0.057	11.08 ± 0.33	105.8 ± 3.1	0.1047 ± 0.0059
18.518 ± 0.053	13.04 ± 0.37	143.6 ± 4.1	0.0908 ± 0.0048
18.651 ± 0.050	14.60 ± 0.40	183.9 ± 5.1	0.0794 ± 0.0039
18.776 ± 0.047	14.38 ± 0.42	205.0 ± 6.0	0.0701 ± 0.0033
18.893 ± 0.044	14.81 ± 0.44	237.3 ± 7.0	0.0624 ± 0.0027
19.004 ± 0.042	14.52 ± 0.45	260.1 ± 8.0	0.0558 ± 0.0023
19.109 ± 0.039	13.81 ± 0.46	274.8 ± 9.0	0.0502 ± 0.0020
19.209 ± 0.038	12.44 ± 0.46	274 ± 10	0.0455 ± 0.0017
19.304 ± 0.036	12.90 ± 0.48	312 ± 12	0.0414 ± 0.0015
19.395 ± 0.034	12.08 ± 0.48	320 ± 13	0.0378 ± 0.0013
19.481 ± 0.033	10.07 ± 0.46	291 ± 14	0.0346 ± 0.0011
19.565 ± 0.032	9.66 ± 0.47	303 ± 15	0.0319 ± 0.0010
19.645 ± 0.030	8.86 ± 0.47	301 ± 16	0.02941 ± 0.00089
19.758 ± 0.046	7.73 ± 0.34	294 ± 13	0.0263 ± 0.0012
19.900 ± 0.044	6.22 ± 0.34	273 ± 15	0.02277 ± 0.00099
20.034 ± 0.041	4.86 ± 0.34	243 ± 17	0.01993 ± 0.00081
20.216 ± 0.070	3.62 ± 0.25	217 ± 15	0.0166 ± 0.0012

TABLE 13 A

SPECTRUM FOR ASSEMBLY WITH COMPOSITION U233/Th/BeO = 1/3.4/1400

ROTOR SPEED = 7200 r.p.m.

Lethargy	Flux Per Unit Lethargy	Flux Per Unit Energy	Energy (eV)
$11.30^{+0.33}_{-0.39}$	5.96 ± 0.22	0.0480 ± 0.0018	124^{+59}_{-35}
$11.59^{+0.28}_{-0.33}$	5,26 ± 0.22	0.0568 ± 0.0023	92^{+36}_{-23}
$11.85^{+0.25}_{-0.29}$	5.07 ± 0.22	0.0708 ± 0.0030	72^{+24}_{-16}
$12.08^{+0.23}_{-0.25}$	5.15 ± 0.23	0.0905 ± 0.0040	57^{+17}_{-12}
$12.28^{+0.21}_{-0.23}$	5.60 ± 0.24	0.1205 ± 0.0051	46^{+12}_{-9}
$12.47^{+0.19}_{-0.21}$	4.79 ± 0.23	0.1241 ± 0.0060	$38.6^{+8.9}_{-6.6}$
$12.63^{+0.17}_{-0.19}$	5.27 ± 0.25	0.1620 ± 0.0075	$32.6^{+6.8}_{-5.2}$
$12.79^{+0.16}_{-0.17}$	4.93 ± 0.24	0.1769 ± 0.0088	$27.8^{+5.3}_{-4.1}$
$12.94^{+0.15}_{-0.16}$	4.70 ± 0.25	0.195 ± 0.010	$24.1^{+4.2}_{-3.3}$
$13.07^{+0.14}_{-0.15}$	4.64 ± 0.25	0.221 ± 0.012	$21.0^{+3.4}_{-2.7}$
13.25 ± 0.15	4.58 ± 0.18	0.262 ± 0.010	17.5 ± 2.6
13.48 ± 0.13	4.50 ± 0.19	0.323 ± 0.014	14.0 ± 1.8
13.68 ± 0.12	4.40 ± 0.20	0.386 ± 0.017	11.4 ± 1.3
13,87 ± 0.11	4.64 ± 0.21	0.490 ± 0.022	9.5 ± 1.0
14,04 ± 0.10	4.55 ± 0,21	0.568 ± 0.027	8,01 ± 0.79
14,193 ± 0.090	4.18 ± 0.22	0.610 ± 0.031	6.86 ± 0.62
14.337 ± 0.084	4.36 ± 0.23	0.734 ± 0,038	5.94 ± 0,50
14.471 ± 0.079	4.42 ± 0.24	0.852 ± 0.045	5.19 ± 0.41
14.597 ± 0,074	4.45 ± 0.24	0.972 ± 0.053	4.58 ± 0.34
14.770 ± 0,088	3.96 ± 0.17	1.029 ± 0.045	3.85 ± 0.34
14.983 ± 0.079	3.90 ± 0,18	1.252 ± 0.059	3,11 ± 0.25
15.175 ± 0.072	3.80 ± 0.19	1.479 ± 0.075	2,57 ± 0.37
15.43 ± 0.10	3.36 ± 0.14	1.684 ± 0.072	2.00 ± 0.20
15.727 ± 0.088	3.64 ± 0.16	2.46 ± 0.11	1,48 ± 0.13
15.987 ± 0.077	3.49 ± 0.18	3.06 ± 0.16	1.140 ± 0.089
16.218 ± 0.069	3.41 ± 0.19	3.76 ± 0.21	0.905 ± 0.062
16.51 ± 0.11	3.52 ± 0.15	5.22 ± 0.23	0.674 ± 0.074

TABLE 13 B

SPECTRUM FOR ASSEMBLY WITH COMPOSITION U233/Th/BeO = 1/3.4/1400

ROTOR SPEED = 1800 r.p.m.

Lethargy	Flux Per Unit Lethargy	Flux Per Unit Energy	Energy (eV)
$14.20^{+0.30}_{-0.35}$	4.31 ± 0.14	0.629 ± 0.021	$6.8^{+2.9}_{-1.8}$
$14.50^{+0.26}_{-0.30}$	4.02 ± 0.15	0.775 ± 0.029	$5.2^{+1.8}_{-1.2}$
$14.72^{+0.23}_{-0.26}$	3.93 ± 0.16	0.970 ± 0.040	$4.1^{+1.2}_{-0.8}$
$14.94^{+0.21}_{-0.24}$	3.90 ± 0.17	1.194 ± 0.053	$3.26^{+0.87}_{-0.62}$
$15.13^{+0.19}_{-0.21}$	3.82 ± 0.18	1.424 ± 0.068	$2.68^{+0.63}_{-0.47}$
$15.31^{+0.18}_{-0.19}$	3.71 ± 0.18	1.650 ± 0.083	$2.24^{+0.48}_{-0.36}$
$15.47^{+0.16}_{-0.18}$	3.78 ± 0.19	1.99 ± 0.10	$1.90^{+0.37}_{-0.29}$
$15.63^{+0.15}_{-0.16}$	3.54 ± 0.20	2.17 ± 0.12	$1.64^{+0.29}_{-0.23}$
15.83 ± 0.16	3.68 ± 0.15	2.76 ± 0.12	1.33 ± 0.21
16.08 ± 0.14	3.37 ± 0.16	3.23 ± 0.15	1.04 ± 0.15
16.30 ± 0.12	3.50 ± 0.17	4.20 ± 0.21	0.84 ± 0.10
16.50 ± 0.11	3.64 ± 0.19	5.32 ± 0.27	0.685 ± 0.075
16.68 ± 0.10	3.79 ± 0.20	6.62 ± 0.35	0.572 ± 0.069
16.92 ± 0.12	3.67 ± 0.15	8.15 ± 0.33	0.450 ± 0.053
17.20 ± 0.10	3.75 ± 0.17	11.09 ± 0.49	0.338 ± 0.035
17.452 ± 0.091	4.64 ± 0.19	17.60 ± 0.73	0.264 ± 0.024
17.674 ± 0.081	4.82 ± 0.21	22.84 ± 0.98	0.211 ± 0.017
17.873 ± 0.073	5.74 ± 0.24	32.2 ± 1.4	0.173 ± 0.013
18.055 ± 0.067	6.44 ± 0.26	44.6 ± 1.8	0.1442 ± 0.0097
18.221 ± 0.062	7.27 ± 0.29	59.6 ± 2.3	0.1221 ± 0.0075
18.375 ± 0.057	8.19 ± 0.31	78.3 ± 3.0	0.1047 ± 0.0060
18.517 ± 0.053	9.40 ± 0.35	103.5 ± 3.8	0.0908 ± 0.0048
18.651 ± 0.050	10.02 ± 0.37	126.1 ± 4.6	0.0795 ± 0.0040
18.775 ± 0.047	9.69 ± 0.38	138.1 ± 5.4	0.0701 ± 0.0038
18.893 ± 0.044	9.73 ± 0.39	156.0 ± 6.3	0.0624 ± 0.0027
19.004 ± 0.042	8.47 ± 0.39	151.7 ± 7.0	0.0558 ± 0.0023
19.109 ± 0.040	9.06 ± 0.41	180.3 ± 8.3	0.0503 ± 0.0020
19.209 ± 0.038	7.80 ± 0.41	171.6 ± 9.1	0.0455 ± 0.0017
19.304 ± 0.036	7.34 ± 0.42	177.9 ± 9.8	0.0414 ± 0.0015
19.437 ± 0.055	6.35 ± 0.30	175.3 ± 8.3	0.0362 ± 0.0020
19.678 ± 0.091	4.79 ± 0.22	168.5 ± 7.8	0.0285 ± 0.0026
19.965 ± 0.079	3.07 ± 0.24	144 ± 12	0.0214 ± 0.0017

TABLE 14 A

SPECTRUM FOR ASSEMBLY WITH COMPOSITION U233/Th/BeO = 1/1.7/700

ROTOR SPEED = 7200 r.p.m.

Lethargy	Flux Per Unit Lethargy	Flux Per Unit Energy	Energy (eV)
$11.25^{+0.33}_{-0.40}$	7.29 ± 0.21	0.0565 ± 0.0017	129^{+63}_{-36}
$11.56^{+0.29}_{-0.34}$	6.67 ± 0.21	0.0699 ± 0.0022	95^{+38}_{-24}
$11.82^{+0.25}_{-0.29}$	6.65 ± 0.22	0.0904 ± 0.0030	74^{+25}_{-17}
$12.05^{+0.23}_{-0.26}$	6.08 ± 0.22	0.1042 ± 0.0037	58^{+17}_{-12}
$12.26^{+0.21}_{-0.23}$	6.36 ± 0.22	0.1341 ± 0.0047	47^{+12}_{-9}
$12.45^{+0.19}_{-0.21}$	5.76 ± 0.22	0.1463 ± 0.0056	$39.4^{+9.2}_{-6.8}$
$12.62^{+0.17}_{-0.19}$	6.06 ± 0.23	0.1829 ± 0.0070	$33.2^{+7.0}_{-5.3}$
$12.77^{+0.16}_{-0.18}$	5.75 ± 0.23	0.2032 ± 0.0082	$28.3^{+5.4}_{-4.2}$
$12.92^{+0.15}_{-0.16}$	5.26 ± 0.23	0.2149 ± 0.0094	$24.5^{+4.3}_{-3.4}$
$13.06^{+0.14}_{-0.15}$	5.82 ± 0.24	0.273 ± 0.011	$21.3^{+3.5}_{-2.8}$
13.18 ± 0.14	5.19 ± 0.24	0.276 ± 0.013	18.8 ± 2.6
13.31 ± 0.14	4.67 ± 0.24	0.280 ± 0.014	16.7 ± 2.2
13.42 ± 0.12	4.91 ± 0.25	0.330 ± 0.017	14.9 ± 1.8
13.53 ± 0.12	4.99 ± 0.25	0.374 ± 0.019	13.4 ± 1.6
13.63 ± 0.11	5.05 ± 0.26	0.418 ± 0.022	12.1 ± 1.3
13.77 ± 0.11	4.75 ± 0.19	0.453 ± 0.018	10.5 ± 1.2
13.95 ± 0.10	4.83 ± 0.19	0.550 ± 0.022	8.78 ± 0.90
14.108 ± 0.095	4.60 ± 0.20	0.616 ± 0.027	7.47 ± 0.71
14.258 ± 0.088	4.74 ± 0.21	0.737 ± 0.032	6.42 ± 0.57
14.398 ± 0.082	4.43 ± 0.21	0.793 ± 0.038	5.59 ± 0.46
14.528 ± 0.077	4.36 ± 0.22	0.890 ± 0.044	4.90 ± 0.38
14.651 ± 0.072	4.64 ± 0.23	1.071 ± 0.053	4.34 ± 0.31
14.766 ± 0.068	4.07 ± 0.23	1.054 ± 0.058	3.86 ± 0.26
14.926 ± 0.081	4.07 ± 0.17	1.235 ± 0.051	3.29 ± 0.27
15.123 ± 0.074	4.03 ± 0.18	1.489 ± 0.065	2.70 ± 0.20
15.303 ± 0.067	3.94 ± 0.19	1.742 ± 0.082	2.26 ± 0.15
15.468 ± 0.062	3.52 ± 0.19	1.837 ± 0.099	1.92 ± 0.12
15.620 ± 0.058	3.78 ± 0.20	2.30 ± 0.12	1.646 ± 0.095
15.825 ± 0.084	3.31 ± 0.15	2.47 ± 0.11	1.34 ± 0.11
16.074 ± 0.074	3.21 ± 0.17	3.07 ± 0.16	1.045 ± 0.078
16.295 ± 0.066	3.66 ± 0.19	4.36 ± 0.22	0.838 ± 0.055

TABLE 14 B

SPECTRUM FOR ASSEMBLY WITH COMPOSITION U233/Th/BeO = 1/1.7/700

ROTOR SPEED = 1800 r.p.m.

Lethargy	Flux Per Unit Lethargy	Flux Per Unit Energy	Energy (eV)
$13.83^{+0.35}_{-0.43}$	4.60 ± 0.13	0.465 ± 0.013	$9.8^{+5.3}_{-3.0}$
$14.16^{+0.30}_{-0.36}$	4.85 ± 0.14	0.681 ± 0.020	$7.11^{+3.1}_{-1.9}$
$14.44^{+0.27}_{-0.31}$	4.26 ± 0.14	0.796 ± 0.027	$5.36^{+1.9}_{-1.2}$
$14.69^{+0.24}_{-0.27}$	4.34 ± 0.15	1.038 ± 0.037	$4.18^{+1.3}_{-0.9}$
$14.91^{+0.21}_{-0.24}$	4.22 ± 0.16	1.258 ± 0.048	$3.35^{+0.91}_{-0.65}$
$15.11^{+0.19}_{-0.22}$	4.19 ± 0.17	1.527 ± 0.062	$2.75^{+0.66}_{-0.49}$
$15.29^{+0.18}_{-0.20}$	3.79 ± 0.17	1.654 ± 0.076	$2.29^{+0.50}_{-0.38}$
$15.45^{+0.16}_{-0.18}$	3.67 ± 0.18	1.889 ± 0.093	$1.94^{+0.38}_{-0.30}$
$15.61^{+0.15}_{-0.17}$	3.33 ± 0.18	2.00 ± 0.11	$1.67^{+0.30}_{-0.24}$
15.81 ± 0.16	3.30 ± 0.14	2.43 ± 0.10	1.36 ± 0.22
16.06 ± 0.14	3.37 ± 0.15	3.18 ± 0.14	1.06 ± 0.15
16.28 ± 0.12	3.34 ± 0.16	3.94 ± 0.19	0.85 ± 0.11
16.48 ± 0.11	3.29 ± 0.17	4.74 ± 0.25	0.693 ± 0.078
16.67 ± 0.10	3.16 ± 0.18	5.46 ± 0.31	0.578 ± 0.060
16.91 ± 0.12	2.96 ± 0.13	6.51 ± 0.30	0.455 ± 0.054
17.19 ± 0.10	3.27 ± 0.15	9.59 ± 0.44	0.341 ± 0.035
17.444 ± 0.091	3.06 ± 0.16	11.50 ± 0.61	0.266 ± 0.024
17.667 ± 0.081	3.73 ± 0.18	17.54 ± 0.85	0.213 ± 0.017
17.867 ± 0.074	4.05 ± 0.20	23.3 ± 1.1	0.174 ± 0.013
18.049 ± 0.067	4.49 ± 0.22	30.9 ± 1.5	0.1450 ± 0.0098
18.216 ± 0.062	4.87 ± 0.24	39.7 ± 1.9	0.1227 ± 0.0075
18.370 ± 0.057	5.29 ± 0.26	50.3 ± 2.4	0.1052 ± 0.0060
18.513 ± 0.053	5.51 ± 0.26	60.4 ± 2.9	0.0912 ± 0.0049
18.646 ± 0.050	6.08 ± 0.29	76.2 ± 3.6	0.0798 ± 0.0040
18.771 ± 0.047	5.38 ± 0.29	76.3 ± 4.2	0.0704 ± 0.0033
18.889 ± 0.044	5.08 ± 0.30	81.1 ± 4.9	0.0626 ± 0.0028
19.051 ± 0.067	4.71 ± 0.22	88.5 ± 4.2	0.0532 ± 0.0035
19.34 ± 0.11	3.19 ± 0.16	79.9 ± 4.1	0.0399 ± 0.0043

TABLE 15

FLUX RATIOS AT THERMAL PEAK

Nominal Assembly Composition				Ratio of Experimental to Theoretical Flux
U233	U235	Th	BeO	
	1		6545	0.97 ± 0.1
	1		4360	1.05 ± 0.1
	1		2185	1.11 ± 0.1
	1		1120	1.27 ± 0.05
	1		740	1.11 ± 0.05
	1	3.6	1500	1.10 ± 0.05
	1	1.8	750	1.12 ± 0, 05
1		6.8	2800	1.25 ± 0.05
1		3.4	1400	1.30 ± 0.05
1		1.7	700	1.55 ± 0.05

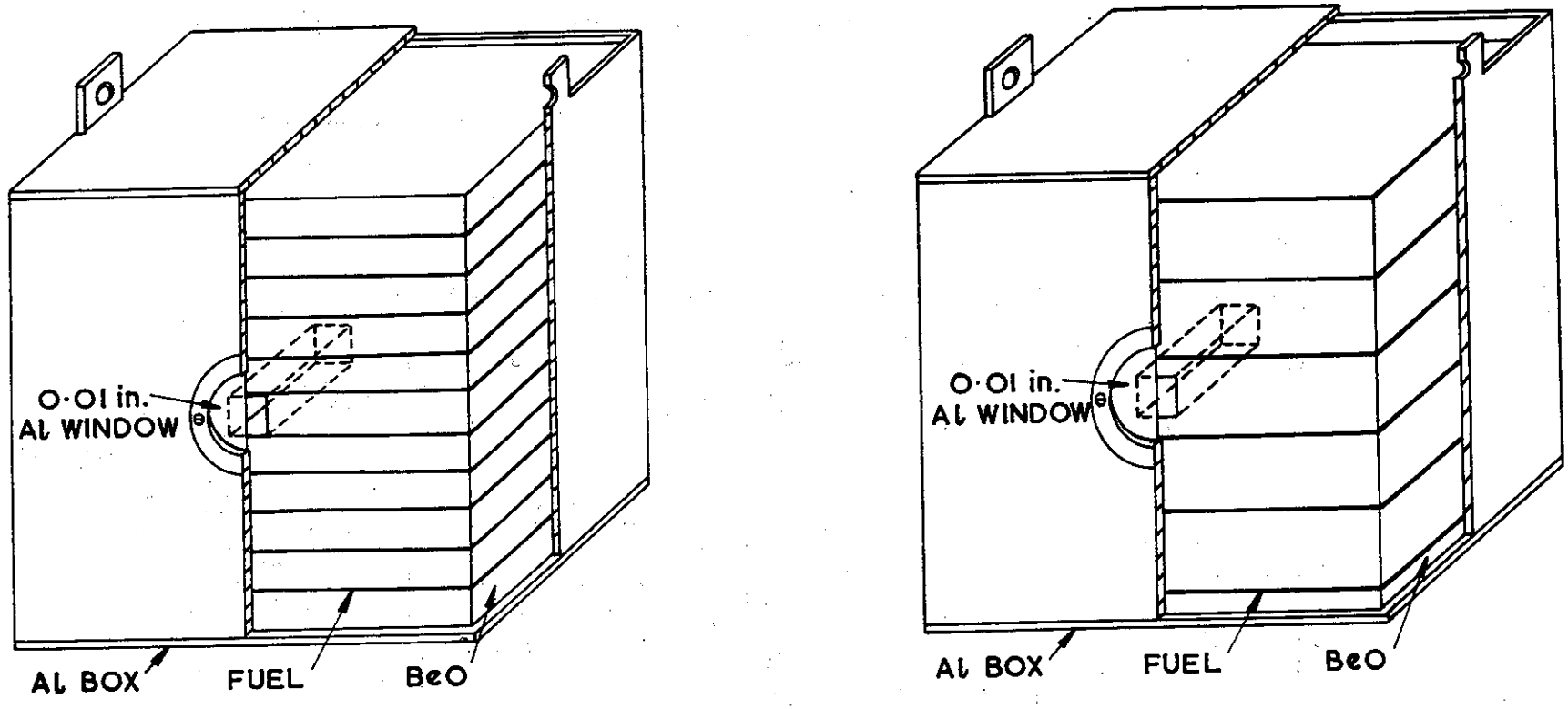

FIGURE 1. BERYLLIA MODERATED ASSEMBLIES

P1083

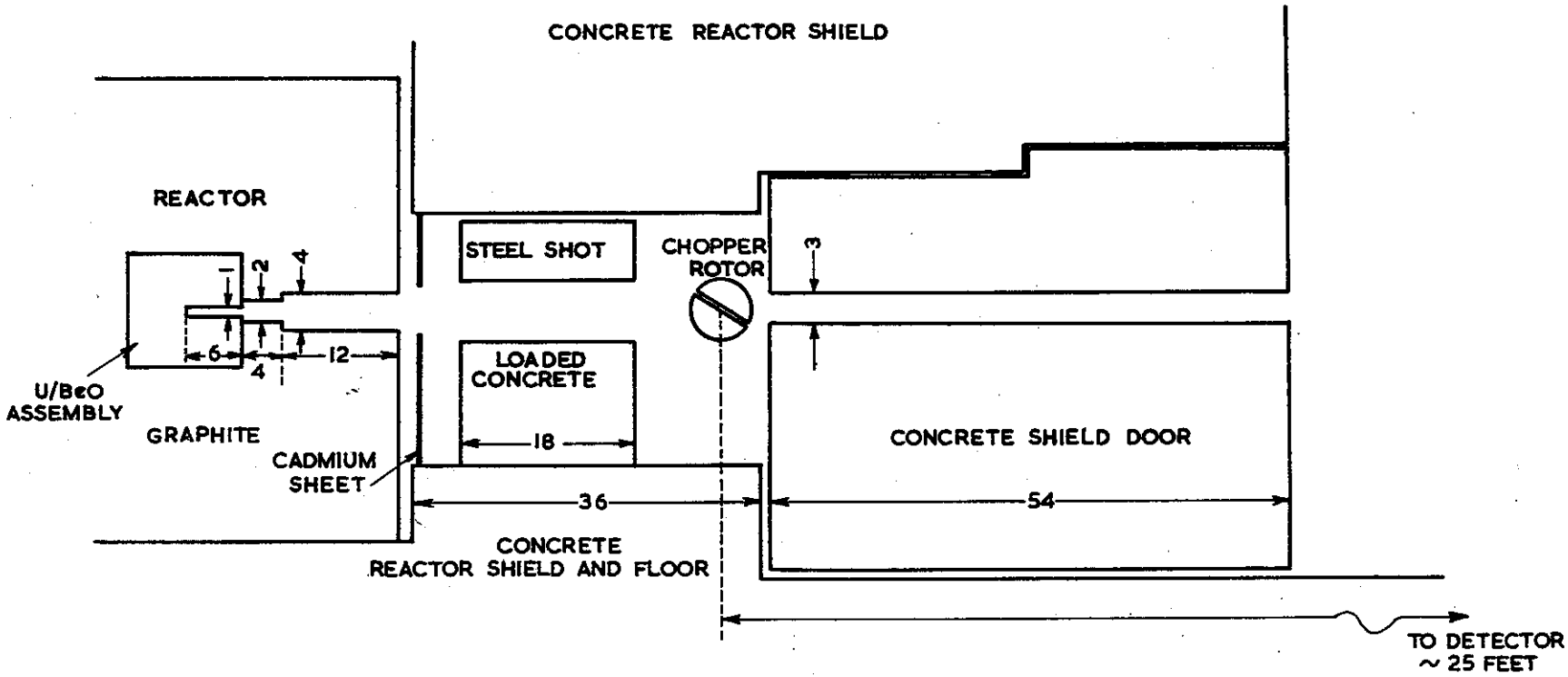

ALL DIMENSIONS IN INCHES

FIGURE 2. VERTICAL SECTION THROUGH FLIGHT PATH IN THE REACTOR

P10 83

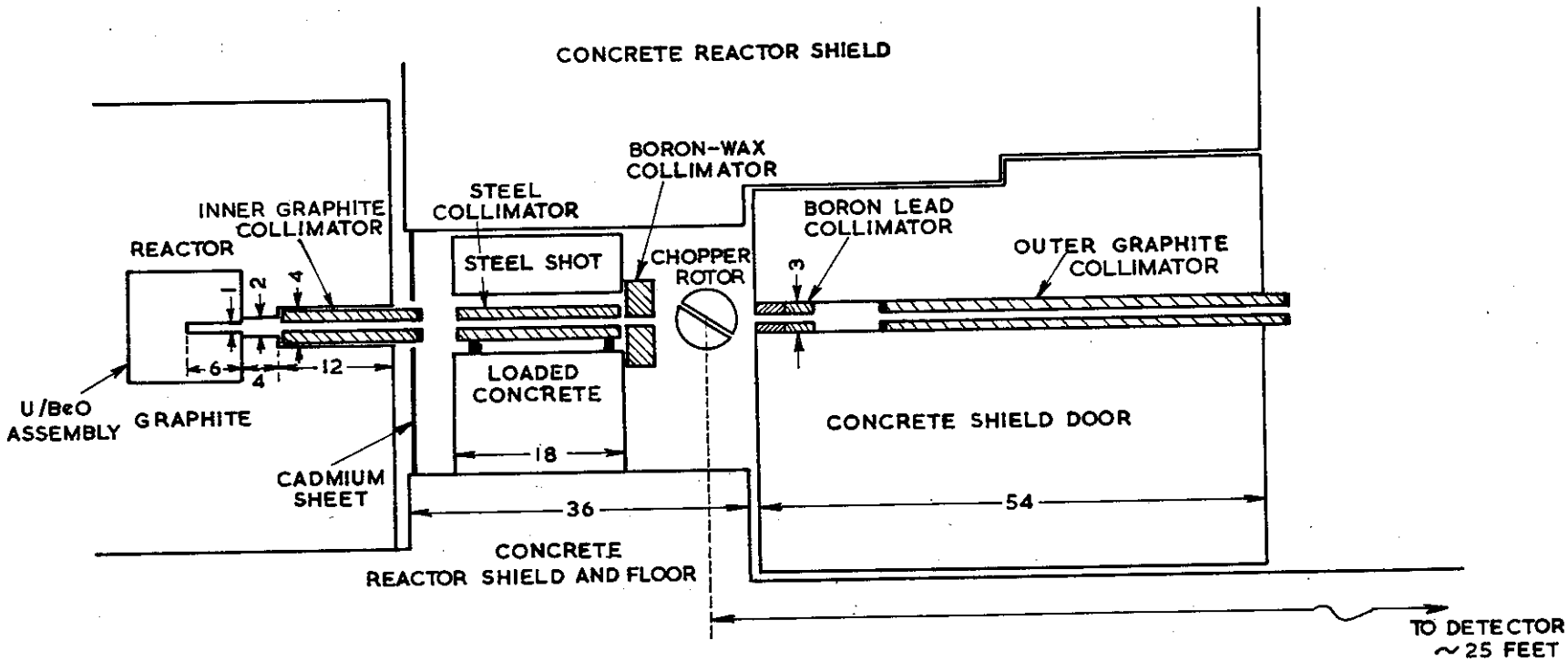

ALL DIMENSIONS IN INCHES

P1083

FIGURE 3. TYPICAL COLLIMATOR ARRANGEMENT

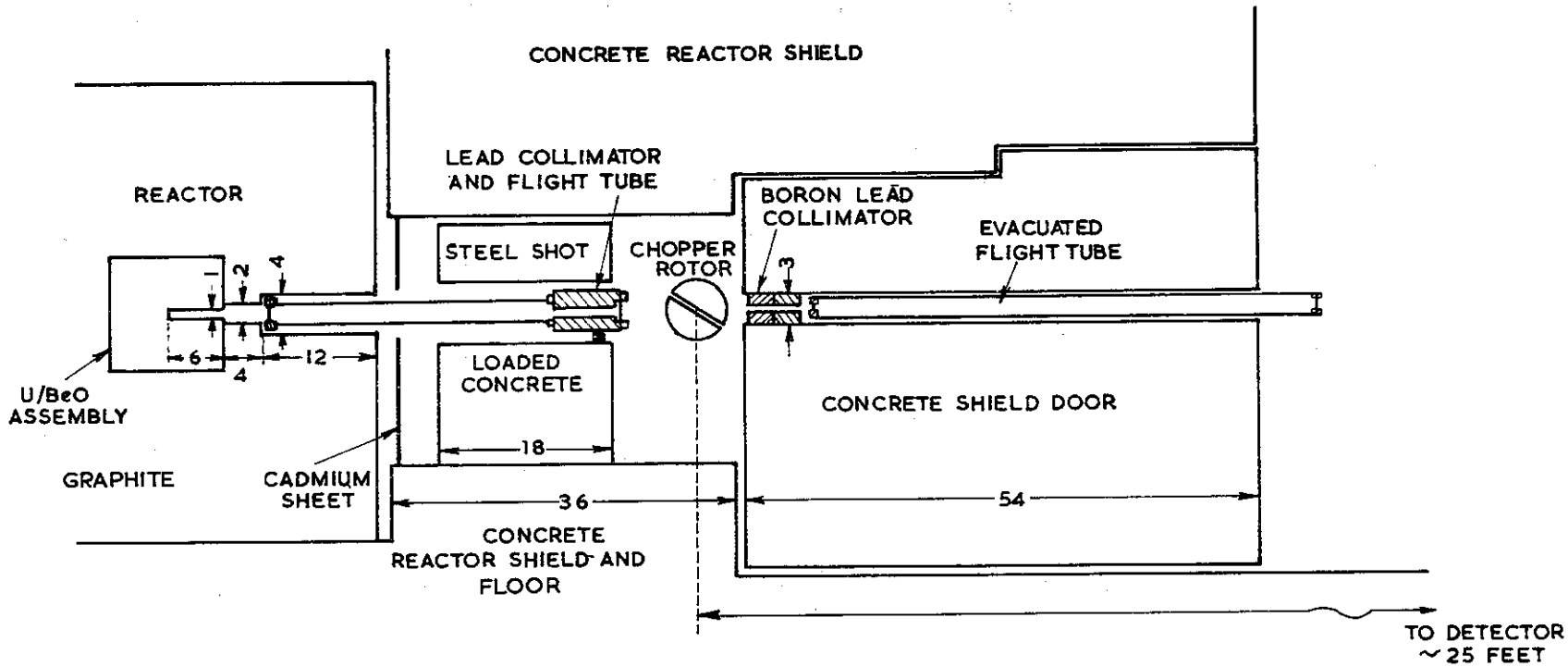

ALL DIMENSIONS IN INCHES

FIGURE 4. TYPICAL COLLIMATOR ARRANGEMENT

P1083

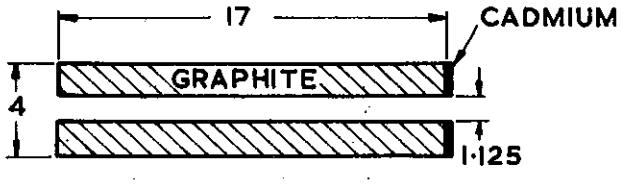

OUTSIDE – 4" square section
BEAM HOLE – 1·25" by 1·125" rectangular section

INNER GRAPHITE COLLIMATOR

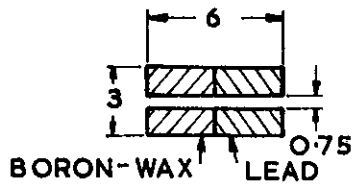

OUTSIDE – 3" square section
BEAM HOLE – 0·75" square section whole unit clad in Al

BORON – LEAD COLLIMATOR

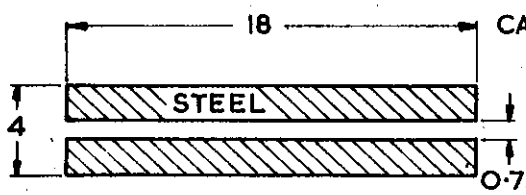

OUTSIDE – 4" square section
BEAM HOLE – 0·75" square section

STEEL COLLIMATOR

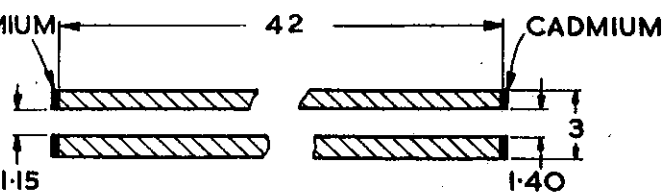

OUTSIDE – 3" square section
BEAM HOLE – Rectangular section tapering from 1·40" by 1·45" to 1·15" by 1·22"

OUTER GRAPHITE COLLIMATOR

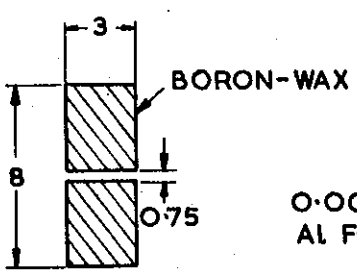

OUTSIDE – 8" square section
BEAM HOLE – 0·75" square section whole unit clad in brass

BORON-WAX COLLIMATOR

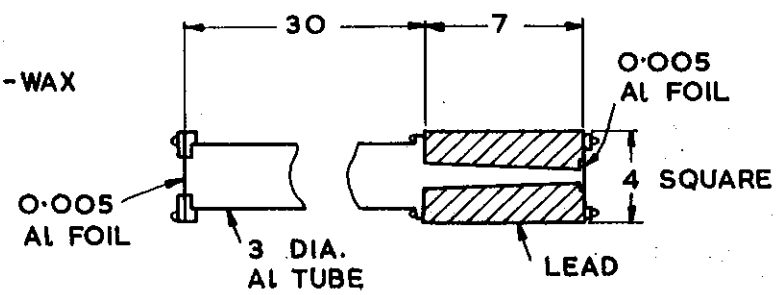

BEAM HOLE in lead is 1" square tapering to 0·75" square

LEAD COLLIMATOR AND FLIGHT TUBE

ALL DIMENSIONS IN INCHES

FIGURE 5. VERTICAL SECTIONS THROUGH COLLIMATORS

P1083

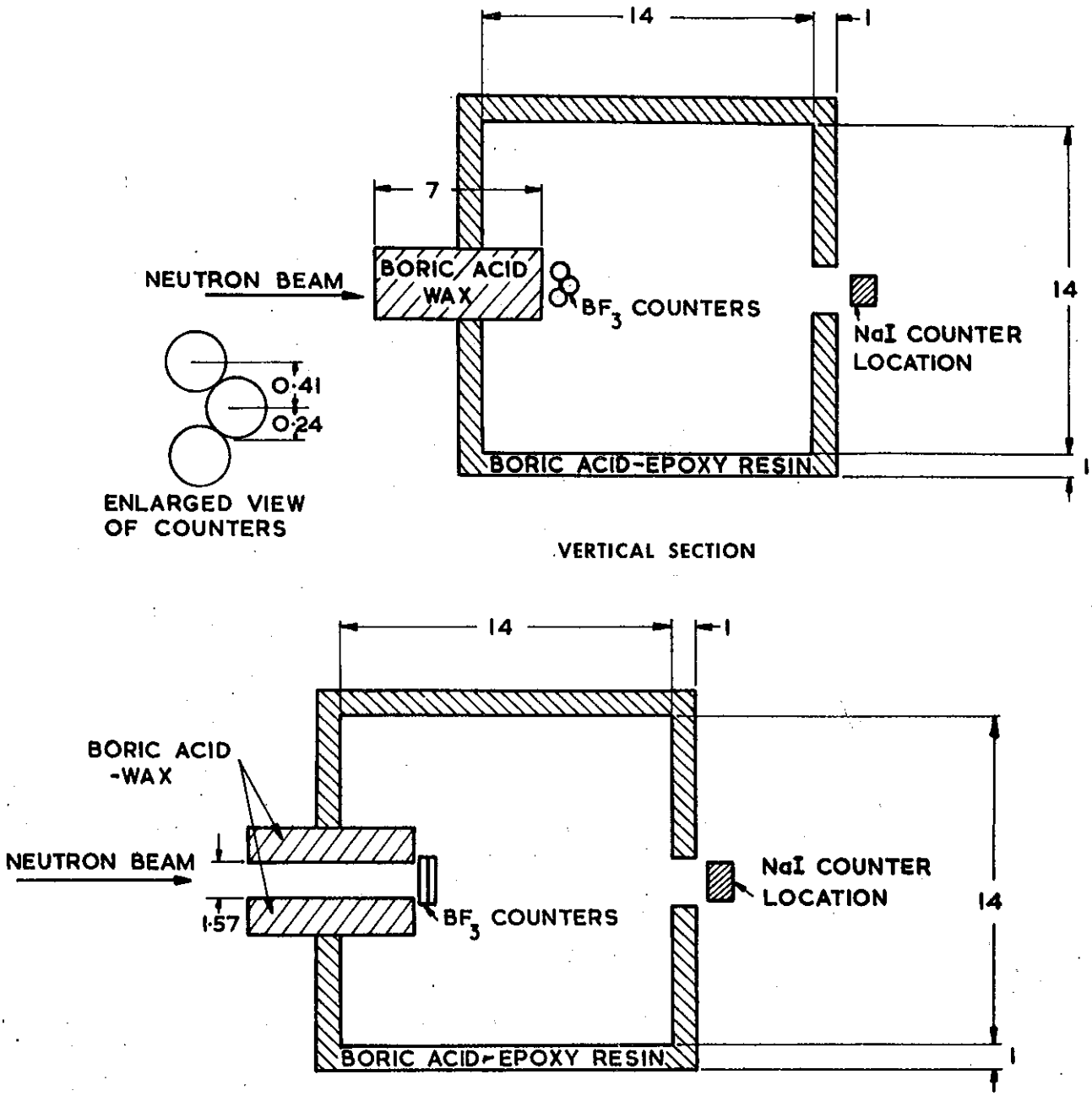

ALL DIMENSIONS IN INCHES

P1083

FIGURE 6. LAYOUT OF BF_3 COUNTER SYSTEM

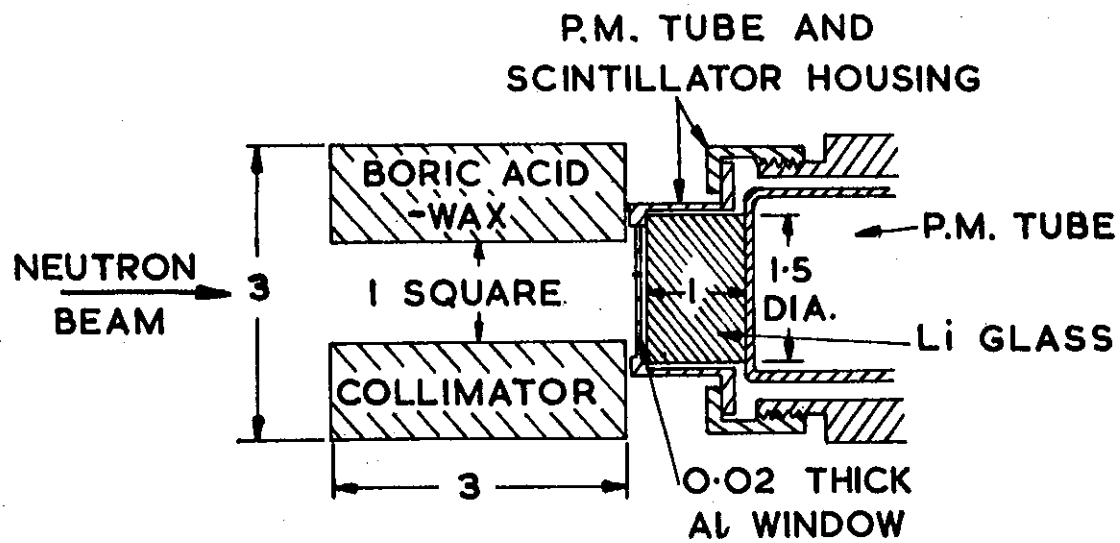

ALL DIMENSIONS IN INCHES

P1083

FIGURE 7. Li-GLASS SCINTILLATION DETECTOR LAYOUT

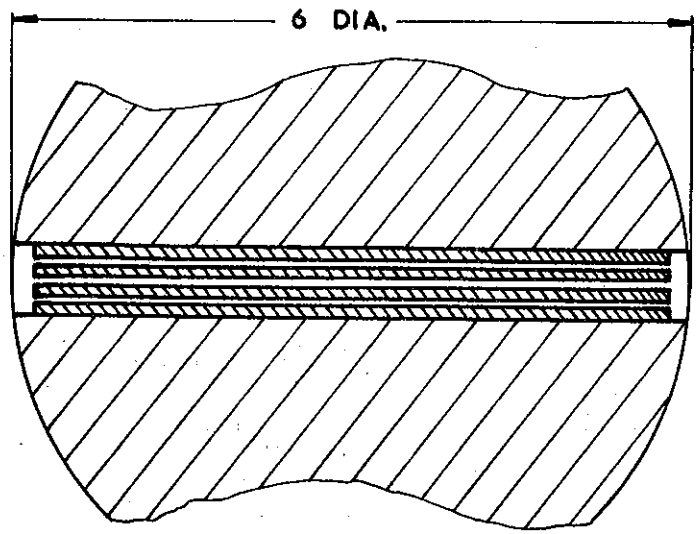

SECTION PERPENDICULAR TO AXIS OF ROTATION

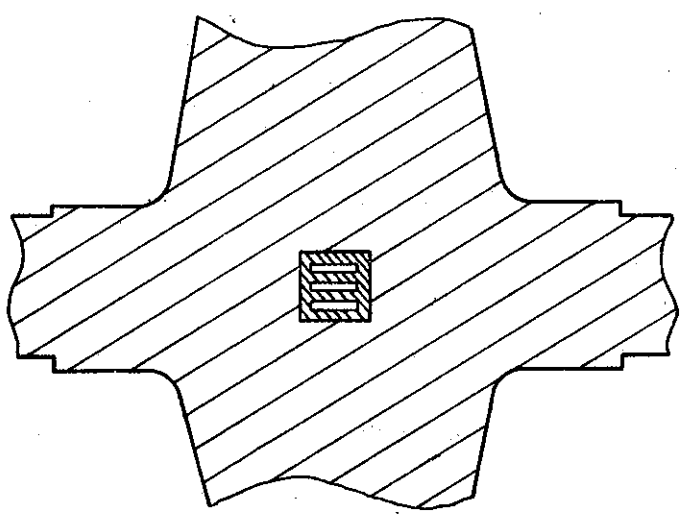

SECTION THROUGH AXIS OF ROTATION

WIDTH OF EACH SLIT	0·424
HEIGHT OF EACH SLIT	0·065
THICKNESS OF SLIT WALLS	0·103
LENGTH OF SLIT	
a) WITH S.S. ROTOR BODY	5·63
b) WITH MONEL ROTOR BODY	5·54

ALL DIMENSIONS IN INCHES

FIGURE 8. SECTIONS THROUGH ROTOR SHOWING SLIT INSERT

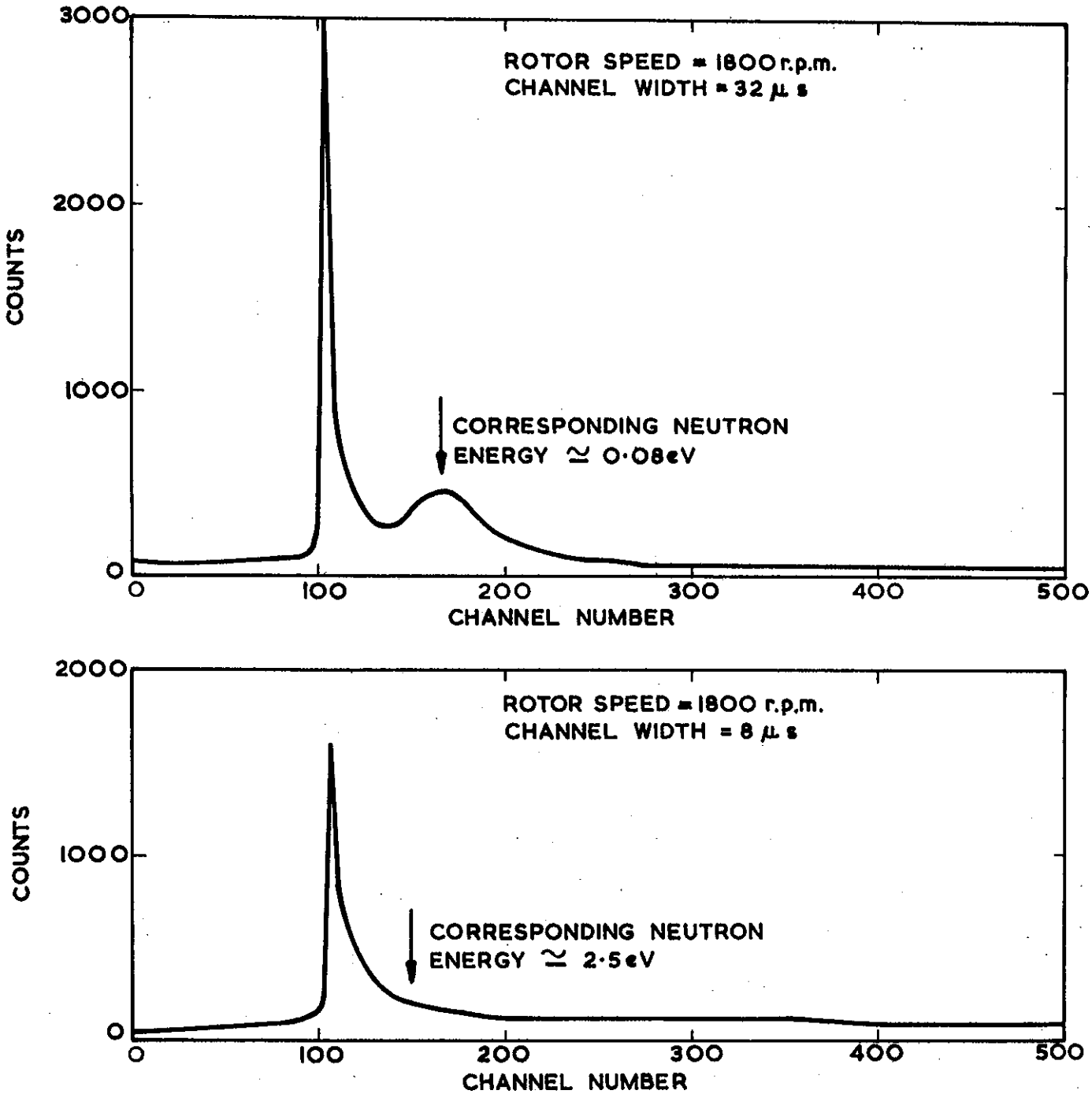

FIGURE 9. COUNT DISTRIBUTIONS FOR ASSEMBLY WITH U233/Th/BeO = 1/6.8/2800

P1083

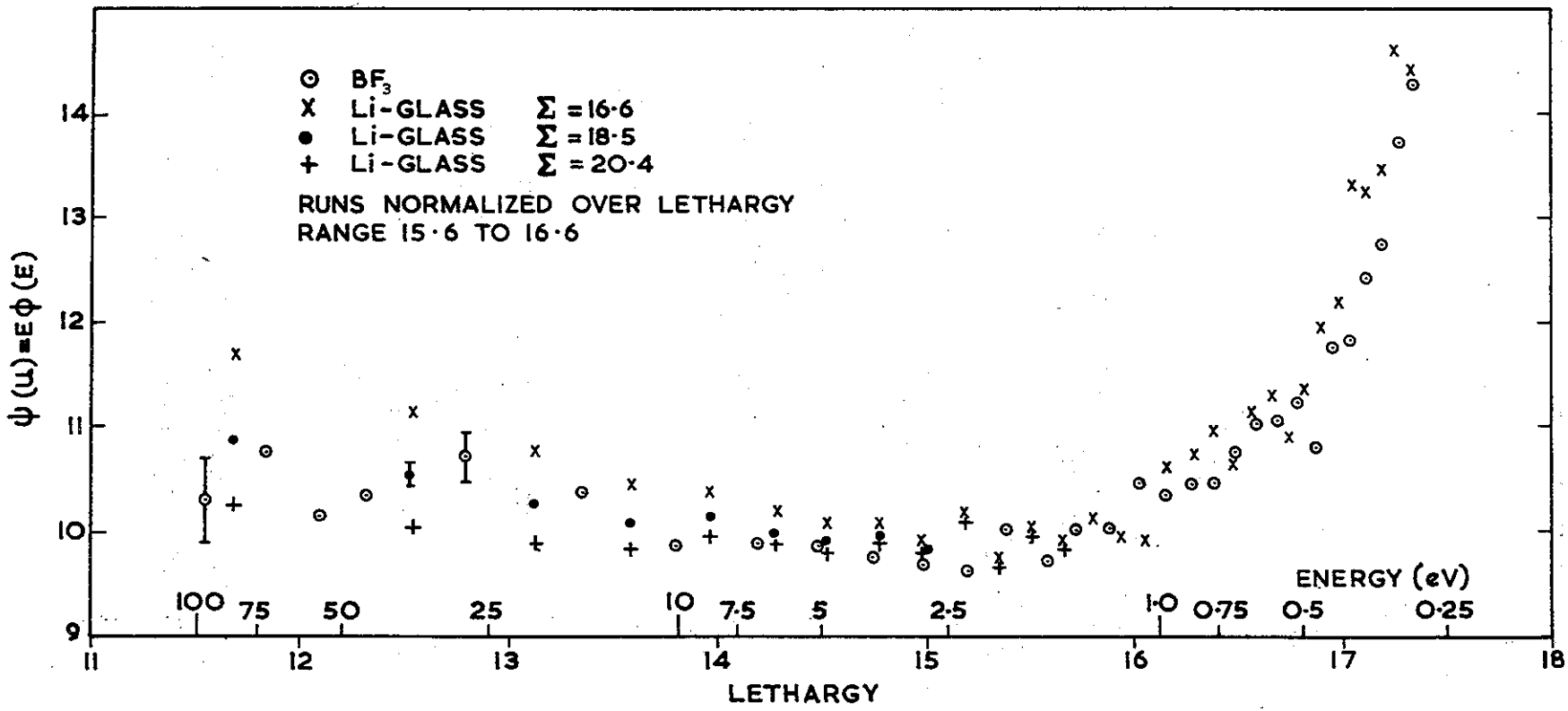

FIGURE 10. COMPARISON OF BF_3 AND Li-GLASS DETECTORS

P1083

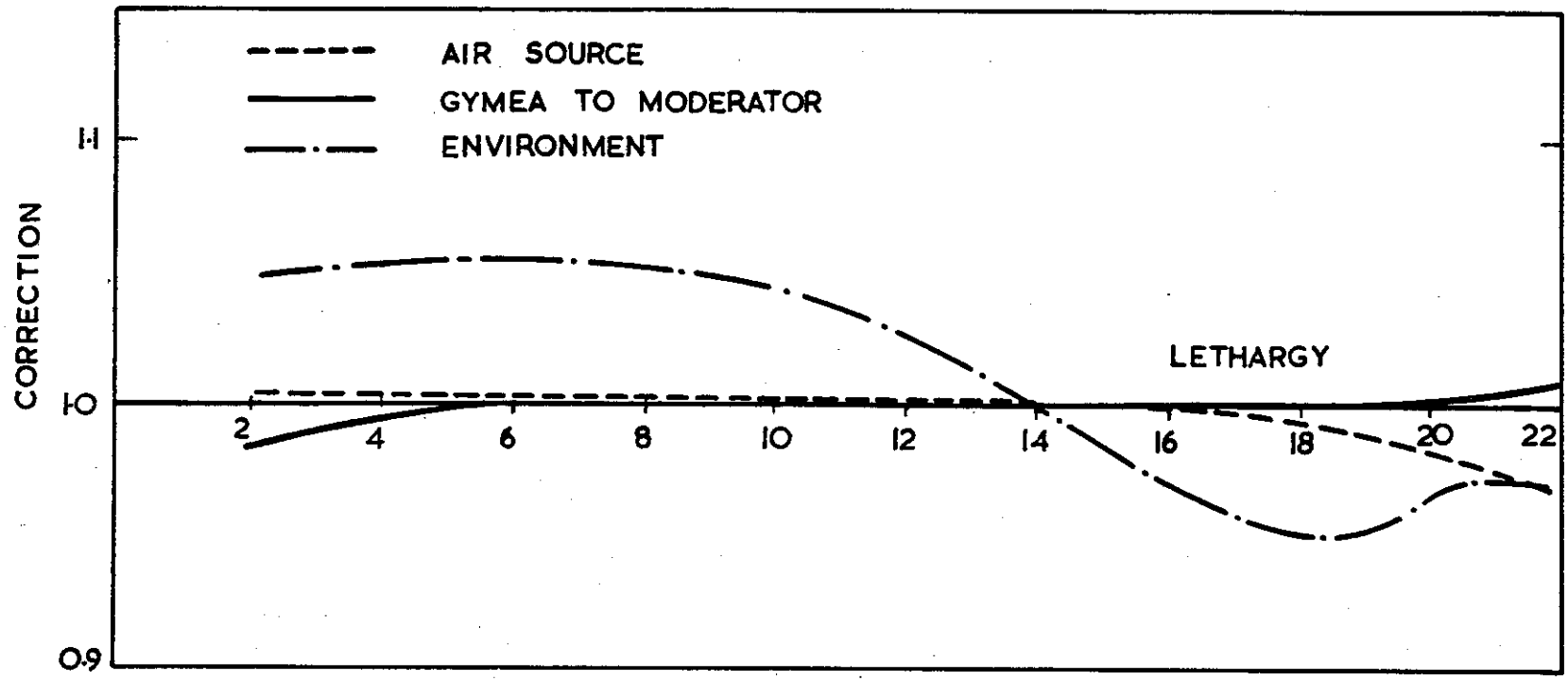

FIGURE 11. CORRECTION FACTORS FOR ASSEMBLY WITH U235/BeO = 1/6545

P1083

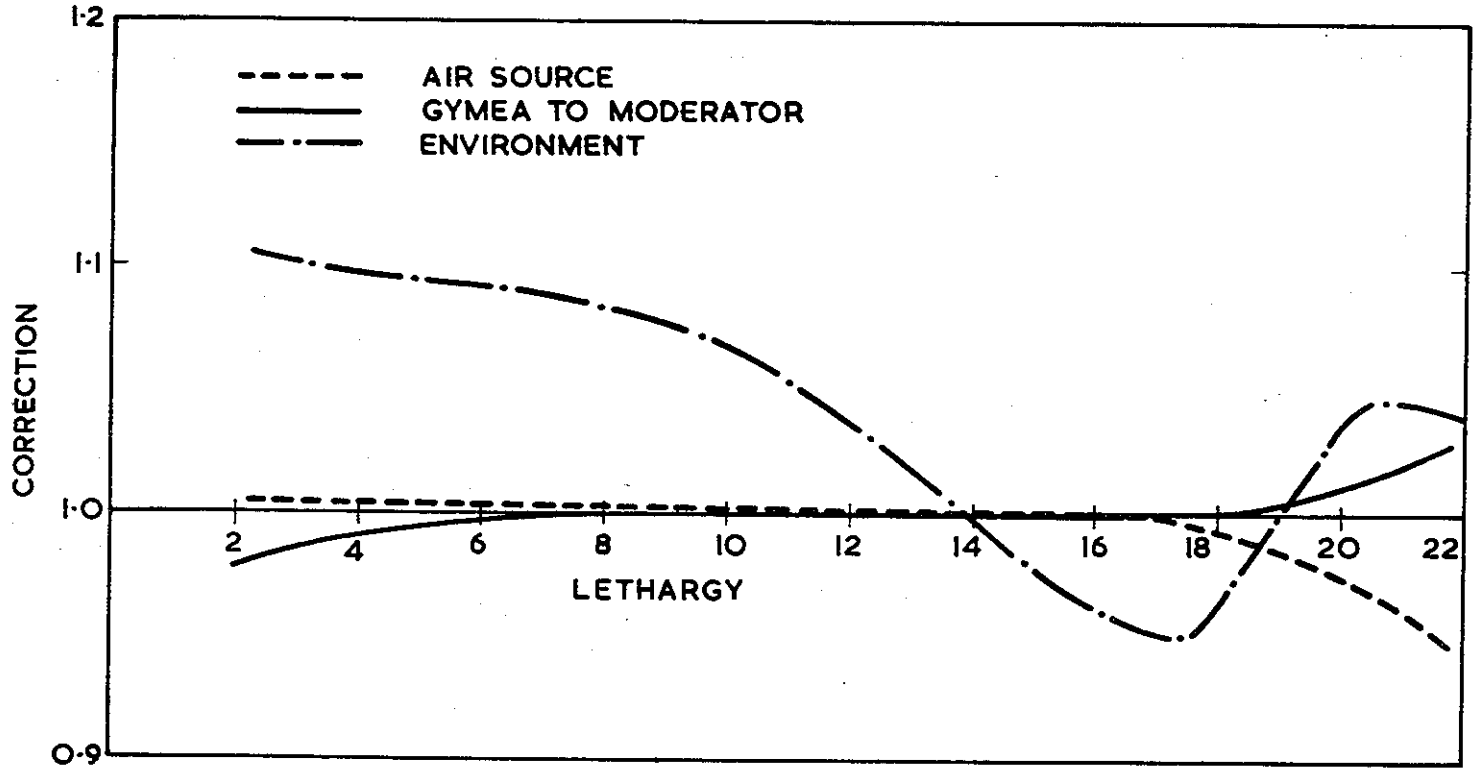

FIGURE 12. CORRECTION FACTORS FOR ASSEMBLY WITH U235/BeO = 1/4360

P1083

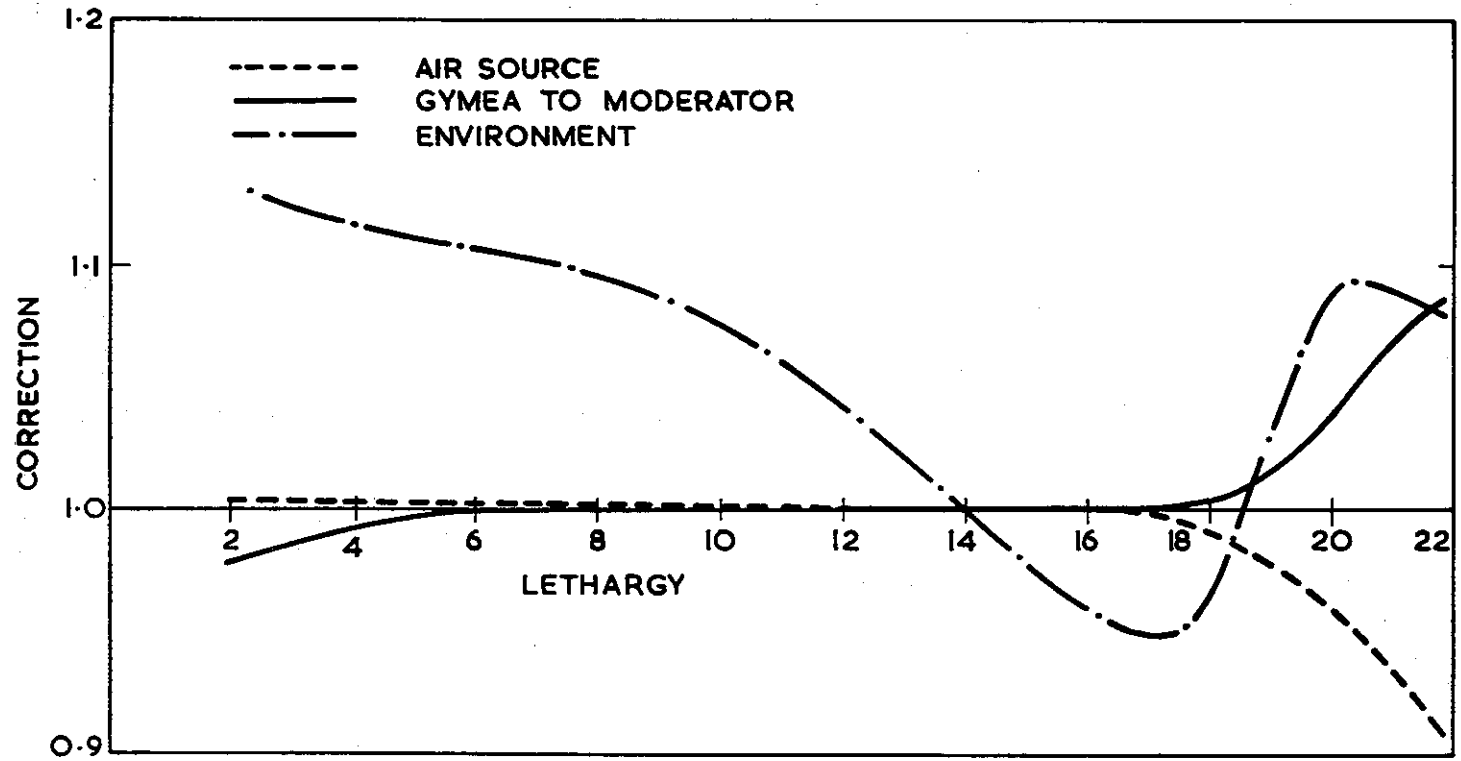

FIGURE 13. CORRECTION FACTORS FOR ASSEMBLY WITH U235/BeO = 1/2185

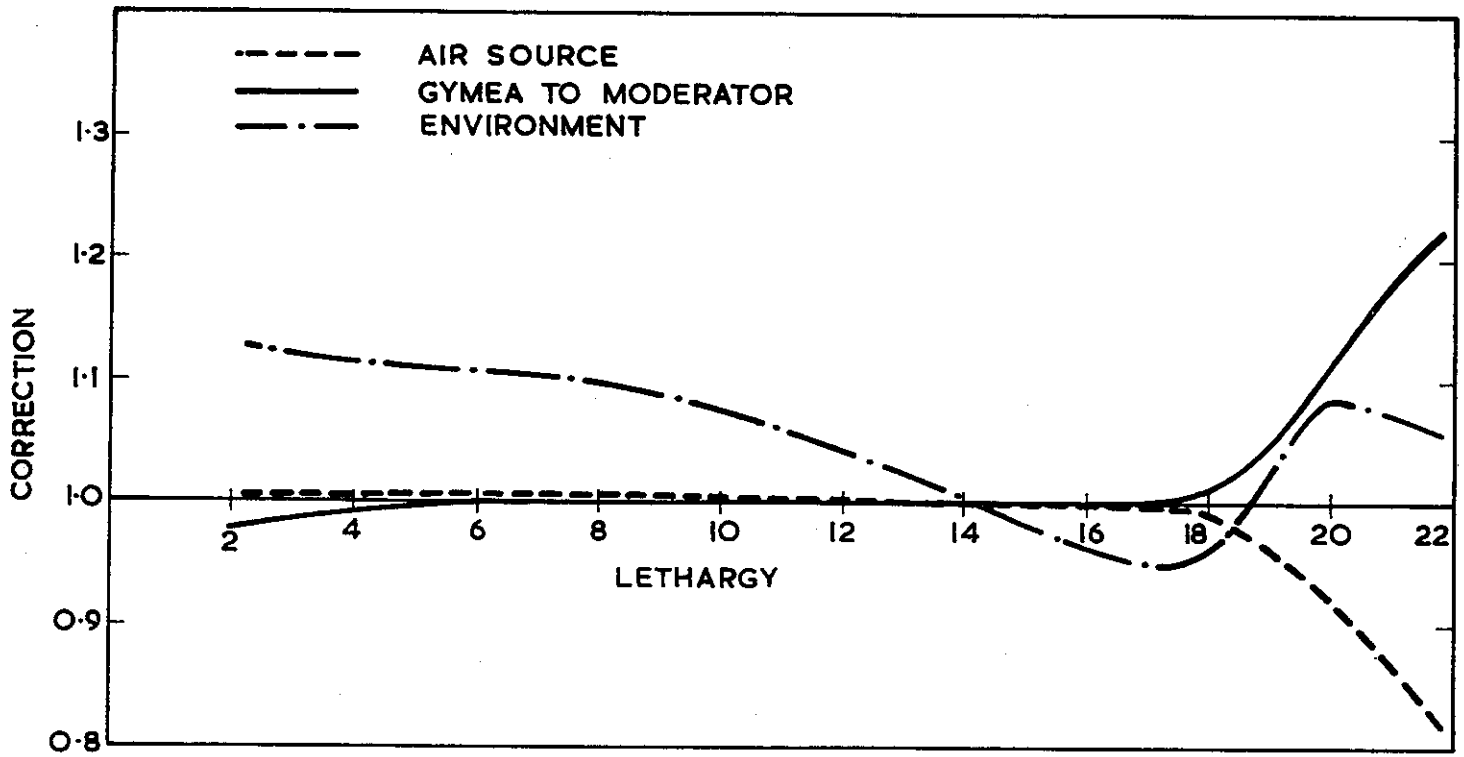

FIGURE 14. CORRECTION FACTORS FOR ASSEMBLY WITH U235/BeO = 1/1120

P1083

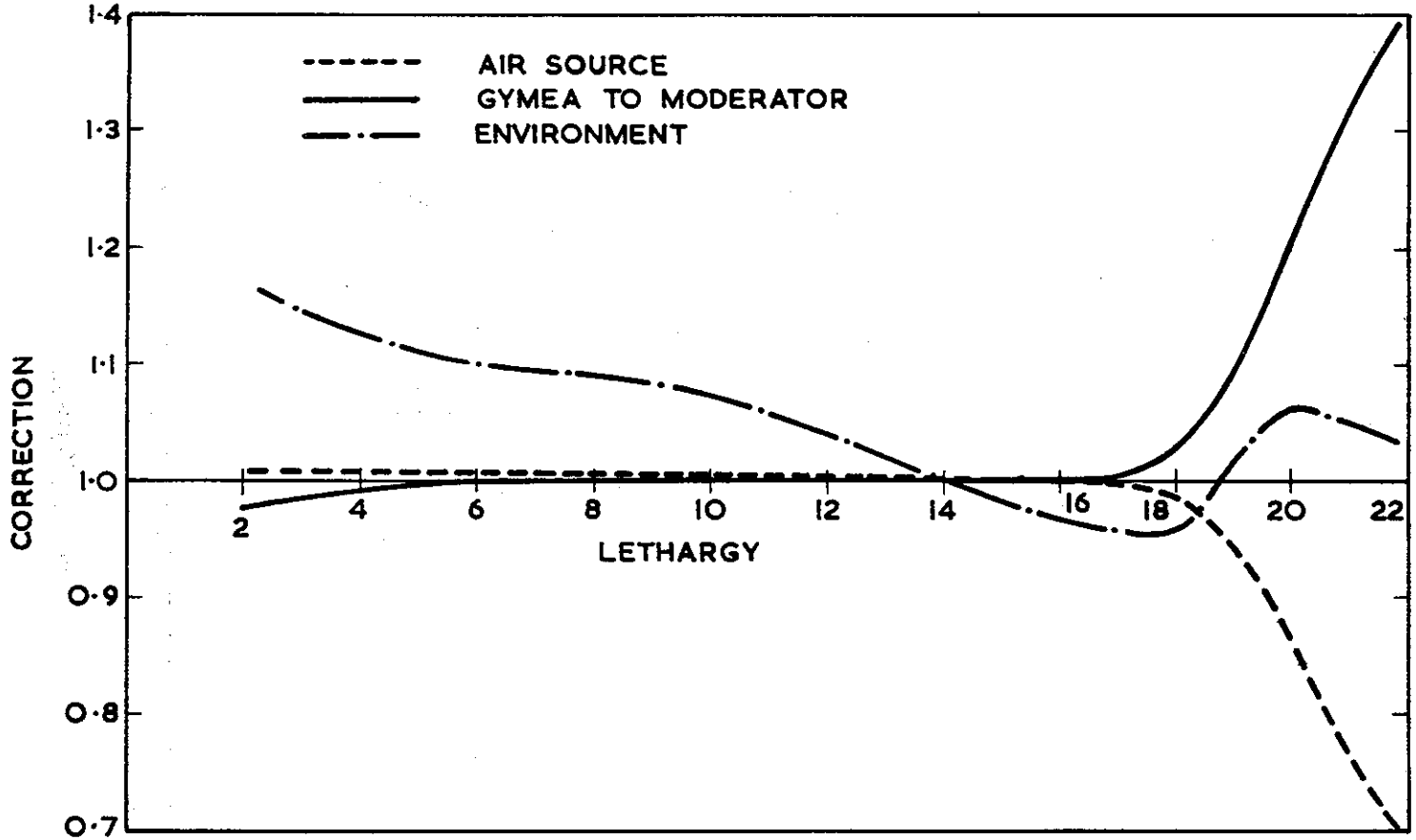

FIGURE 15. CORRECTION FACTORS FOR ASSEMBLY WITH U235/BeO = 1/740

P1083

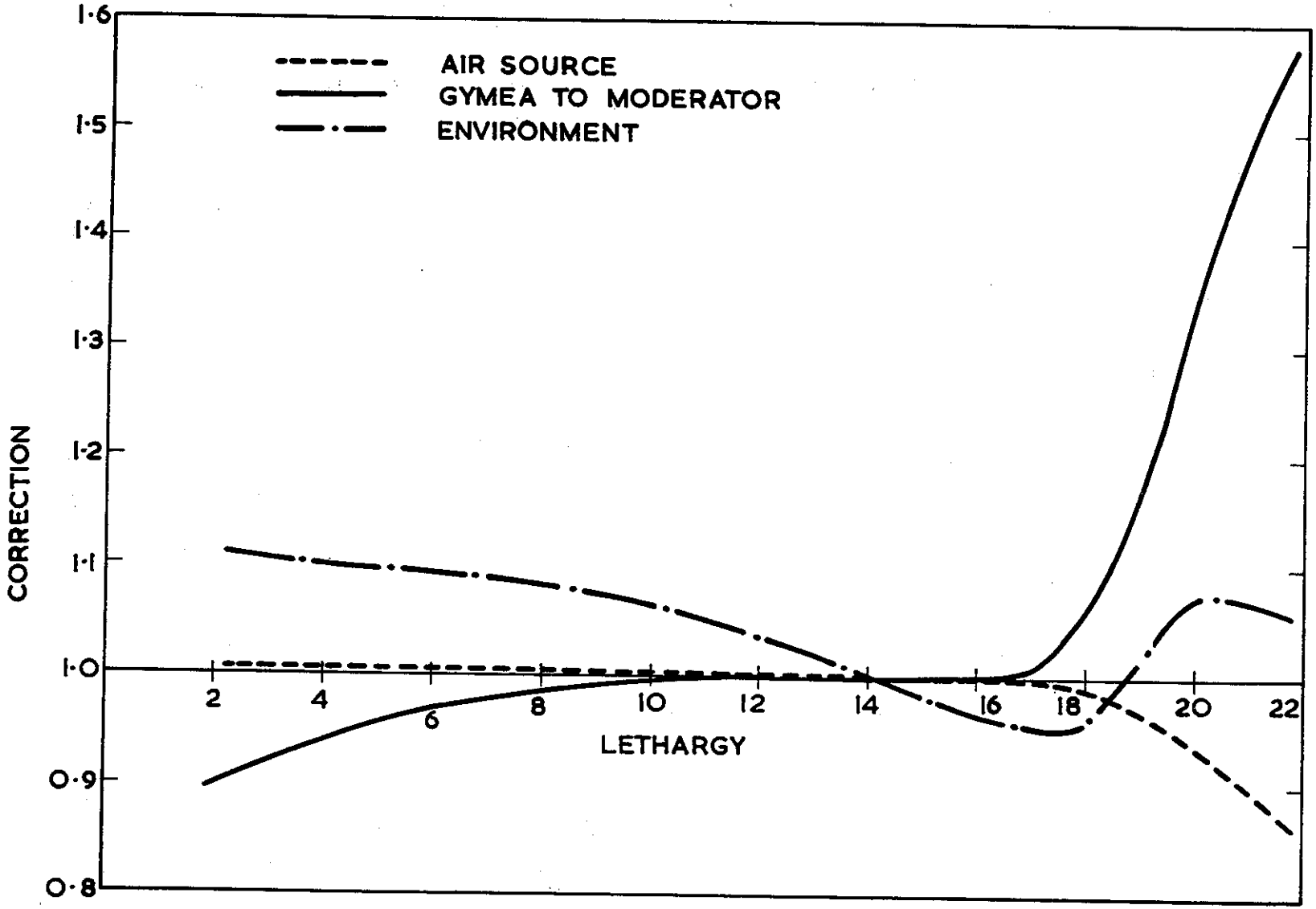

FIGURE 16. CORRECTION FACTORS FOR ASSEMBLY WITH U235/Th/BeO = 1/3.6/1500

P1083

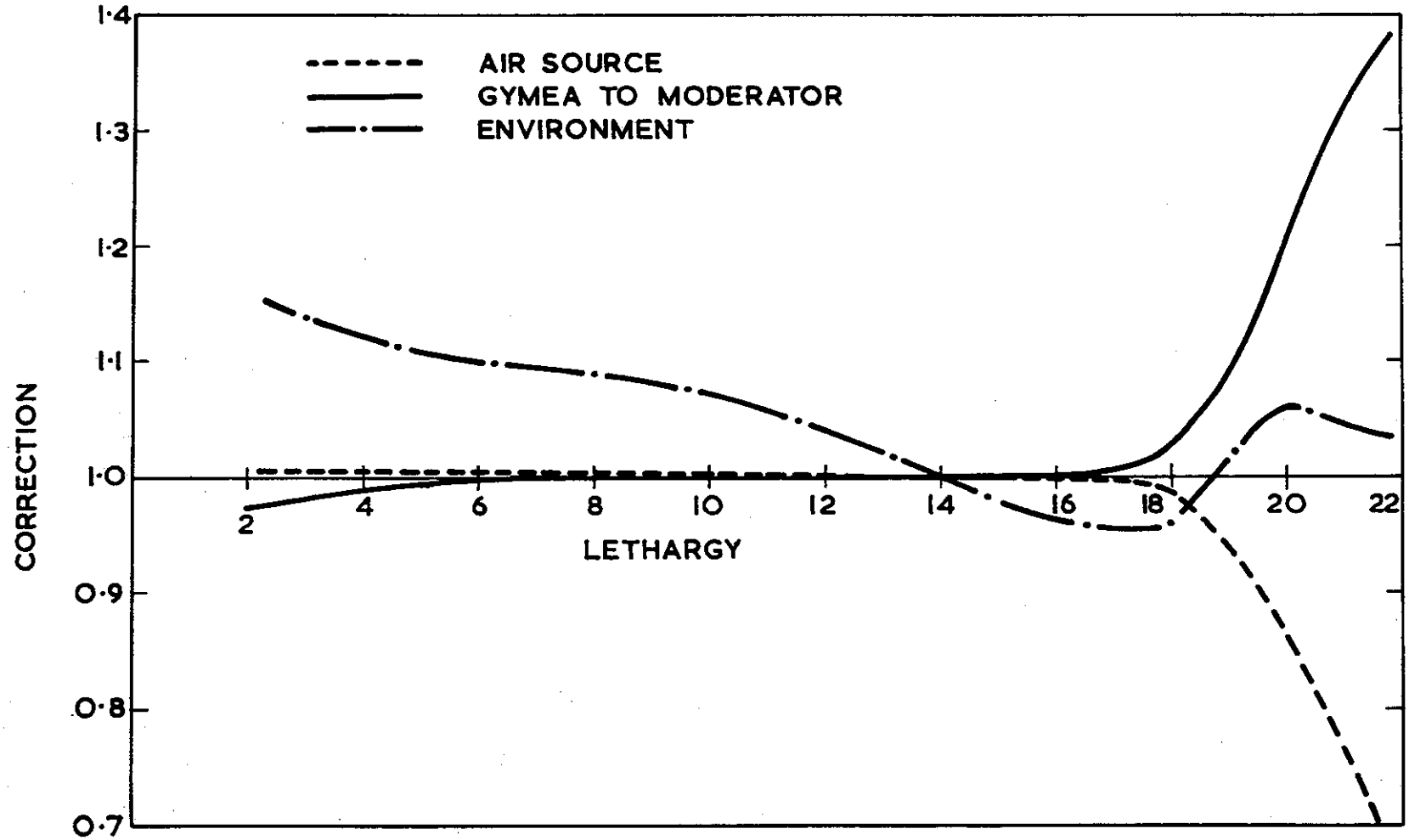

FIGURE 17. CORRECTION FACTORS FOR ASSEMBLY WITH U235/Th/BeO = 1/1.8/750

P1083

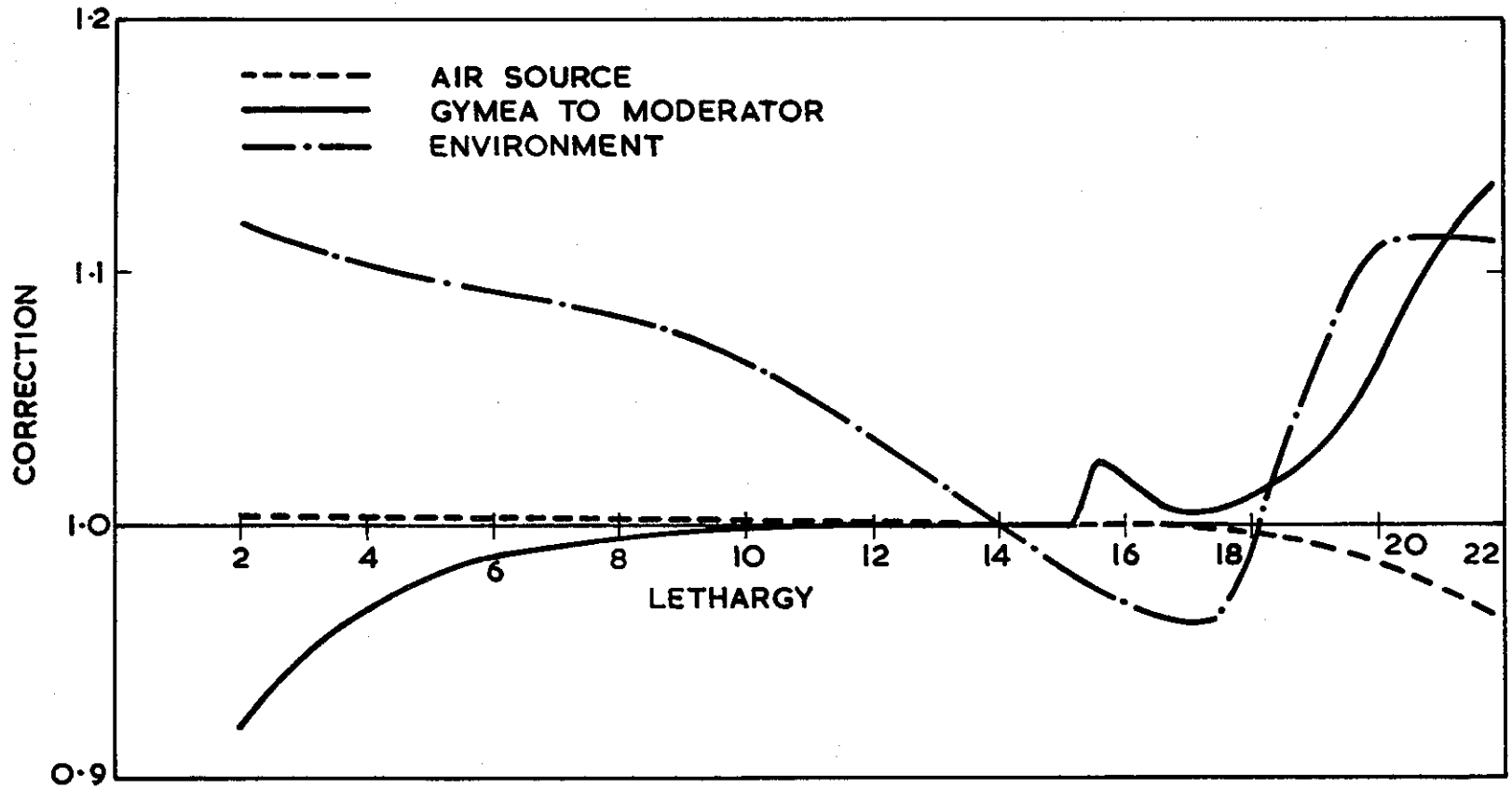

FIGURE 18. CORRECTION FACTORS FOR ASSEMBLY WITH U233/Th/BeO = 1/6.8/2800

P1083

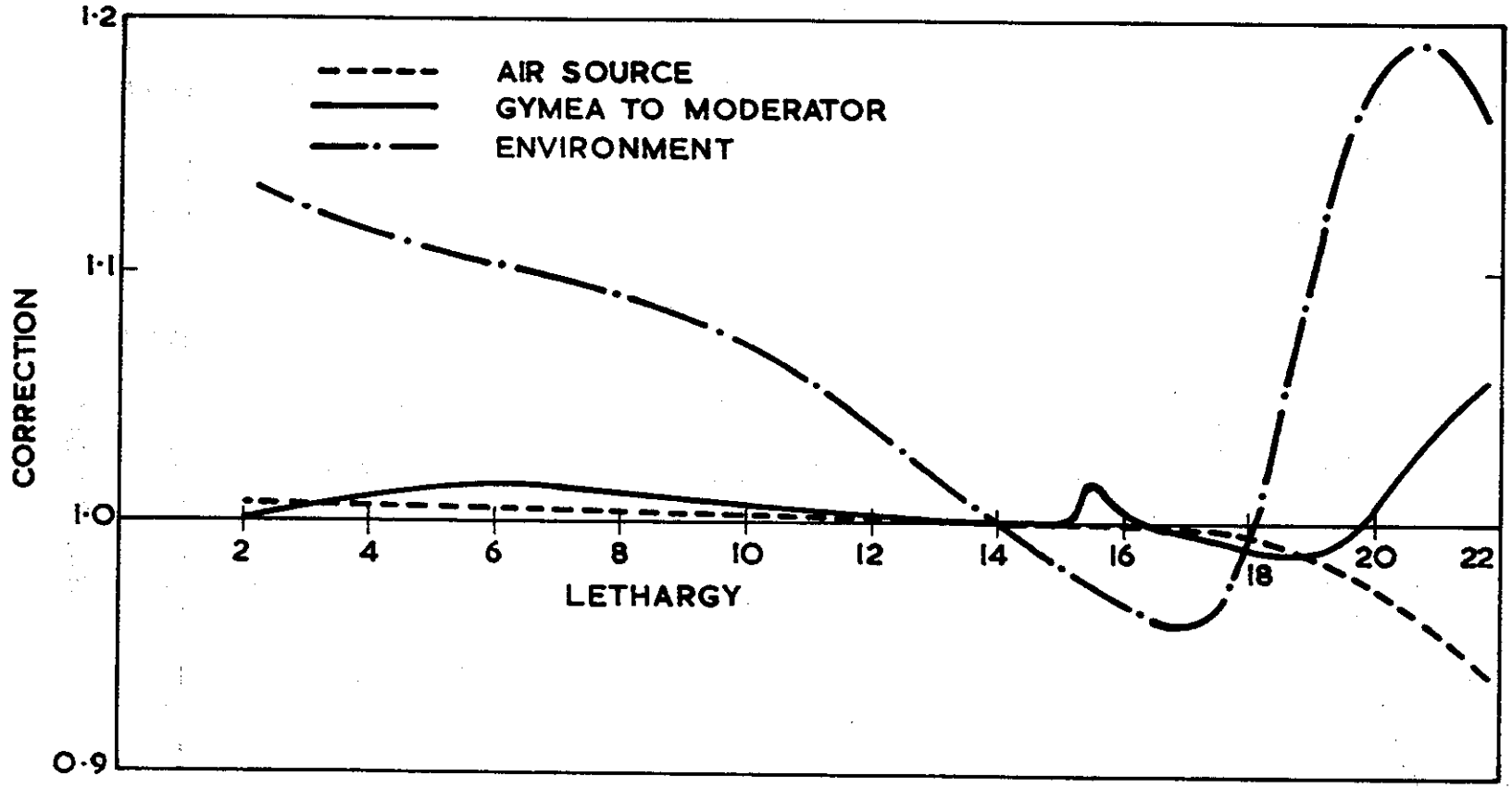

FIGURE 19. CORRECTION FACTORS FOR ASSEMBLY WITH U233/Th/BeO = 1/3.4/1400

P1083

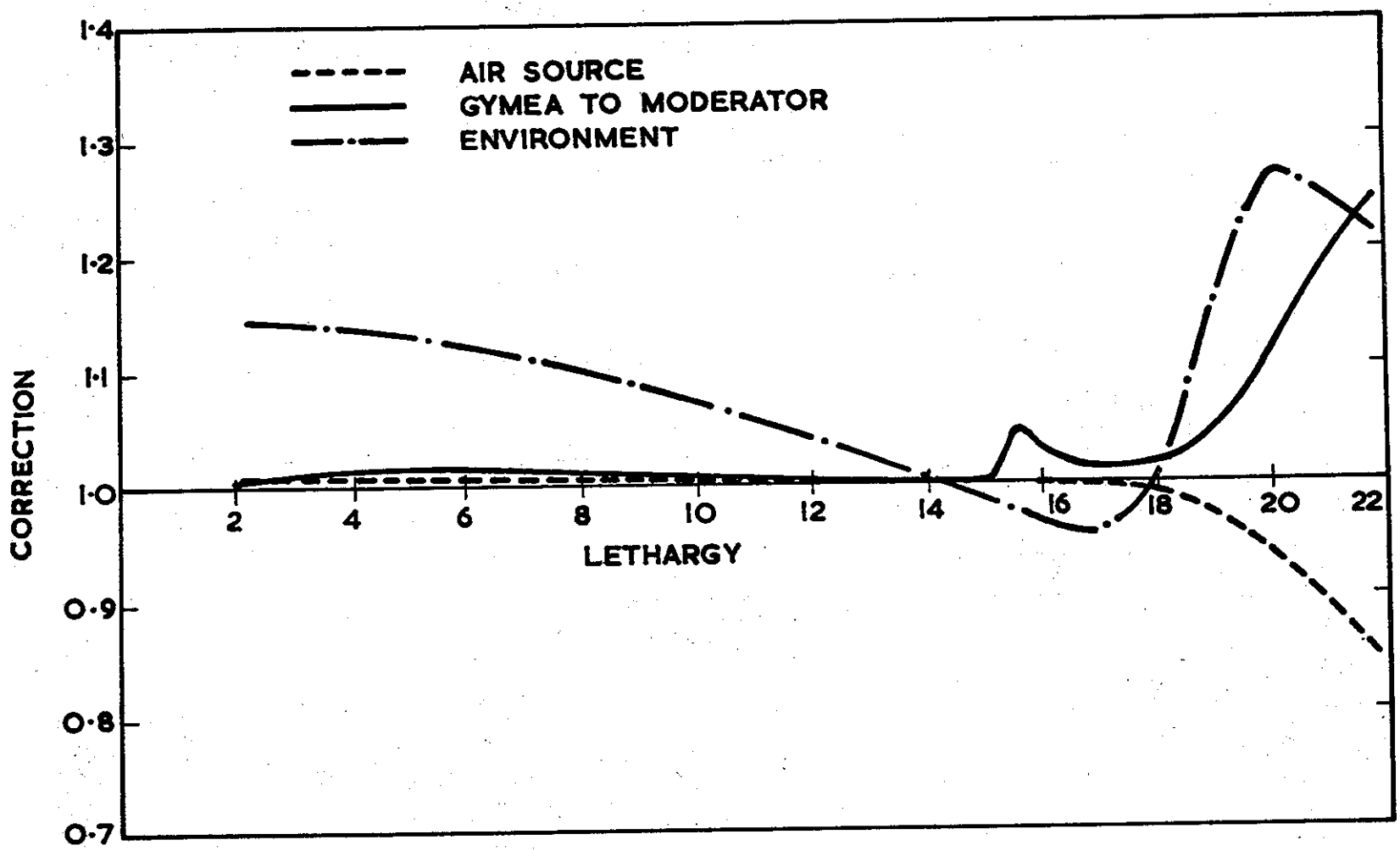

FIGURE 20. CORRECTION FACTORS FOR ASSEMBLY WITH U233/Th/BeO = 1/1.7/700

P1083

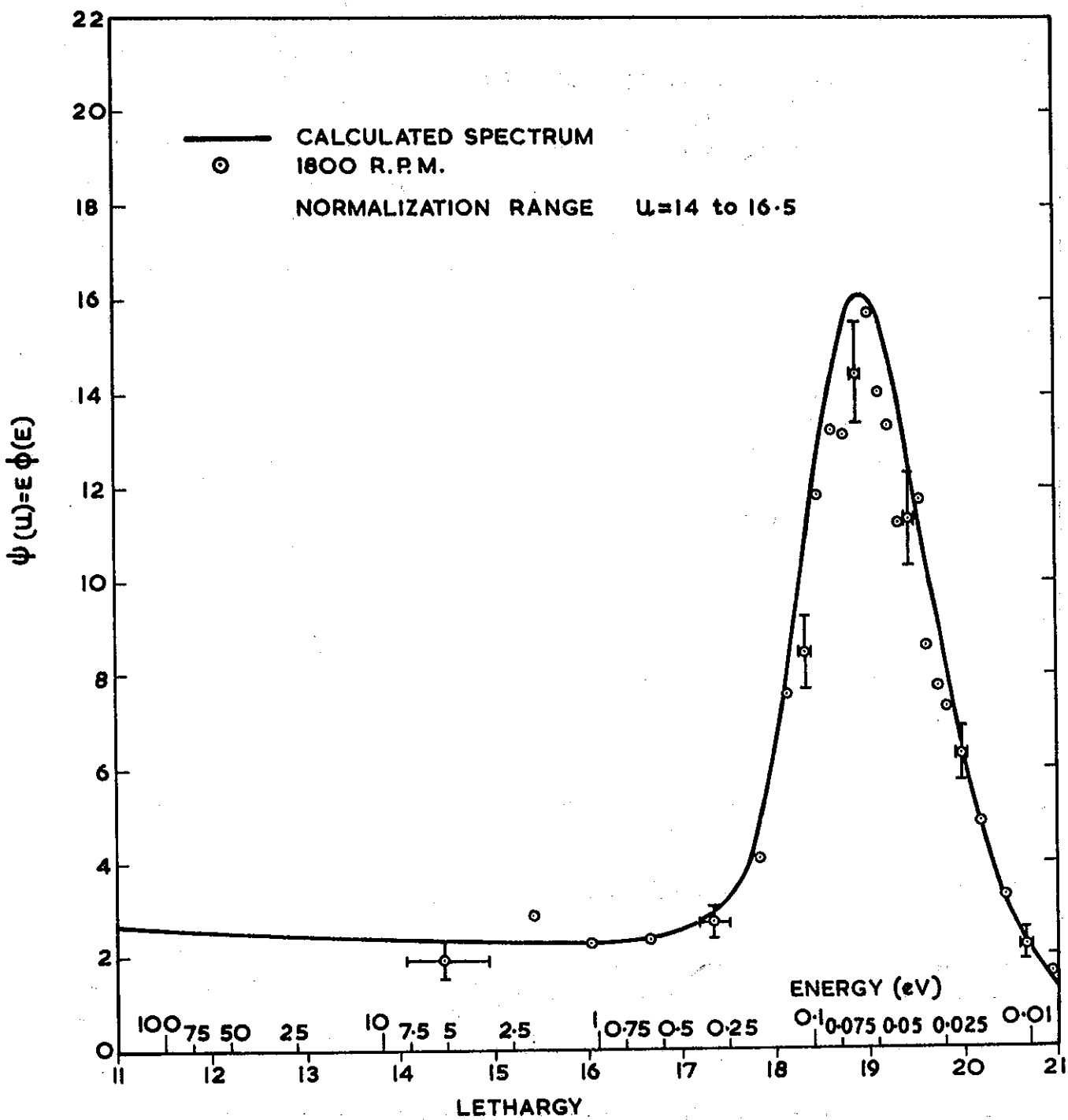

FIGURE 21. SPECTRA FOR ASSEMBLY WITH U235/BeO = 1/6545

P1083

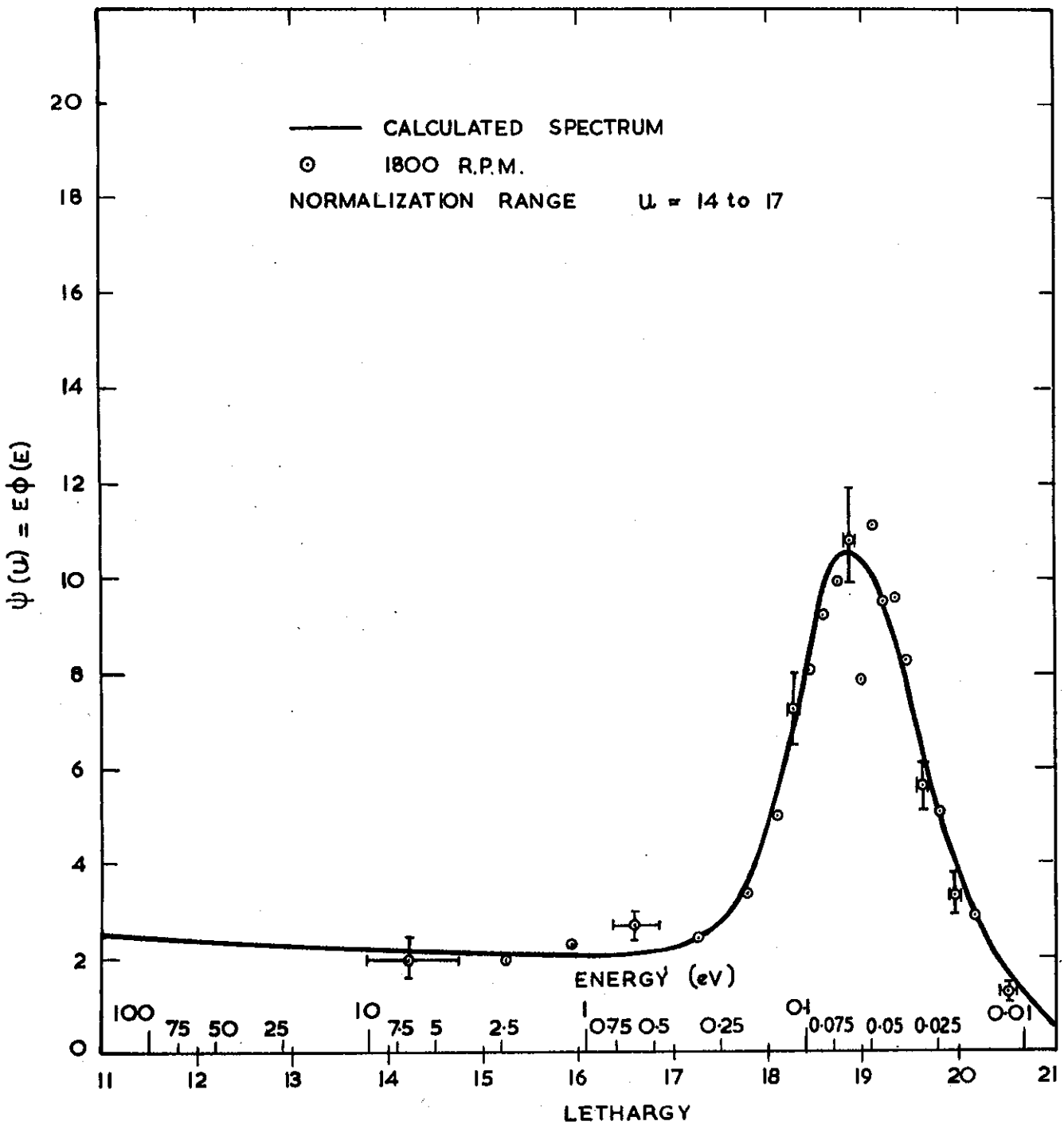

FIGURE 22. SPECTRA FOR ASSEMBLY WITH U235/BeO = 1/4360

P1083

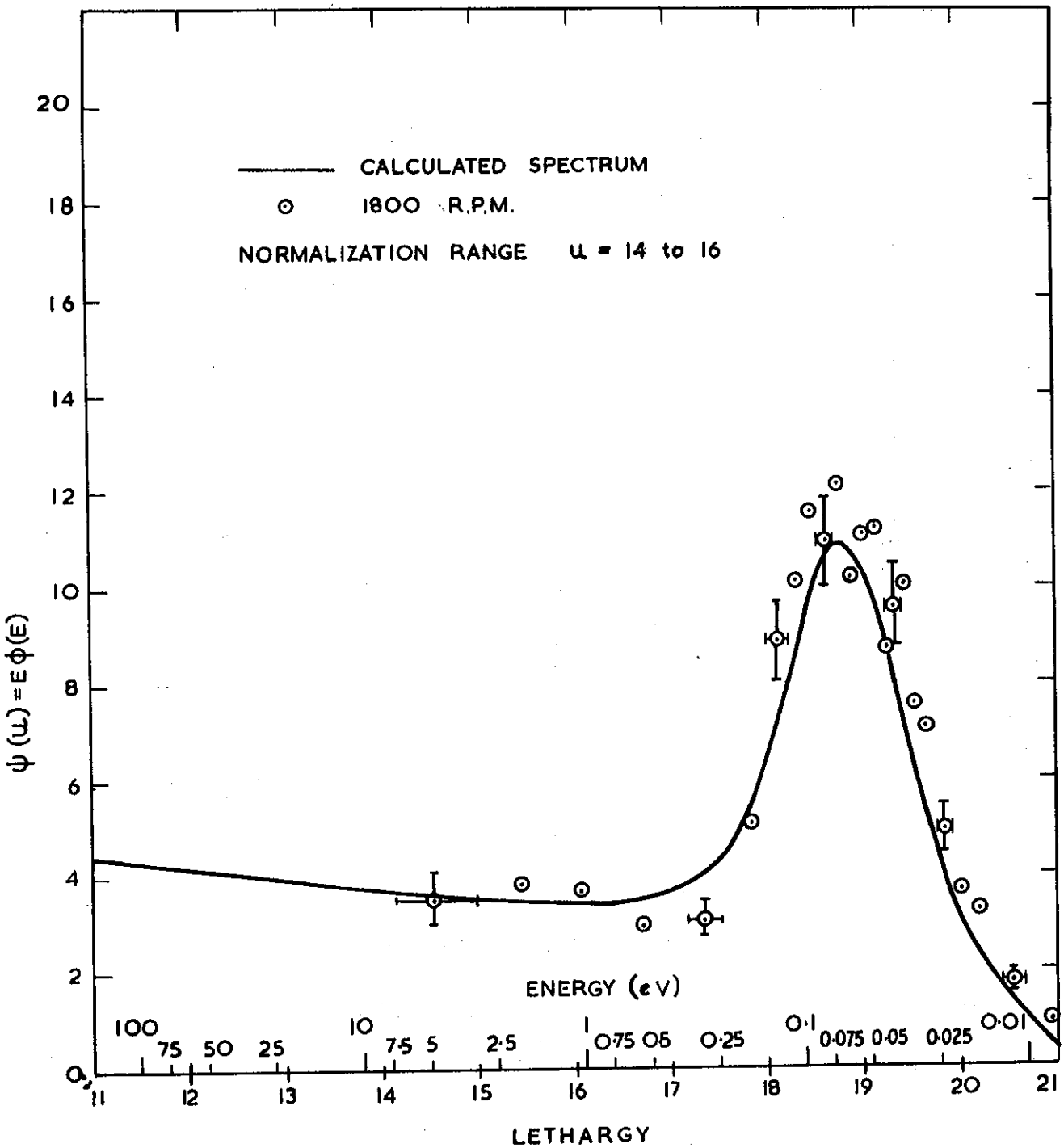

FIGURE 23. SPECTRA FOR ASSEMBLY WITH U235/BeO = 1/2185

P1083

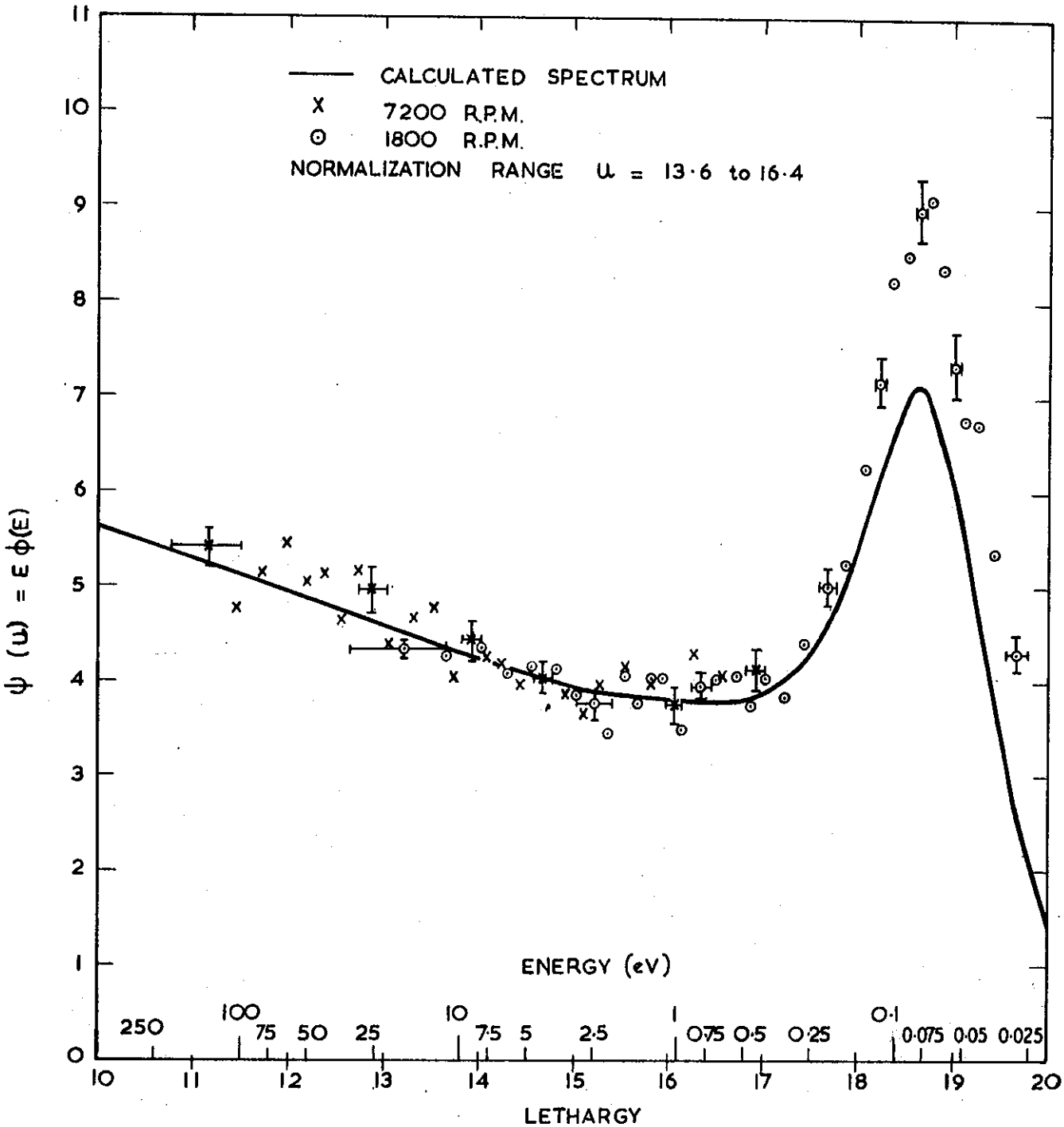

FIGURE 24. SPECTRA FOR ASSEMBLY WITH U235/BeO = 1/1120

P1083

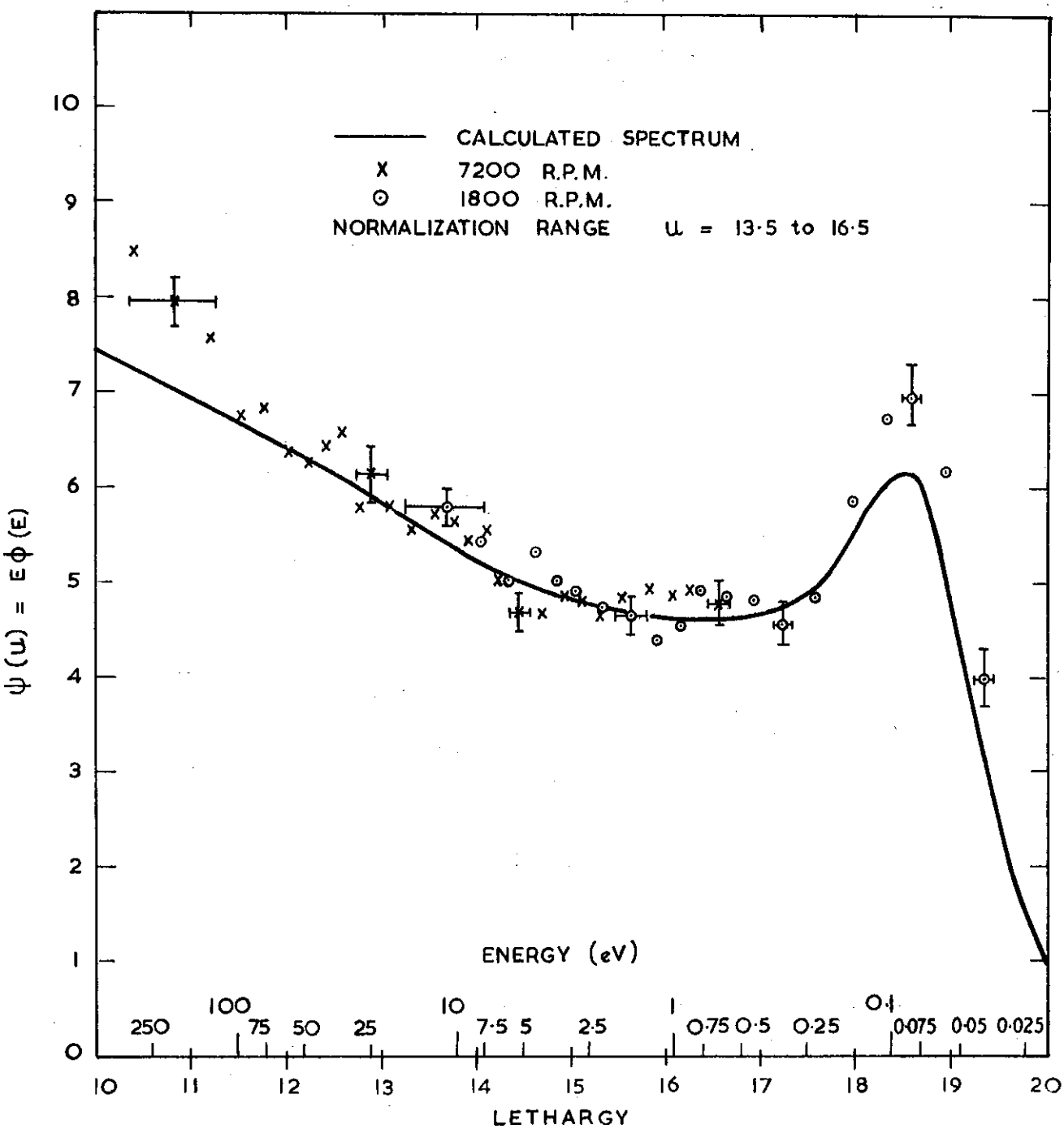

PIO83

FIGURE 25. SPECTRA FOR ASSEMBLY WITH U235/BeO = 1/740

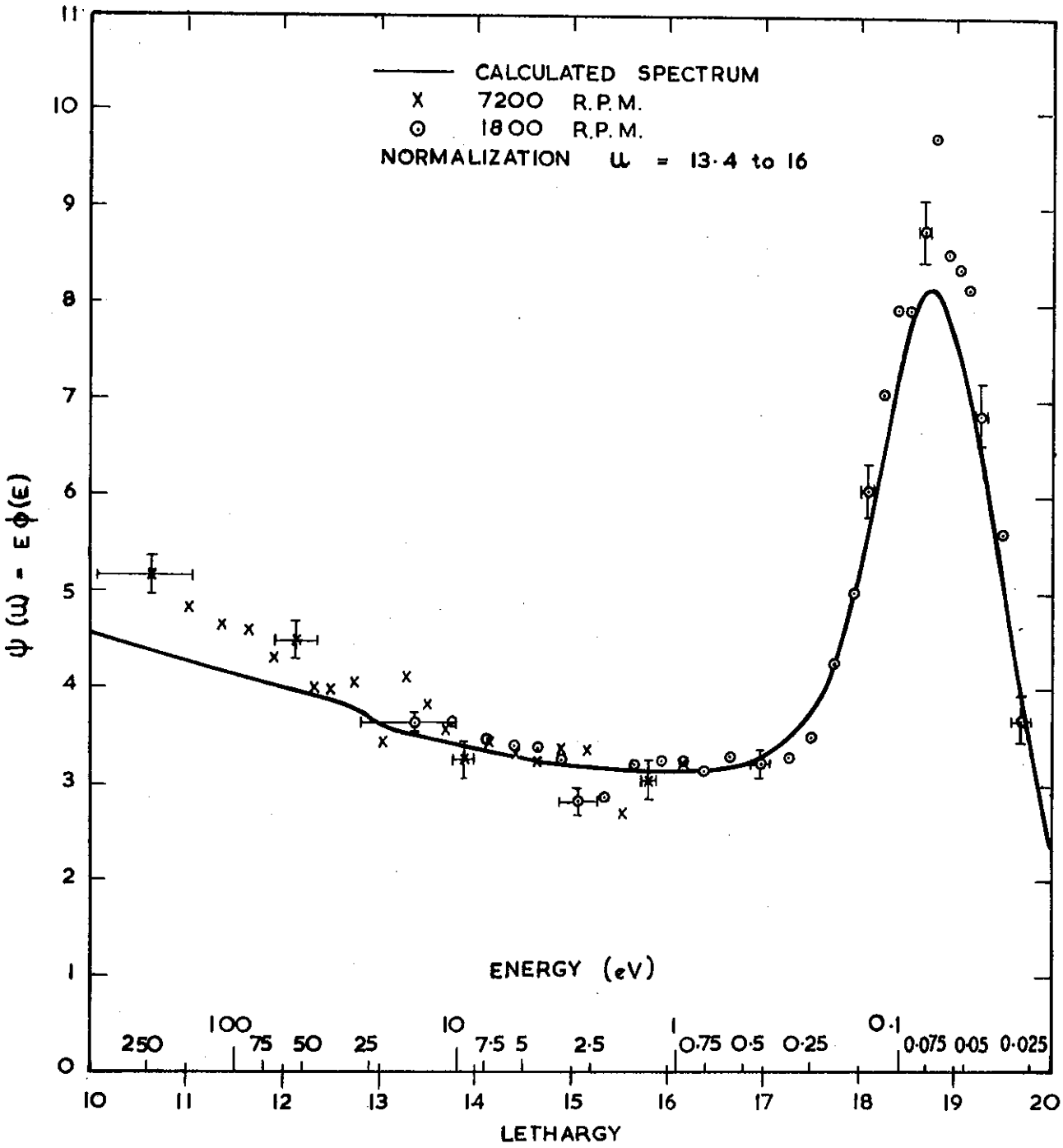

FIGURE 26. SPECTRA FOR ASSEMBLY WITH U235/Th/BeO = 1/3.6/1500

P1083

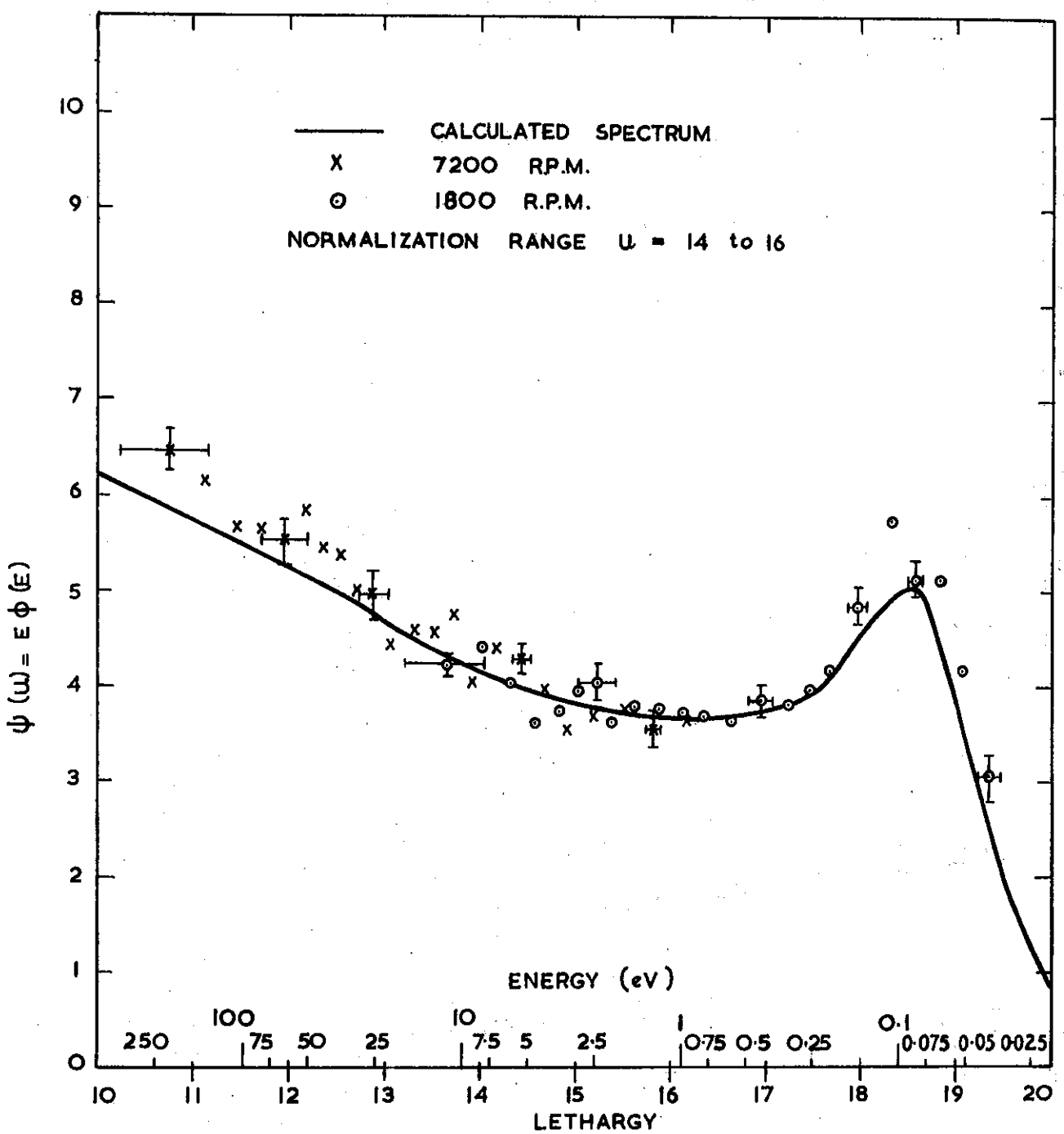

FIGURE 27. SPECTRA FOR ASSEMBLY WITH U235/Th/BeO = 1/1.8/750 P1083

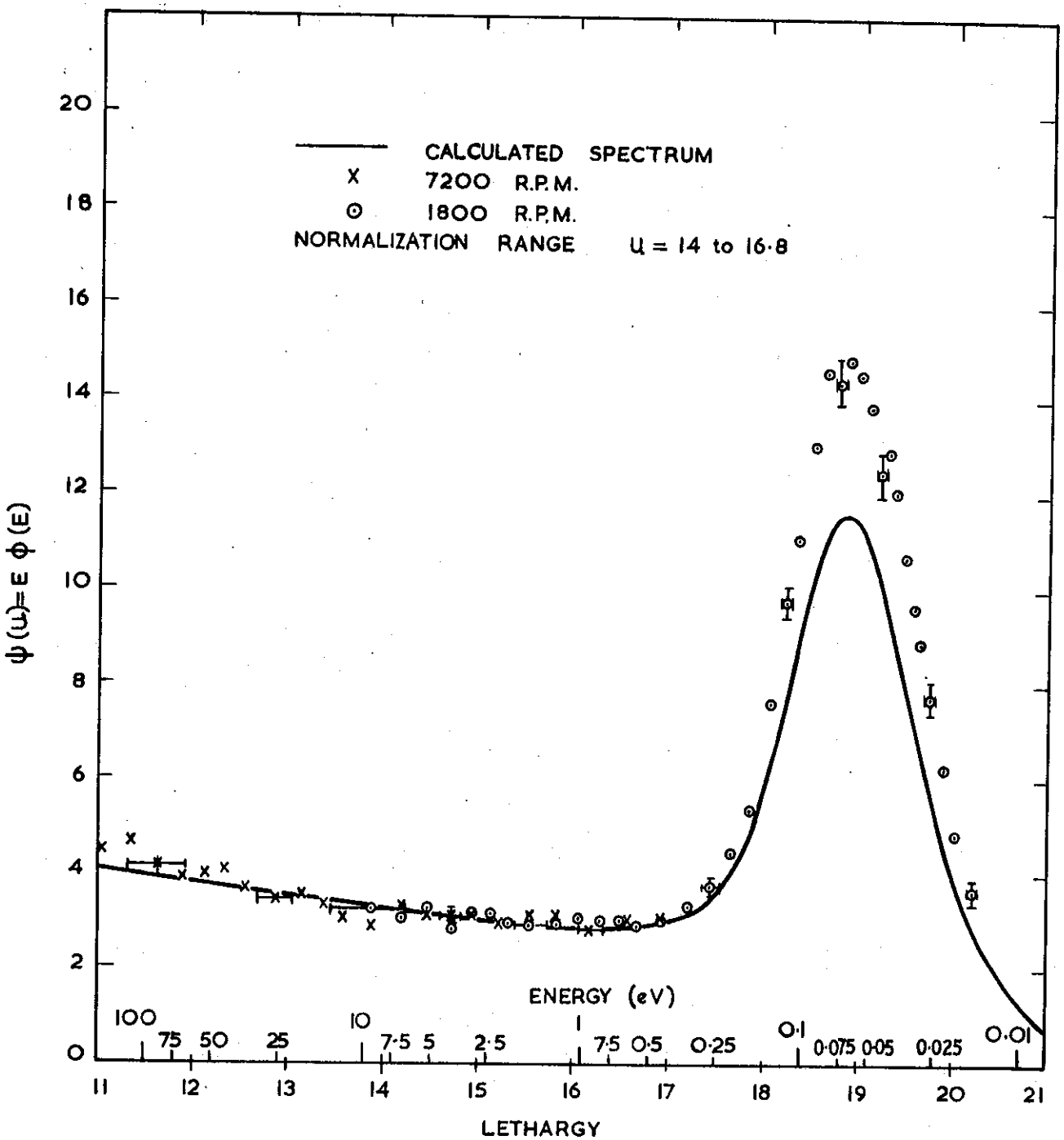

FIGURE 28. SPECTRA FOR ASSEMBLY WITH U233/Th/BeO =1/6.8/2800

P1083

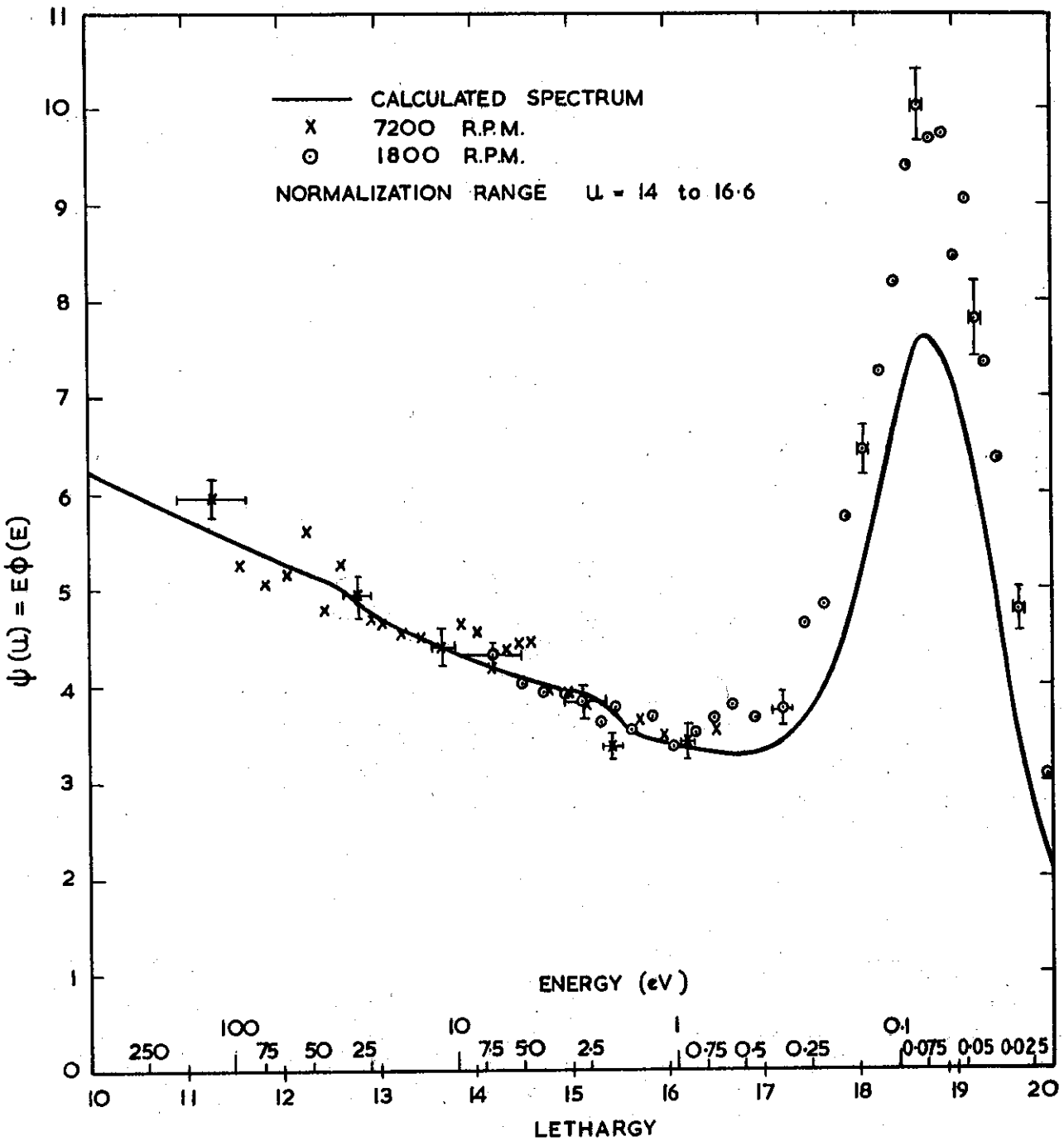

FIGURE 29. SPECTRA FOR ASSEMBLY WITH U233/Th/BeO = 1/3.4/1400

P1083

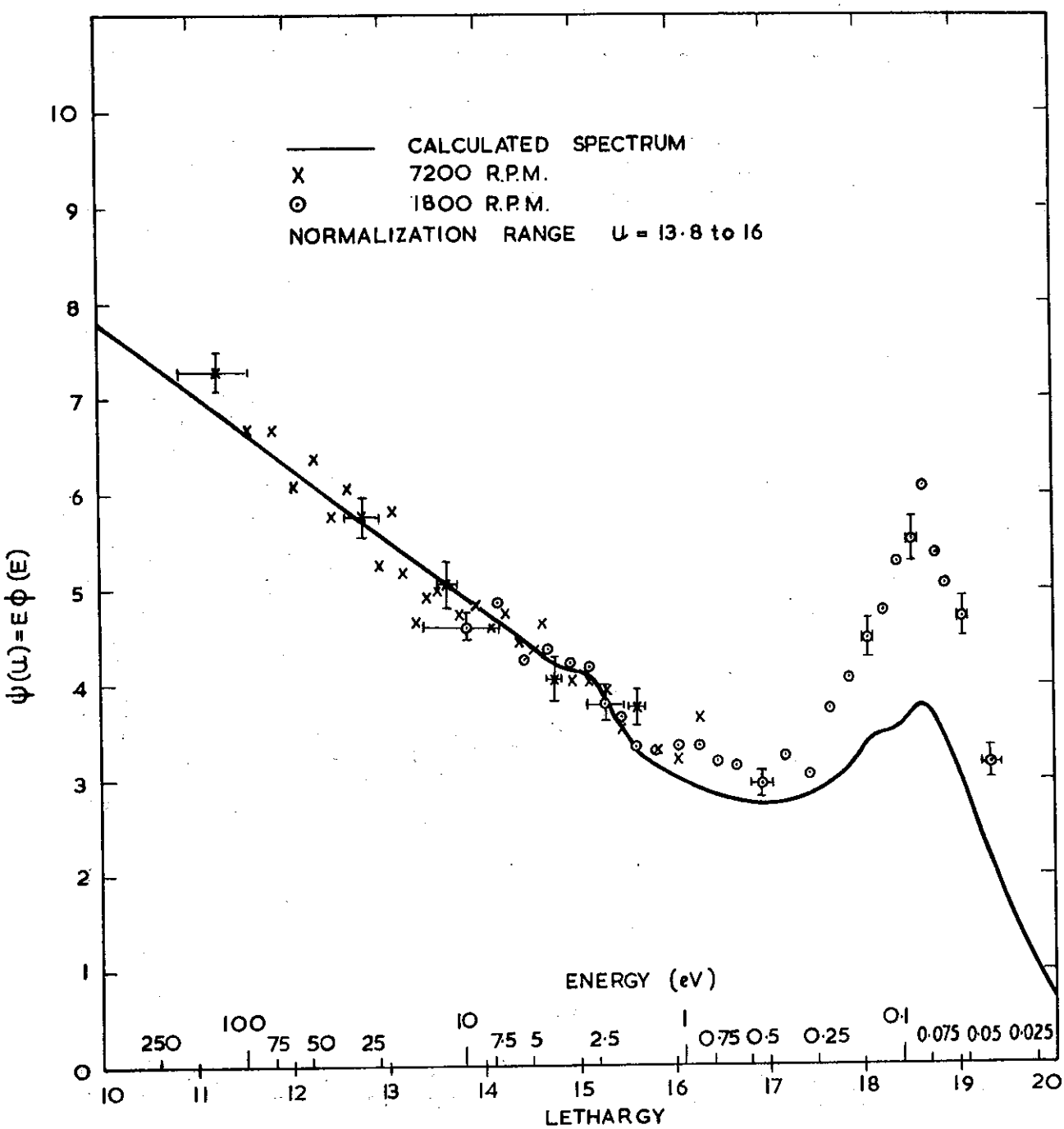

FIGURE 30. SPECTRA FOR ASSEMBLY WITH U233/Th/BeO = 1/1.7/700

PIO83

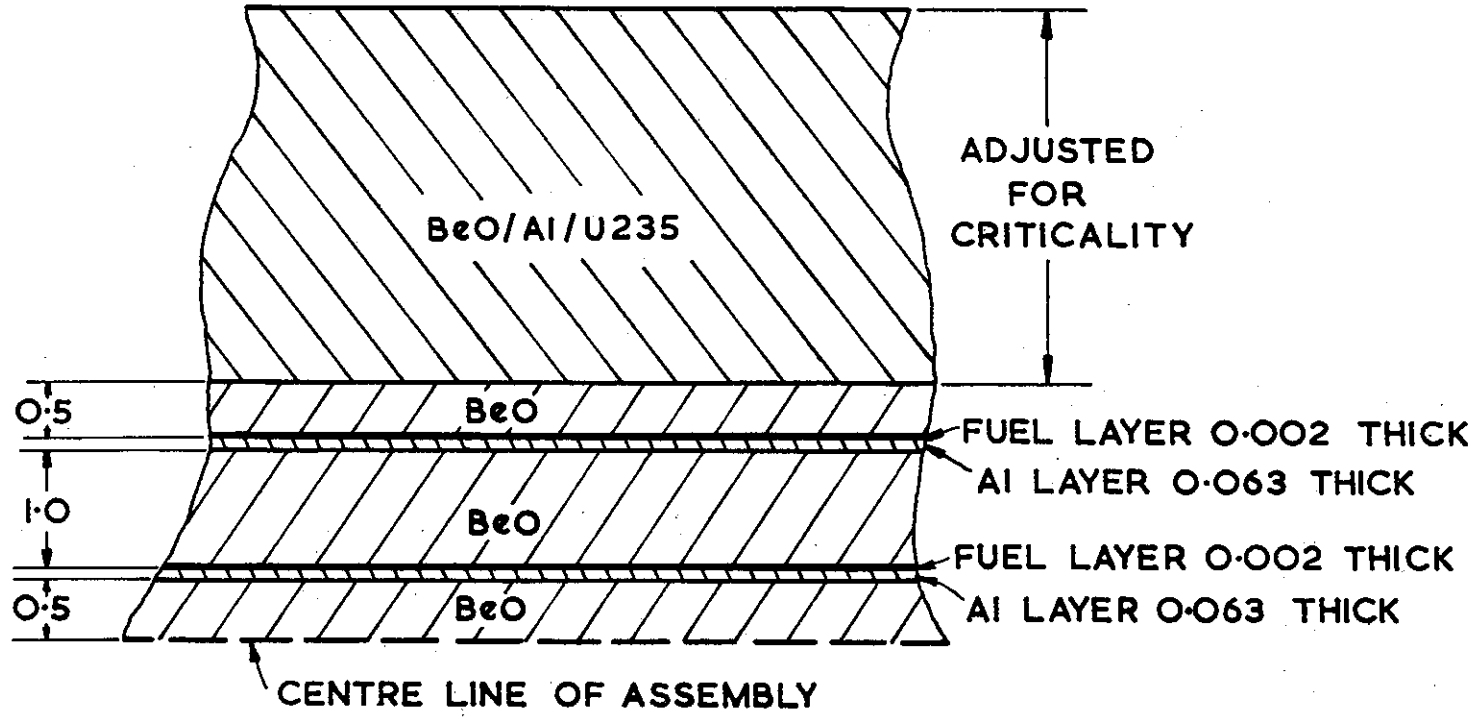

ALL DIMENSIONS IN INCHES

FIGURE 31. TYPICAL CONFIGURATION ASSUMED FOR DSN CALCULATIONS ON U235/BeO ASSEMBLIES

P1083

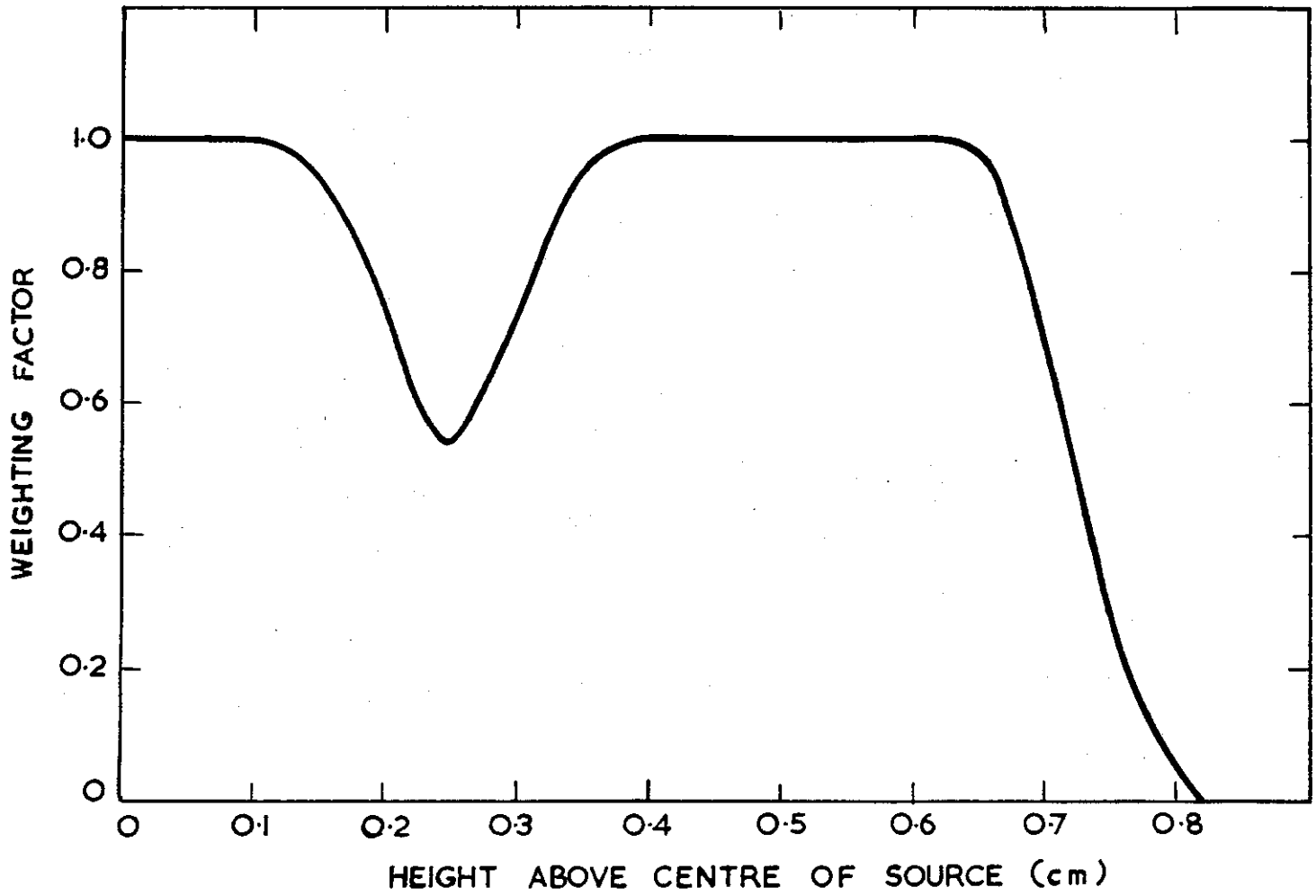

FIGURE 32. CHOPPER SENSITIVITY ALONG SOURCE PLANE

P1083

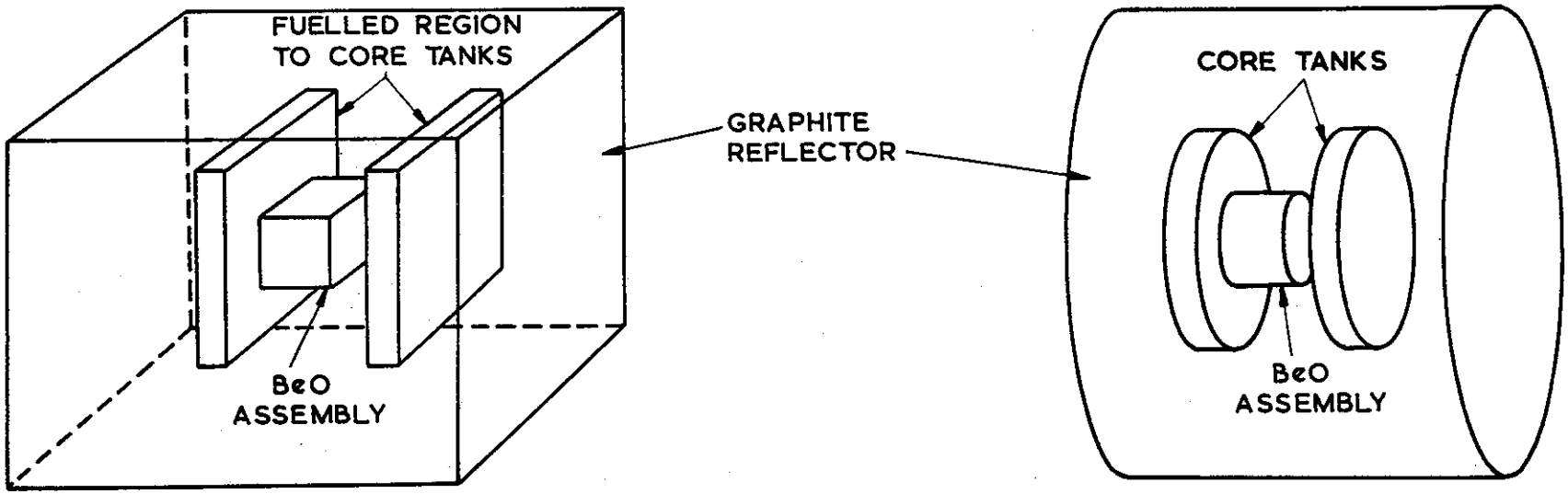

FIGURE 33. GHOST VIEW OF MOATA AND CYLINDRICAL MODEL USED IN CRAM CALCULATIONS

P1083